1-1-2018

Expression Analysis of MicroRNAs and MicroRNA-like RNAs in Aspergillus Flavus-Infected Aflatoxin Resistant and Susceptible Maize Inbred Lines

Amanda Benton Harper

Expression analysis of microRNAs and microRNA-like RNAs in Aspergillus flavus-infected aflatoxin resistant and susceptible maize inbred lines

By

Amanda Benton Harper

A Thesis
Submitted to the Faculty of
Mississippi State University
in Partial Fulfillment of the Requirements
for the Degree of Master of Science
in Biochemistry
in the College of Agriculture and Life Sciences

Mississippi State, Mississippi

December 2018

Expression analysis of microRNAs and microRNA-like RNAs in Aspergillus flavus-infected aflatoxin resistant and susceptible maize inbred lines

By

Amanda Benton Harper

Approved:

_____

Din-Pow Ma
(Major Professor)

_____

W. Paul Williams
(Committee Member)

_____

Sam K.C. Chang
(Committee Member)

_____

Kenneth O. Willeford
(Graduate Coordinator)

_____

George Hopper
Dean
College of Agriculture and Life Sciences

Name: Amanda Benton Harper

Date of Degree: December 14, 2018

Institution: Mississippi State University

Major Field: Biochemistry

Major Professor: Din-Pow Ma

Title of Study: Expression analysis of microRNAs and microRNA-like RNAs in Aspergillus flavus-infected aflatoxin resistant and susceptible maize inbred lines

Pages in Study: 101

Candidate for Degree of Master of Science

Corn (*Zea mays*) is frequently infected by a soil fungal pathogen *Aspergillus flavus*. The fungus produces aflatoxins, which cause liver cancer. Maize inbred lines that are resistant to infection by *A. flavus* have been developed, and these inbred lines provide excellent models for studying molecular mechanisms of maize resistance to the fungus. MicroRNA-like RNAs (milRNAs) recently identified in *A. flavus* had been found to be correlated with aflatoxin production conditions, suggesting that the milRNAs might play a role in the regulation of aflatoxin production. In this research, small RNAs were isolated from kernels of maize (resistant Mp719 and susceptible Va35) inoculated with *A. flavus* NRRL 3357 (aflatoxigenic) and NRRL 21882 (nonaflatoxigenic) and then subjected to RNA sequencing. Sequencing had identified 69 *A. flavus* milRNAs and 691 *Z. mays* miRNAs. The differential expression of some maize miRNAs revealed their potential role in response to inoculation, *A. flavus* growth, and aflatoxin production.

ACKNOWLEDGEMENTS

I would like to thank my major professor, Dr. Din-Pow Ma for his encouragement and patience as I completed this research and thesis. I want to also thank my committee, Drs. Paul Williams and Sam Chang, for their support and insight in this process. I would like to also thank the other member of our lab, Katy Franks, for her help and friendship during my graduate study. A special thanks to Dr. Williams and the USDA/ARS for the corn samples used for this project, as well as to Dr. Chuan-Yu Hsu, Tony Arick, and the Institute for Genomics, Biocomputing and Biotechnology at Mississippi State University, for technical support and the use of equipment and facilities. Finally, I would like to thank my family, for their encouragement, support, and love, as well as the graduate students in the Dorman 450 office – Jeremy, Dafne, Felix, Gizem, Norbert, and Saroj – for their knowledge and friendship.

TABLE OF CONTENTS

LIST OF TABLES

LIST OF FIGURES

LIST OF ABBREVIATIONS

A	adenine
BAC	bacterial artificial chromosome
bp	base pair
C	cytosine
cDNA	complementary DNA
DEPC	diethyl pyrocarbonate
DNA	deoxyribonucleic acid
EDTA	ethylenediaminetetraacetic acid
G	guanine
GWAS	genome-wide association study
MFE	minimum free energy
miRNAs	microRNAs
milRNAs	microRNA like RNAs
nt	nucleotide
PCA	Principal Component Analysis
PCR	polymerase chain reaction
PEG	polyethylene glycol
ppb	parts per billion
QTL	quantitative trait locus

RCF	relative centrifugal force
RNA	ribonucleic acid
RT-qPCR	reverse transcription quantitative PCR
SDS	sodium dodecyl sulfate
T	thymine
UTR	untranslated region
WGS	whole genome sequencing

CHAPTER I

INTRODUCTION

Aspergillus flavus, a fungus, is the major producer of aflatoxins, which have detrimental effects on agricultural products and their consumers. *A. flavus* infects a variety of crops under favorable conditions during pre- and post-harvest stages, and the fungus produces aflatoxins as secondary metabolites (Yu 2012; Klich 2007; Kensler et al. 2011). The toxins, when ingested, can act as carcinogens in humans and animals, and they often lead to liver disease, malnutrition, and suppressed immunity (Yu 2012; Klich 2007; Warburton and Williams 2014). In order to combat this worldwide issue, research attention has been focused on both *A. flavus* and its hosts to better understand the processes of infection and subsequent formation of aflatoxins (Warburton and Williams 2014).

Maize (*Zea mays*) is one of the major food crops in the world (Farfan et al. 2015). The plant was domesticated in Mexico about 9000 years ago (Xiao et al. 2017; Schnable et al. 2009). Maize is one of the crops infected by *A. flavus*, which causes ear rot in the plant and produces aflatoxins (Smart et al., 1990). Maize resistance to *A. flavus* and aflatoxin production is not fully understood. Research exploring the genetic basis for resistance is ongoing, but it has revealed the complexity of resistance mechanisms. It has been shown in some plants that miRNAs may respond to fungal infection, but the role of

maize miRNAs in resistance to *A. flavus* has not yet been explored (Kulcheski et al. 2011; Baldrich et al. 2015).

MicroRNAs (miRNAs) are small, non-coding RNAs that range from ~18-24 nucleotides, and they are produced by plants and animals (Axtell et al. 2011, Lee et al. 2010), while microRNA-like RNAs (milRNAs) are produced by fungi (Lee et al. 2010). Both miRNAs and milRNAs play important roles in post-transcriptional modification. They act as the guide for the RNA-induced silencing complex (RISC) to cleave target mRNAs or halt mRNA translation. They have been shown to play a role in growth and development, response to biotic and abiotic stresses, and activation of gene expression (Huntley et al. 2016; Zhang et al. 2014). The main difference between miRNAs and milRNAs occurs in their biogenesis, in that the miRNA/milRNA biogenesis mechanisms in plants, animals and fungi diverged with the different kingdoms (Lee et al. 2010). Neither the response of maize miRNAs to *A. flavus* infection, nor the response of *A. flavus* milRNAs to growth on resistant or susceptible maize lines has ever been explored.

In this research two maize inbred lines, Va35 and Mp719, infected by *A. flavus* strains, NRRL 3357 and NRRL 21882 were used for the study of the host-pathogen interaction of maize and *A. flavus*. The inbred line Va35 is susceptible to aflatoxin production by *A. flavus.* The inbred line Mp719, developed at the USDA-ARS at Mississippi State, is resistant to aflatoxin production by *A. flavus* (Williams and Windham 2012). In comparison to Va35, Mp719 has significantly lower levels of aflatoxin accumulation, about fifteen times less (Williams and Windham 2012). NRRL 3357 is an aflatoxigenic strain of *A. flavus*, and its genome has been recently sequenced (Nierman et al. 2015). NRRL 21882, a nonaflatoxigenic strain of *A. flavus,* lacks the

aflatoxin gene pathway, and it has been used as part of biological control agents against other aflatoxigenic strains of *A. flavus* (Mylroie et al. 2016). These different *A. flavus* strains have provided excellent materials for studying the host-pathogen interactions between maize and *A. flavus*.

CHAPTER II

LITERATURE REVIEW

Aspergillus flavus

The genus *Aspergillus* was first described in 1729 by an Italian priest and biologist Pier Antonio Micheli (Amaike and Keller 2011; Bennett 2010). The morphology of the conidiophore reminded Micheli of the aspergillum, a device for sprinkling holy water, and it then became the name for these fungi. *Aspergillus* species are found all over the world, primarily in soil, where they grow as saprophytes and acquire nutrients from decaying vegetation (Bennett 2010). Their spores are airborne, so the fungi can spread and grow almost anywhere, providing that the environment has the appropriate moisture and a food source (Bennett 2010). Many *Aspergillus* species have industrial importance, such as production of citric acid by *A. niger* and fermentation of rice soy sauce by *A. oryzae* and *A. sojae* (Bennett 2010). In developed countries, *A. flavus* and its secondary metabolites, aflatoxins, present an economic problem because the contamination of the toxins decreases the value of affected crops. Estimated annual losses due to aflatoxins in US corn amount to $280 million, and when including cotton, peanuts, and tree nuts the losses total to more than $1 billion (Nierman et al. 2015). These figures do not even include other cost factors such as testing for toxins, handling contaminated materials, and further research spending.

Life Cycle

A. flavus is a pathogenic fungus that grows in soil worldwide and affects a large variety of crops including cereals, oilseeds, spices, and nuts (Bennett 2010; Bhatnagar-Mathur et al. 2015). The fungus is yellow-green in color, existing primarily in its asexual state as an anamorph, and it has been isolated from soil in all major biomes on earth (Klich 2007; Hedayati et al. 2007). The sexual state, or teleomorph, of *A. flavus* has recently been described from laboratory crosses as *Petromyces flavus* (Horn et al. 2009). This is likely the cause of the large number of polymorphisms among wild *A. flavus* populations (Hedayati et al. 2007; Horn et al. 2009).

The microscopic features of *A. flavus* are shown in Figure 2.1. Conidiophores have thick, coarse, uncolored walls and are less than 1 mm in length. Vesicles are elongate when young (Figure 2.1B), later becoming subglobose or globose (Figure 2.1A), varying from 10 to 65 μm in diameter. Phialides can be uniseriate (Figure 2.1B) or biseriate (Figure 2.1A) with the primary branches up to 10 μm in length and the secondary up to 5 μm in length. Conidia are typically round with small spines and are between 3.5 to 4.5 μm in diameter (Hedayati et al. 2007).

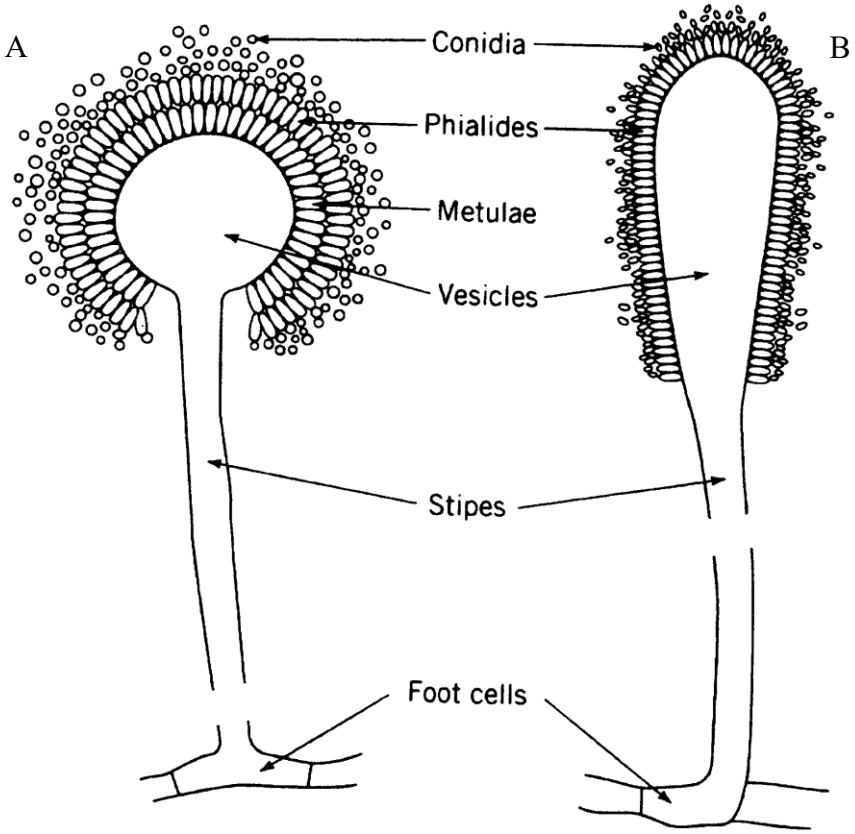

Figure 2.1 Conidiophores of *Aspergillus*

Conidiophores are shown with young (B) and old (A) vesicles. Image retrieved from Klich (2007).

In the soil, *A. flavus* utilizes decomposing plant tissues as its food source by breaking down sugar polymers into usable energy sources (Bennett 2010). The conidia can become airborne or be carried by an insect vector, and if given the opportunity, *A. flavus* will infect many plant or animal hosts (Bennett 2010; Bhatnagar-Mathur et al. 2015; Warburton and Williams 2014).

Infection

A. flavus can cause disease in both animals and plants (Bennett 2010; Hedayati et al. 2007). In humans, *A. flavus* can cause an allergic response or an infection, in addition

to the health effects of ingesting aflatoxins (Bennett 2010). Specifically, contact with fungal spores through inhalation, skin contact, or ingestion can lead to an allergic response, with populations in tropical climates being the most likely to be affected (Hedayati et al. 2007; Bennett 2010). *A. flavus* can also cause infections in the eye, the skin, upper respiratory tract, or other systems through the exposure of wounds by injury or surgery or through spread of previous infections (Hedayati et al. 2007). Varying resistance has been shown to antifungals, but *A. flavus* seems to be more virulent and more resistant than the other *Aspergillus* species (Hedayati et al. 2007).

A. flavus infection leads to rot of the food products or roots of the plants, such as ear rot of the kernels in corn or yellow mold in peanut seedlings (Klich 2007). Infection can occur both at pre-harvest, due to damage, drought stress, or excessive rain, and at post-harvest, due to excessive rain and improper storage conditions (Bhatnagar-Mathur et al. 2015; Amaike and Keller 2011). Spores will infect the plant through the damage to the seed or during pollination, in the case of maize (Bhatnagar-Mathur et al. 2015). Since pre-harvest infection relies primarily on environmental factors, several strategies such as good agricultural practices, limiting injury to plants, competitive inhibition by nonaflatoxigenic strains of *A. flavus*, and resistant crop lines have been used to prevent infection and aflatoxin production (Klich 2007). There are various treatment methods for contaminated products that give mixed results (Klich 2007).

Aflatoxin production

Aspergillus flavus poses a serious problem for agriculture because of the production of aflatoxins. Aflatoxins are secondary metabolites produced by *A. flavus*, *A. parasiticus*, *A. nomius, A. pseudotamarii, A. bombycis, A. ochraceoroseus,* and

Emericella venezuelens (Yu et al. 2004; Klich 2007). Aflatoxins were first identified in the early 1960s in the wake of the "Turkey 'X' Disease" outbreak, when contaminated feed led to widespread death of turkeys, ducks, and chickens (Kensler et al. 2011). There are six different aflatoxins – B_1, B_2, G_1, G_2, M_1, and M_2 – that impact agricultural products and consumers (Klich 2007). *A. flavus* produces only B_1 and B_2, while *A. parasiticus* produces B_1, B_2, G_1, and G_2 (Klich 2007). Aflatoxins M_1 and M_2, found in cow's milk, are by-products from the consumption of aflatoxins B_1 and B_2 (Yu 2012). The US Food and Drug Administration limits aflatoxins in human and animal food products to 20 ppb, except for milk, which is limited to 0.5 ppb (Kensler et al. 2011; Warburton and Williams 2014). There are similar regulations in many other countries worldwide, that affect the sale and trade of impacted agricultural products. In areas of the world that depend on subsistence farming, these regulations do not prevent ingestion of affected products (Warburton and Williams 2014). Aflatoxin exposure has also been hypothesized to play a role in worsening disease epidemics such as AIDS in developing countries (Warburton and Williams 2014).

Aflatoxin exposure can lead to liver disease, malnutrition, and suppressed immunity, and it can also cause cancer in animals and humans with prolonged exposure (Kensler et al. 2011; Klich 2007; Warburton and Williams 2014). Of the six molecules, Aflatoxin B_1 is the most prevalent and the most carcinogenic, and it is also the most potent naturally occurring carcinogen (Klich 2007). The function of aflatoxins in the fungus has not yet been elucidated, although it may be in response to oxidative stress (Fountain et al. 2014) and changes in nutrient availability in the host (Mellon, Dowd, and Cotty 2005).

Biosynthesis of Aflatoxins

The genome of *A. flavus* strain NRRL 3357 has been sequenced and is accessible at NCBI under the whole-genome shotgun (WGS) accession number EQ963472 (Nierman et al. 2015). The genome is predicted to contain 13,485 protein-coding genes and several biosynthetic gene clusters, which could code for more secondary metabolites beyond aflatoxins. The aflatoxin biosynthesis pathway gene cluster, a 70 kb DNA fragment containing 25 genes, has been characterized and annotated in *A. parasiticus* (GenBank accession number AY371490) (Yu et al. 2004).

The biosynthesis pathway of aflatoxins in *A. flavus,* as shown in Figure 2.2, is facilitated by the enzymes encoded by the genes *aflA-aflQ,* while the other genes in the biosynthesis cluster play other roles related to the production of aflatoxin. Fatty acid synthase α subunit (*aflA*), fatty acid synthase β subunit (*aflB),* and polyketide synthase (*aflC*) are involved in the first step of aflatoxin biosynthesis, the conversion of acetate to norsolorinic acid (NOR). The reduction of NOR to averantin (AVN) is carried out by a reductase (*alfD*), NOR-reductase (*alfE*), and a dehydrogenase (*alfF*). A hydroxyl group is added to AVN by a cytochrome P450 monooxygenase (*alfG*) to produce 5'-hydroxyaverantin (HAVN). HAVN is then converted to averufin (AVF) via one of two intermediates: oxoaverantin (OAVN) by an alcohol dehydrogenase (*aflH*) or averufanin (AVNN). AVF is then acted upon by an oxidase (*aflI*) to form versiconal hemiacetal acetate (VHA). VHA is converted to versiconal (VAL) by an esterase (*aflJ*). VERB synthase (*aflK*) converts VAL to versicolorin B (VERB), and a desaturase (*aflL*) converts VERB to versicolorin A (VERA). Both a dehydrogenase (*aflM*) and a monooxygenase (*aflN*) conduct the production of demethylsterigmatocystin (DMST). At this juncture,

dihydrodemethylsterigomatocystin (DHDMST) is also produced from VERA. *O*-methyltransferase B (*aflO*) converts DMST to sterigmatocystin (ST) and DHDMST to dihydrosterigmatocystin (DHST). *O*-methyltransferase A (*aflP*) converts ST to *O*-methylsterigmatocystin (OMST) and DHST to *O*-methyl-dihydrosterigmatocystin (DHOMST). An oxidoreductase (*aflQ*) catalyzes the final reaction of OMST to either aflatoxin B1 or G1 and the final reaction of DHOMST to either aflatoxin B2 or G2. Other genes from the cluster with known functions related to aflatoxin biosynthesis are *aflR* and *aflS*, which encode a transcription activator and transcription enhancer, respectively, that regulate the pathway.

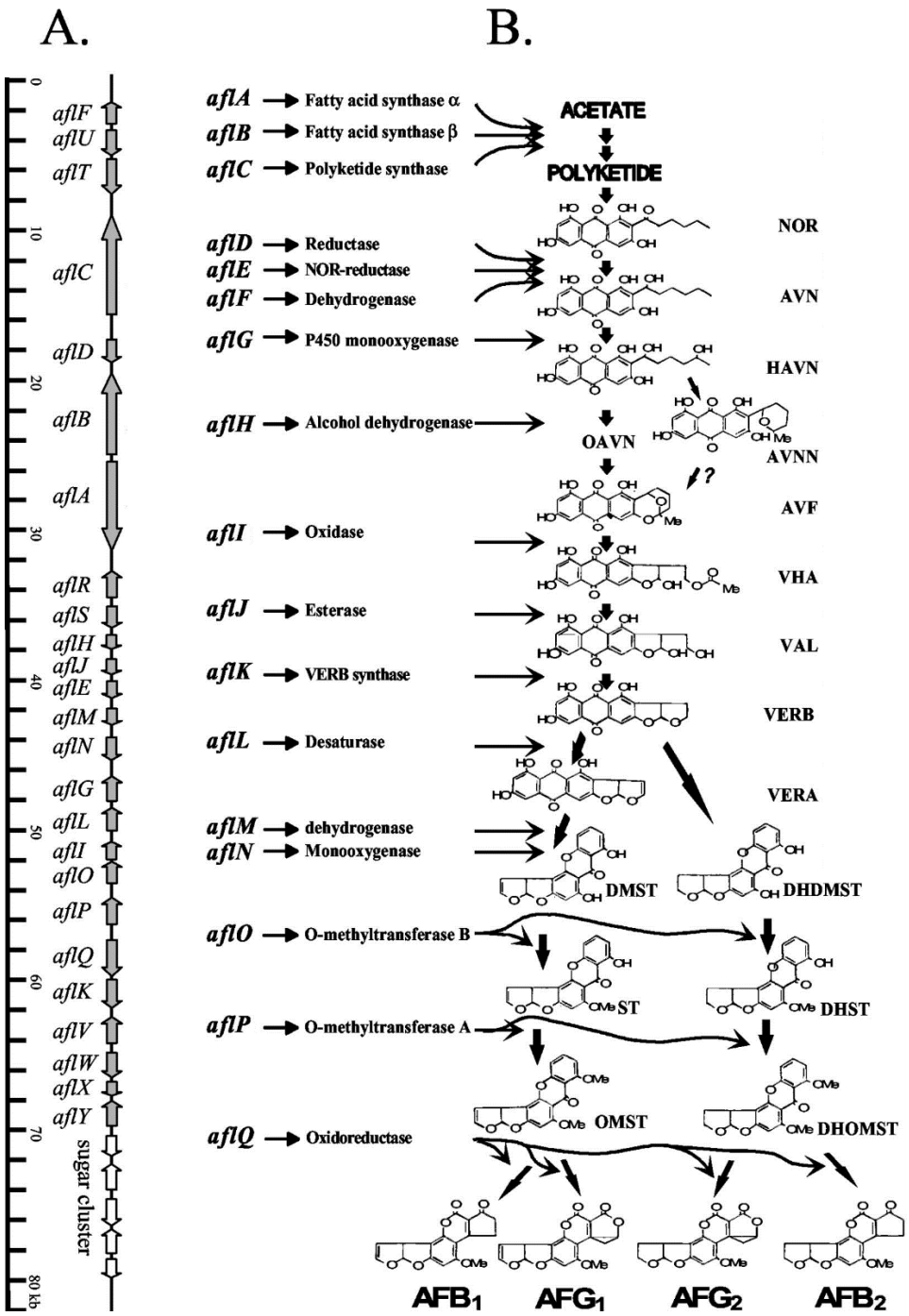

Figure 2.2 Aflatoxin biosynthesis pathway gene cluster and illustrated biosynthesis pathway

(A) Aflatoxin biosynthesis pathway gene cluster including the sugar cluster in *A. parasiticus* and *A. flavus*. Arrows indicate the direction of gene transcription. (B) Aflatoxin biosynthesis pathway with gene names, corresponding enzymes, and biosynthesis steps they catalyze. Modified from Yu et al. (2004).

Some other strains of *A. flavus* have been isolated, and they do not produce aflatoxins at all. The nonaflatoxigenic strain NRRL 21882 lacks the genes in the aflatoxin gene cluster beginning with the *aflB* gene (Amaike and Keller 2011). This strain was isolated from a peanut plant (Abbas et al. 2011), and it is marketed as Afla-Guard, which is often used as a competitive inhibitor for aflatoxigenic strains of *A. flavus* (Amaike and Keller 2011). It has been shown that co-inoculation of maize with the strain NRRL 21882 can significantly reduce aflatoxin accumulation in maize (Mylroie et al. 2016).

Zea mays

Maize (*Zea mays*), originated in Mexico, where it was first domesticated from the grass teosinte about 9000 years ago (Xiao et al. 2017; Schnable et al. 2009). Its genome has been duplicated several times via long terminal repeat retrotransposons, and nearly 85% of the genome is made up of transposable elements (Schnable et al. 2009). The 2.3 Gb genome of the maize inbred line B73 was sequenced through the combined effort of the National Science Foundation, the US Department of Agriculture, and the Department of Energy using the bacterial artificial chromosome (BAC) approach and Roche 454 WGS reads to improve coverage (Schnable et al. 2009; Law et al. 2015).

Maize is one of three major food crops in the world, with 883 million tons produced in 2011 (Farfan et al. 2015). Most of the maize grown worldwide is produced in temperate regions, where the yield is the highest; however, a portion of maize is also grown in sub-tropical regions of the world, where the crop is more susceptible to drought stress and *Aspergillus flavus* infection (Farfan et al. 2015). About 9% of US-grown maize is grown in the southeastern states, including Mississippi, which have a sub-tropical climate (Farfan et al. 2015).

The infection of maize by *A. flavus* typically begins in the ear through the silk at the top when it becomes a honey-brown color. Alternatively, infection can occur at damage sites (Smart et al. 1990; Luo et al. 2009). Microscopic analysis has shown that the fungus can colonize spikelets (see Figure 2.3) through the junction of the glumes and rachilla or through the air space between the rachis and spikelets. Subsequently, *A. flavus* can penetrate the kernel through the rachilla (Smart et al. 1990; Luo et al. 2009).

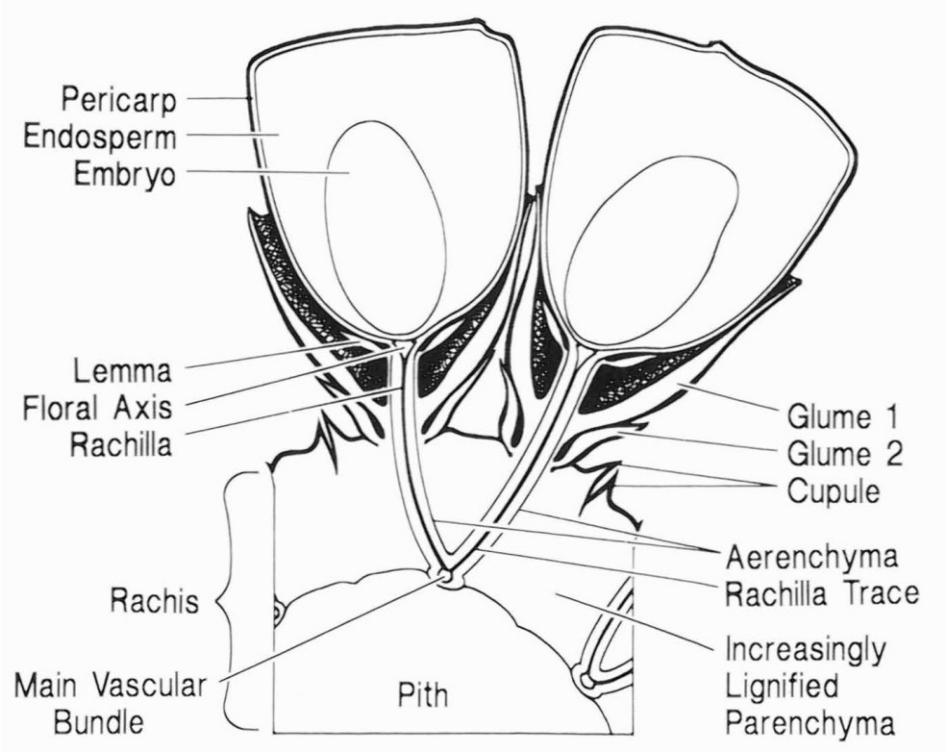

Figure 2.3 Maize kernels in spikelet pair

Image taken from Smart et al. (1990). Some structures have been omitted from the illustration.

Maize Resistance to *A. flavus* and Aflatoxin Production

Research has been conducted to study the mechanisms of maize resistance to *A. flavus* and aflatoxin production (Warburton and Williams 2014). Resistant maize inbred

lines have been produced, and analysis of resistance has been conducted at the physical and molecular level. There are physical and chemical barriers to *A. flavus* infection of the maize kernel. The pericarp and aleurone layers present a physical barrier that *A. flavus* must break through, and certain resistant lines have been shown to increase the production of certain chemicals at the pericarp which inhibit *A. flavus* (Luo et al. 2009). Furthermore, several comparative protein analyses of maize kernels have collectively identified resistance-associated proteins, including antifungal proteins and stress-related proteins, such as chitinases, catalases, and trypsin inhibitors (Luo et al. 2009). Maize silk has also been analyzed for resistance-associated proteins, and chitinases (PRm3 chitinase, chitinase 1, and chitinase A) were shown to have higher activity in resistant maize than in susceptible maize silks (Peethambaran et al. 2010).

Maize genome analysis has identified a variety of genes relevant to maize response to *A. flavus* infection. Information about resistance at the genetic level can inform and improve breeding techniques. Genome-wide association studies (GWAS) have made it possible to identify quantitative trait loci (QTLs), which map the genes that cause certain traits, as well as the location of the genes (Xiao et al. 2017). Microarray analysis has also been used to compare resistant and susceptible maize lines, with some results further validating of known QTLs (Kelley et al. 2009; Shan and Williams 2014). RT-qPCR expression data has been used, along with a computational analysis pipeline, to determine the relationships and potential significance of RNA transport pathway genes in *A. flavus* resistance (Asters et al. 2014; Shan and Williams 2014).

Resistant inbred lines have been developed using phenotypic and genotypic knowledge of resistance, but there are certain complications such as the resistance can be

linked to the growing environment and the plants do not produce as high yields as commercial maize lines (Warburton and Williams 2014). Several resistant maize inbred lines including Mp313e, Mp420, Mp715, Mp717, and Mp719 have been developed at the USDA ARS laboratory located at Mississippi State University. The maize line Mp719, used in these experiments, is a cross between Mp715 and Va35, a susceptible line (Williams and Windham 2012). The lineage of Mp719 can be tracked back to Tuxpan, which is derived from Tuxpeño, one of the most productive and successful corn lines from Mexico (Shan and Williams 2014).

Another option for combating *A. flavus* and aflatoxins is genetic modification. A transgenic maize had been produced that had a gene cassette for RNA interference, which targeted the *aflC* gene (Thakare et al. 2017). The *alfC* gene encodes a polyketide synthase that is important in the first steps of aflatoxin biosynthesis. Following infection with *A. flavus*, the transgenic kernels accumulated no aflatoxin, demonstrating the successful host-induced gene silencing of *A. flavus* (Thakare et al. 2017).

Another avenue for maize resistance lies in microRNAs (miRNAs). There is increasing evidence of the role of miRNAs in plant response to abiotic and biotic stresses via their ability to affect gene expression (Kulcheski et al. 2011; Baldrich et al. 2015). In soybeans, miRNAs have been shown to respond to both drought stress and fungal infection by *Phakopsora pachyrhizi* which causes Asian soybean rust, with most miRNAs being down-regulated in infected susceptible plants, but unaffected in resistant plants (Kulcheski et al. 2011). Rice miRNAs have been shown to regulate gene expression in different tissues in response to fungal infection by *Magnaporthe oryzae,* the

cause of rice blast (Baldrich et al. 2015). The role of miRNAs in maize in response to *A. flavus* infection is not yet known.

microRNAs and microRNA-like RNAs

microRNAs (miRNAs) are small, non-coding RNAs that range from ~18-24 nucleotides, and they play important roles in post-transcriptional modification. They are found in plants and animals. microRNA-like RNAs (milRNAs) have recently been found in fungi. Both miRNAs and milRNAs have been shown to play roles in controlling growth and development, response to stressors, and possibly regulation of gene expression (Huntley et al. 2016; Zhang et al. 2014). Two miRNAs, lin-4 and let-7, were first found in the nematode *Caenorhabditis elegans*, and they were involved in the control of developmental timing of the organism (Axtell et al. 2011). miRNAs and milRNAs represent a diverse and controlled system for post-transcriptional control in plants, animals, and fungi. Currently the microRNA database, miRBase, contains more than 48,000 mature miRNA sequences from 271 species, but does not include fungal milRNAs (Kozomara and Griffiths-Jones 2014).

Plant microRNAs

In plants, miRNAs act as guides for mRNA cleavage or translational repression (Axtell et al. 2011; Eldem et al. 2013; Rogers and Chen 2013; Borges and Martienssen 2016). The miRNA gene is transcribed by RNA polymerase II to form a pri-miRNA (Figure 2.4) containing a hairpin with extended sequences on either end, to the 5’ cap and 3’ poly-A tail. The hairpin undergoes further processing by a RNase III Dicer-like protein (DCL1), in a conjunction with RNA-binding proteins DAWDLE (DDL), TOUGH

(TGH), SERRATE (SE), HYPONASTIC LEAVES1 (HYL1), CAP BINDING COMPLEX PROTEIN 20 (CBP20), and CAP BINDING COMPLEX PROTEIN 80 (CBP80) to produce a pre-miRNA hairpin with a 3' overhang. DDL, TGH, SE, and HYL1 have been shown to play a role in stabilizing the system to ensure that DCL1 can accurately and efficiently generate the pre-miRNA (Rogers and Chen 2013). This hairpin is then further cleaved to remove the loop and produce a double-stranded complex (miRNA/miRNA*), and the 3' end of miRNA in the complex is 2'-O-methylated by HEN1 to produce the mature miRNA sequence that is protected from degradation (Axtell et al. 2011; Eldem et al. 2013; Rogers and Chen 2013). The miRNA/miRNA* duplex leaves the nucleus, exported by HASTY (HST), and then becomes a part of RISC (RNA-induced silencing complex) bound to an Argonaute (AGO) protein (Axtell et al. 2011; Eldem et al. 2013; Rogers and Chen 2013; Borges and Martienssen 2016). The AGO-bound complex uses the sense miRNA strand as a guide and seeks its transcriptional target for splicing or inhibition. In order to bind the mRNA target, the sequence of the miRNA must have a perfect or near-perfect complementarity (Axtell et al. 2011). By and large, plant miRNAs mediate mRNA cleavage; however, some miRNAs will not cleave the transcript, but bind mRNA to block its translation (Axtell et al. 2011; Eldem et al. 2013; Rogers and Chen 2013). Alternatively, a complex with AGO4 has been shown to modify its target gene by methylation to prevent transcription altogether (Rogers and Chen 2013).

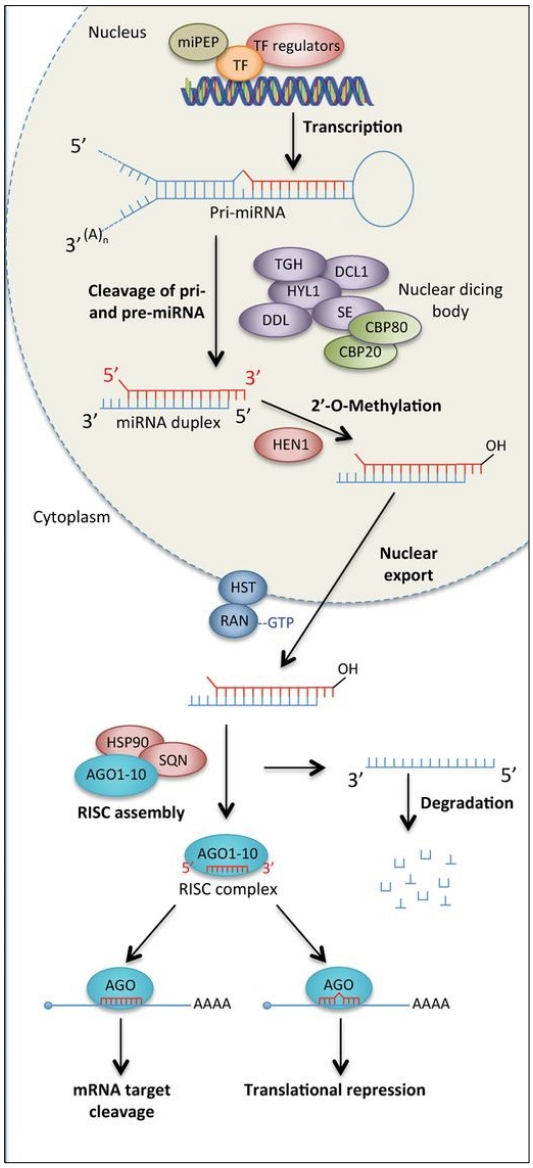

Figure 2.4 Plant miRNA biosynthesis pathway

Retrieved from Huntley et al. (2016).

The proteins involved in miRNA cleavage are highly conserved, and in general this is how miRNAs are produced in the cell; however, some variations do exist, especially between plants and animals (Eldem et al. 2013). In plants, miRNA genes are transcribed almost exclusively from non-protein coding regions and are variable in size

from 70 to hundreds of nucleotides (Axtell et al. 2011). Plant miRNAs also must have nearly perfect complementarity to the mRNA sequence target (Axtell et al. 2011). There is also some variation in the biosynthesis pathways for some plant miRNAs, in which the larger, proto-miRNAs, which make less precise hairpins, are processed by other Dicer-like proteins, namely DCL2, -3, and -4 (Axtell et al. 2011).

Z. mays microRNAs

There are 325 mature *Z. mays* miRNA sequences annotated in miRBase (Kozomara and Griffiths-Jones 2014). They are found on all maize chromosomes and are expressed in various tissues (Zhang et al. 2009). Maize miRNAs have been predicted to predominantly target transcription factors as well as proteins related to physiological and metabolic processes, including growth and development as well as in stress response (Zhang et al. 2009; Zhang et al. 2006). The role of maize miRNAs in response to *A. flavus* infection or aflatoxin production has not been explored.

Fungal microRNA-like RNAs

Fungi utilize a variety of RNA silencing techniques, including quelling, meiotic silencing by unrepaired DNA (MSUD), and repeat-induced point mutation (RIP) (Chen et al. 2014; Lee et al. 2010). Recently, it was discovered that some fungi, such as the filamentous fungus *Neurospora crassa,* also produce miRNA-like RNAs (milRNAs) (Chen et al. 2014; Lee et al. 2010; Lau et al. 2013). These milRNA molecules, however, are not produced by all fungi; for instance, *Saccharomyces cerevisiae*, lacks the proteins necessary to produce milRNAs (Chen et al. 2014). Fungal milRNAs do not have the same characteristics as plant or animal miRNAs, suggesting that they cannot be predicted using

the same methods (Chen et al. 2014). Overall, there are four different mechanisms of milRNA biosynthesis, and one of the mechanisms is similar to plant miRNA biosynthesis and utilizes only Dicer-like proteins, which are homologous to those used by plants and animals (Lee et al. 2010). Two others utilize a combination of a Dicer-like protein, an AGO protein QDE-2 (QUELLING DEFICIENT-2), an exonuclease QIP, and an RNAse III domain-containing protein (MRPL3). Another mechanism of biogenesis is Dicer-independent and only utilizes the QDE-2 (Lee et al. 2010). milRNAs also seem to play similar roles as miRNAs, in that they affect growth and development by their specialization in different growth stages of the fungus (Lau et al. 2013). Plant and animal miRNAs are separated into families, which are not shared between the kingdoms. In the same way, fungal milRNAs are not similar to the miRNAs in plants or animals (Chen et al. 2014). It has been hypothesized that the miRNA regulatory mechanism was present before the divergence of fungi, plants, and animals (Lee et al. 2010).

A. flavus microRNA-like RNAs

Fungal microRNA-like RNAs have not been annotated and deposited in miRBase (Kozomara and Griffiths-Jones 2014). Using computational and molecular methods, 135 milRNA sequences were predicted and identified in the *A. flavus* NRRL 3357 strain grown *in vitro* under aflatoxin production conditions: water activity (99% and 93%) and temperature (28°C and 37°C) (Bai et al. 2015). Of these, four of the milRNAs (Afl-milR-3, -33, -19, and -107) showed differential expression under different temperature or water activity conditions. Half of the *A. flavus* milRNA sequences identified were computationally targeted to mRNA targets. Of the differentially expressed milRNAs, Afl-mir-3 had 2 and Afl-mir-33 had 3 predicted targets. All but one of these predicted targets

were uncharacterized proteins. The single target, predicted for Afl-mir-33, was the *ustA* gene, which encodes the peptide precursor for a secondary metabolite called ustiloxin B (Umemura et al. 2014). This indicates that milRNAs may play a role in regulating secondary metabolism biosynthesis pathways in *A. flavus*, including the aflatoxin biosynthesis pathway.

CHAPTER III

MATERIALS AND METHODS

Inoculation and Collection of Plant Materials

The maize lines, Mp719 and Va35, were planted in a randomized complete block design with three replications at the R.R. Foil Plant Research Center at Mississippi State University. The ears were self-pollinated and inoculated 18 days after pollination with either the *A. flavus* NRRL 3357, *A. flavus* NRRL 21882, or water, or not inoculated as a control. The inoculum of the two *A. flavus* strains was grown on 50 g of sterile corn cob grits (size 2040, Grit-O-Cobs) with 100 mL of sterile distilled water in 500 mL flasks and incubated at 28°C for 21 days. Conidial spores were obtained by washing the grits with a mixture of 500 mL of sterile distilled H_2O and 0.1% Tween 20 and then filtering the liquid through four layers of cheese cloth. Conidial concentration was calculated using a hemocytometer and the final inoculum concentration was diluted to $9x10^7$ conidia/mL with sterile distilled water. Inoculation was performed by peeling back the husk and injuring the maize kernels with a size of 12 quilting needle (Entaco Limited) dipped in the appropriate inoculum or sterile distilled water. The inoculation was done by alternating 2 rows inoculated and 2 rows uninoculated around the entire ear. After inoculation, the husk was placed back around the ear and 2 shoot bags were secured around the ear with rubber bands. Maize ears were collected 7 days after inoculation and both inoculated and uninoculated kernels were removed from the ears and flash frozen in

liquid nitrogen for subsequent small RNA extractions. Kernels were collected for each of the two maize inbred lines inoculated with *A. flavus* strain NRRL 3357, *A. flavus* strain NRRL 21882, water, and non-inoculated control plants with three replicates of each for a total of 24 unique samples.

Small RNA Extraction

Small RNAs were extracted from the 24 samples using the method of Rosas-Cárdenas et al. (2011) and further purified with the Sigma-Aldrich mirPremier miRNA Isolation Kit for small RNA isolation from plant tissues. A single kernel (0.9-1.0 g) of each sample was ground to fine powder using a mortar and pestle with liquid nitrogen, placed into a 1.5 ml microcentrifuge tube, and kept on ice. To each tube, 500 µl of lithium chloride extraction buffer (100 mM Tris-HCl, pH 9.0, 1% SDS, 100 mM LiCl, 10 mM EDTA) and 500 µl of phenol (pH 8.0) were added. Each sample was mixed, incubated for 5 minutes at 60°C in a water bath, and centrifuged for 10 minutes in a microcentrifuge (Eppendorf 5415D) at 16.1×10^3 RCF. The upper phase was transferred to a new tube containing 600 µl of chloroform-isoamyl alcohol (24:1), mixed, and centrifuged for 10 minutes. The upper phase was transferred to a new tube and incubated for 15 minutes in a 65°C water bath. Following the incubation, 50 µl of 5 M NaCl and 63 µl of 40% PEG 8000 were added, and each sample was mixed, incubated on ice for 30 minutes, and then centrifuged for 10 minutes. The supernatant was transferred to a new 1.5 ml microcentrifuge tube, and 500 µl of phenol-chloroform-isoamyl alcohol (24:1:1) were added to the tube and then mixed. Samples were centrifuged for 10 minutes, and the supernatant was transferred to a new microcentrifuge tube containing 50 µl of 3 M

sodium acetate (pH 5.2) and 1.2 ml 96 % ethanol. The sample was mixed and incubated overnight at -20°C.

After overnight incubation, each sample was centrifuged for 10 minutes. The supernatant was discarded, and the pellet was freeze-dried (Labconco Freeze Dry System and Savant SpeedVac Concentrator). The pellet was resuspended in 50 µl of DEPC-treated water, and an aliquot was taken for later quality analysis. A lysis mix was made by mixing 650 µl of microRNA Lysis Buffer (M1070), 300 µl of Binding Solution (L8042), 50 µl of 96% ethanol, and 10 µl of 2-mercaptoethanol per sample. The lysis mix of 750 µl was added to each sample, and samples were mixed, incubated for 5 minutes in a 55°C water bath, and centrifuged for 5 minutes. The supernatant was added to a filter column (C6866) and centrifuged for 1 minute. The volume of the filtrate was measured with a pipette, and 1.1 volumes of 96% ethanol was added, and the solution was mixed. This mixture, in two portions, was added to a binding column (C6991) and centrifuged for 30 seconds. The column was sequentially washed with 700 µl of 96% ethanol and 500 µl of Binding Solution by centrifugation for 30 seconds and 1 minute, respectively. The column was then washed twice with 500 µl of Wash Solution 2 (W3261) by centrifugation for 30 seconds. The column was further centrifuged for 1 minute to remove any residual solution. An Elution Solution (E8024) of 50 µl was added to the column, incubated for 1 minute at room temperature, and centrifuged for 1 minute. The concentration of eluted RNA samples was determined using the NanoDrop 2000c Spectrophotometer (ThermoFisher) and the RNA quality was checked by electrophoresis on a 1% agarose gel. The isolated RNA was stored at -80°C.

Construction of cDNA Libraries

The purified small RNA samples were used for preparation of cDNA libraries using the NEBNext Multiplex Small RNA Sample Prep Set for Illumina. The concentration of RNA samples was determined by the Qubit Fluorometer (ThermoFisher) with the Qubit MicroRNA Assay Kit and RNA quality was analyzed by the Agilent BioAnalyzer 2100 with the Small RNA Kit. The 3' SR adaptor was ligated to 150 ng of the small RNAs, and the SR RT primer was hybridized to all 3' adaptors, including those that were not bound to small RNAs. This forced the 5' SR adaptor to ligate only to the small RNAs, but not to any excess 3' adaptors. After ligation of the 5' adaptor, the ligated RNA was reverse transcribed to form cDNA and further amplified by PCR with the SR primer and the appropriate Index primer (1-24).

The PCR product was purified using the QIAQuick PCR Purification Kit (Qiagen) according to the manufacturer's instructions and eluted with 27.5 µl of nuclease-free water. The purified product was mixed with 32.5 µl (1.3X) of resuspended AMPure XP beads and incubated at room temperature. The samples were placed on a magnetic stand to separate the beads from the supernatant. The clear supernatant was transferred to a new tube, and 92.5 µl of fresh beads were added and incubated. The final supernatant was analyzed with the Agilent DNA 1000 Kit for the BioAnalyzer and the Qubit dsDNA HS Kit. The library samples were stored at -20°C until being prepared for pooling. Each sample was diluted to 20 nM using the concentration determined by the Qubit and the average library size from the BioAnalyzer. Samples were diluted in EB Buffer (10 mM Tris-HCl, pH 8.5) with 0.1% Tween-20 and pooled for sequencing. The sequences of all adaptors and primers used for library construction are listed in Table 3.1.

Table 3.1 Primers and adaptors used in the construction of miRNA libraries

Primer ID	Sequence
3’ SR Adaptor	5'-rAppAGATCGGAAGAGCACACGTCT-NH_2-3'
SR Primer	5'-AATGATACGGCGACCACCGAGATCTA CACGTTCAGAGTTCTACAGTCCG-s-A-3'
5’ SR Adaptor	5'-rGrUrUrCrArGrArGrUrUrCrUrA rCrArGrUrCrCrGrArCrGrArUrC-3'
SR RT Primer	5'-AGACGTGTGCTCTTCCGATCT-3'
Index Primer	5'-CAAGCAGAAGACGGCATACGAGAT**CGTGAT**GT GACTGGAGTTCAGACGTGTGCTCTTCCGATC-s-T-3'

Bold underlined section represents index. All indices are listed in Table 4.2.

Library Sequencing and Data Analysis

The 24 sample libraries were loaded to a single flow cell and single-end (1x50) sequenced on the Illumina HiSeq 4000 System. Adapters were trimmed and all sequences with length less than 18 bp were removed. Two samples were removed from further analysis as outliers when compared with other samples’ length distribution and alignment to the *A. flavus* NRRL 3357 genome.

By using trimmed reads from infected samples, MIREAP (https://sourceforge.net/projects/mireap/) predicted 236 hypothetical *A. flavus* milRNAs. These were combined with the 135 known *A. flavus* milRNAs from Bai et al. (2015) to generate 371 milRNAs. One hypothetical milRNA was found to overlap with a known milRNA (Afl-milR-96) and was removed to leave a total of 370 milRNAs. These were filtered against the Rfam database (http://rfam.xfam.org/) to eliminate any overlap with other RNA sources (mRNA, tRNA, rRNA, etc.) and 255 (180 hypothetical and 75 known) were removed. The remaining 115 milRNAs were used for the downstream analysis.

miRDeep-P (https://sourceforge.net/projects/mirdp/) was used to analyze trimmed reads, and it predicted 634 novel Maize miRNAs. Briefly, the trimmed reads were mapped to the maize B73 genome using Bowtie (http://bowtie-bio.sourceforge.net/index.shtml) and filtered using the Rfam database (http://rfam.xfam.org/) to eliminate any overlap with other RNA sources (mRNA, tRNA, rRNA, etc.). miRNA precursors were created from overlapping alignments, but any RNA with sizes longer than 280 bp were removed. The precursors were folded using RNAfold (https://www.tbi.univie.ac.at/RNA/index.html), and the reads from the RNA-seq were aligned to them. miRDeep-P was used to call miRNAs from the generated data. The known *Z. mays* miRNAs from miRbase were combined with the hypothetical 634 miRNAs for a total of 924 miRNAs.

The milRNA and miRNA target prediction was performed by miRanda (http://cbio.mskcc.org/miRNA2003/miranda.html). Since neither of the genomes in NCBI (*A. flavus* NRRL 3357 genome and *Z. mays* B73 genome) contain information about UTRs, the 500-bp on either side of the gene were added as artificial 5`-UTRs and 3`-UTRs. Psuedogenes and other non-coding RNA were removed before target prediction. The predicted targets were then filtered based on the six criteria as described by Bai *et al.* (2015) for both milRNAs and miRNAs: (1) No more than four mismatches between the milRNA and target (G-U bases count as 0.5 mismatches); (2) No more than two adjacent mismatches in the milRNA/target duplex; (3) No adjacent mismatches in positions 2–12 of the milRNA/target duplex (5′ of milRNA); (4) No mismatches in positions 10–11 of milRNA/target duplex; (5) No more than 2.5 mismatches in positions 1–12 of the milRNA/target duplex (5′ of milRNA); and (6) Minimum free energy (MFE)

of the milRNA/target duplex should be ≥75% of the MFE of the milRNA bound to its perfect complement.

The trimmed data were also aligned to the mature milRNA or miRNA sequences using BWA (http://bio-bwa.sourceforge.net/). Any mature milRNA or miRNA sequence without alignments in at least 3 of the 24 samples was removed, leaving 69 milRNAs and 691 miRNAs. The variance of milRNAs and miRNAs between infection groups was visualized in PCA (principal component analysis) plots. The RNA-seq data analysis software, edgeR (https://bioconductor.org/biocLite.R), was used to determine differential expression of these milRNAs and miRNAs, and gplots (https://cran.r-project.org/web/packages/gplots/index.html) and RColorBrewer (https://cran.r-project.org/web/packages/RColorBrewer/index.html) were used to visualize the differential expression.

RT-qPCR

The RT-qPCR assay was used to determine the expression of the 135 milRNAs identified by Bai et al. (2015). The Mir-X miRNA First-Strand Synthesis and SYBR qRT-PCR kits (Clontech) were used to first convert the milRNA into cDNA which was then quantified by RT-qPCR analysis. A 3.75 µl of mixture containing 500 µg of the small RNA sample and nuclease-free water was mixed with 5 µl of mRQ Buffer (2X) and 1.25 µl of mRQ Enzyme containing Poly(A) Polymerase and MMLV Reverse Transcriptase, and then incubated for 1 hour at 37°C. After the reverse transcription reaction, the mRQ Enzyme was inactivated at 85°C for 5 minutes. The 10 µl cDNA

sample was subsequently diluted with 90 µl of ddH_2O and used as DNA template for qPCR amplification.

PCR reactions with each sample containing 4.5 µl sterile double-distilled H_2O, 6.25 µl SYBR Advantage Premix (2X), 0.25 µl ROX dye (50X), 0.25 µl (10 µM) mRQ 3' primer, 0.25 µl (10 µl) miRNA-specific 5' primer, and 1 µl cDNA were performed on the QuantStudio 5 Real-Time PCR System (Applied Biosystems) according to the following protocol: 95°C denaturation for 10 seconds, 40 cycles at 95°C for 5 seconds and at 60°C for 20 seconds, and following by melt curve analysis at 95°C for 15 seconds, 60°C for 1 minute, and 95°C for 15 seconds. The miRNA-specific primers are listed in Table A.1. The U6 forward and reverse primers from the Clontech kit were used as an internal control for sample normalization with the delta-delta C_t method (Livak and Schmittgen 2001).

CHAPTER IV

RESULTS

Preparation of Small RNAs and cDNA Libraries

Concentrations of the isolated small RNA samples were determined using the Nanodrop Spectrophotometer and Qubit Fluorometer and are presented in Table 4.1. The representative analysis of a small RNA sample by BioAnalyzer is shown in Figure 4.1. The concentration and the size analysis of the small RNA samples by the BioAnalyzer indicated that they were appropriate for the preparation of cDNA libraries. There is a large difference in the concentration determined between the Nanodrop and Qubit methods, as well as a wide range of concentration differences among samples, including within experimental groups. The BioAnalyzer results also identified the presence of a wide range of miRNA percentages as well, from as low as 20% in a control sample to 80% in an infected sample, with concentrations ranging from ~9 to 80 ng/µl of miRNA-sized sequences.

Table 4.1 Concentrations of small RNAs determined by NanoDrop Spectrophotometer and Qubit Fluorometer

Sample	Conc (ng/ul) determined by NanoDrop	Conc (ng/µl) determined by Qubit
Mp719-3357-1	563.2	74.6
Mp719-3357-2	534.2	68.1
Mp719-3357-3	460.4	55.4
Mp719-21882-1	200.8	91.7
Mp719-21882-2	236.8	95.3
Mp719-21882-3	163.4	77.6
Mp719-H_2O-1	128.6	25.9
Mp719-H_2O-2	130.3	33.8
Mp719-H_2O-3	419.2	67.6
Mp719-Control-1	84.9	32.6
Mp719-Control-2	123.2	34.2
Mp719-Control-3	92.6	32.4
Va35-3357-1	94.7	31.7
Va35-3357-2	201.0	88.7
Va35-3357-3	129.1	62.1
Va35-21882-1	196.8	80.2
Va35-21882-2	209.9	84.9
Va35-21882-3	126.2	39.2
Va35-H_2O-1	142.4	39.2
Va35-H_2O-2	134.5	37.6
Va35-H_2O-3	133.2	32.2
Va35-Control-1	88.7	26.4
Va35-Control-2	106.2	32.4
Va35-Control-3	155.3	32.7

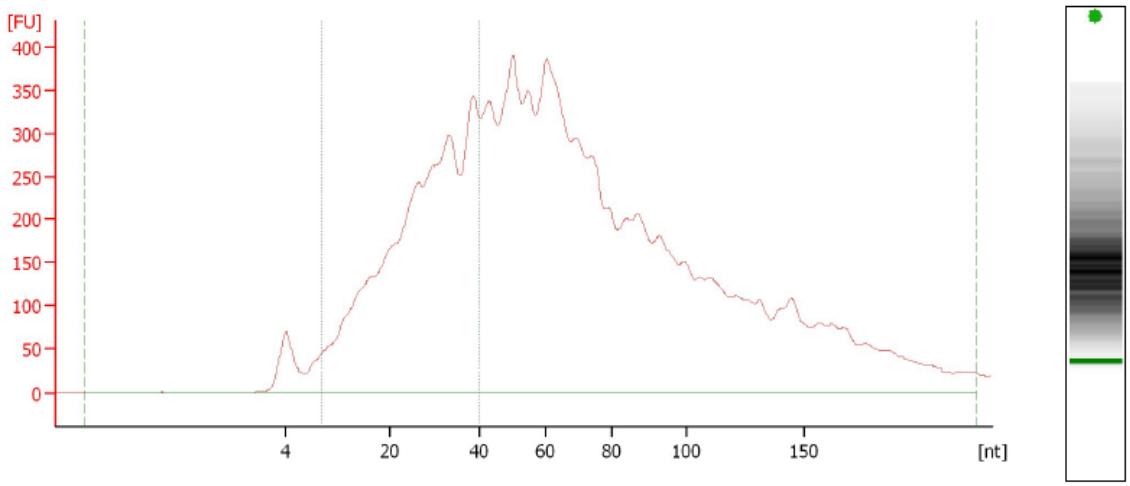

Figure 4.1 Size analysis of the Mp719 21882 replicate 1 small RNA sample

The capillary electrophoresis output (right picture) shows the intensity of small RNAs, which corresponds to the graphical representation (left picture) with intensity ([FU]) as a function of size (nt). The green band represents the marker, which corresponds to the peak at 4 nt. The area between 10 and 40 nt represents the miRNAs which have a concentration of 17,865.2 pg/µl and represents 59% of the sample. The average size in the miRNA range is 27 nt. The Mp719 21882 Replicate 1 sample was analyzed prior to cDNA library preparation.

The concentration of the 24 cDNA libraries determined by the Qubit Fluorometer and the size of the constructed cDNA libraries determined by the BioAnalyzer are presented in Table 4.2. The 24 index sequences assigned to each sample as well as the calculated library concentration in nM are also included in this table. A representative BioAnalyzer analysis of a cDNA library sample before (A) and after (B) size selection by AMPure XP beads is shown in Figure 4.2. There is a wide range of concentration differences between samples, including within the experimental groups. The average size of the constructs is slightly varied, as seen in Figures 4.2A and 4.2B, after treatment by the size selecting AMPure XP beads. The average size of constructed libraries is

relatively the same, between 138-142 nt, and excluding the added 3' and 5' SR Adaptors as well as the primers for library preparation, the average sequence sizes are 20-24 nt.

Table 4.2 The list of 24 cDNA libraries for sequencing with indices, concentrations (determined with Qubit), and average construct sizes

Sample	NEB Index	Index Sequence	Concentration (ng/µl)	Average Construct Size (bp)	Concentration (nM)
Mp719-3357-1	1	ATCACG	3.24	141	34.82
Mp719-3357-2	2	CGATGT	8.58	142	91.55
Mp719-3357-3	3	TTAGGC	7.03	141	75.54
Mp719-21882-1	4	TGACCA	6.63	140	71.75
Mp719-21882-2	5	ACAGTG	12.7	140	137.45
Mp719-21882-3	6	GCCAAT	6.21	141	66.73
Mp719-H_2O-1	7	CAGATC	14.8	141	159.04
Mp719-H_2O-2	8	ACTTGA	13.3	141	142.92
Mp719-H_2O-3	9	GATCAG	15.7	140	169.91
Mp719-Control-1	10	TAGCTT	13.5	140	146.1
Mp719-Control-2	11	GGCTAC	16.1	141	173.01
Mp719-Control-3	12	CTTGTA	10.6	139	115.54
Va35-3357-1	13	AGTCAA	17.1	139	186.40
Va35-3357-2	14	AGTTCC	8.36	141	89.83
Va35-3357-3	15	ATGTCA	10.4	140	112.55
Va35-21882-1	16	CCGTCC	4.29	142	45.77
Va35-21882-2	17	GTAGAG	5.47	141	58.78
Va35-21882-3	18	GTCCGC	3.43	138	37.66
Va35-H_2O-1	19	GTGAAA	7.03	139	76.63
Va35-H_2O-2	20	GTGGCC	6.18	140	66.88
Va35-H_2O-3	21	GTTTCG	3.83	139	41.75
Va35-Control-1	22	CGTACG	9.94	140	107.58
Va35-Control-2	23	GAGTGG	2.42	139	26.38
Va35-Control-3	24	GGTAGC	7.78	140	84.20

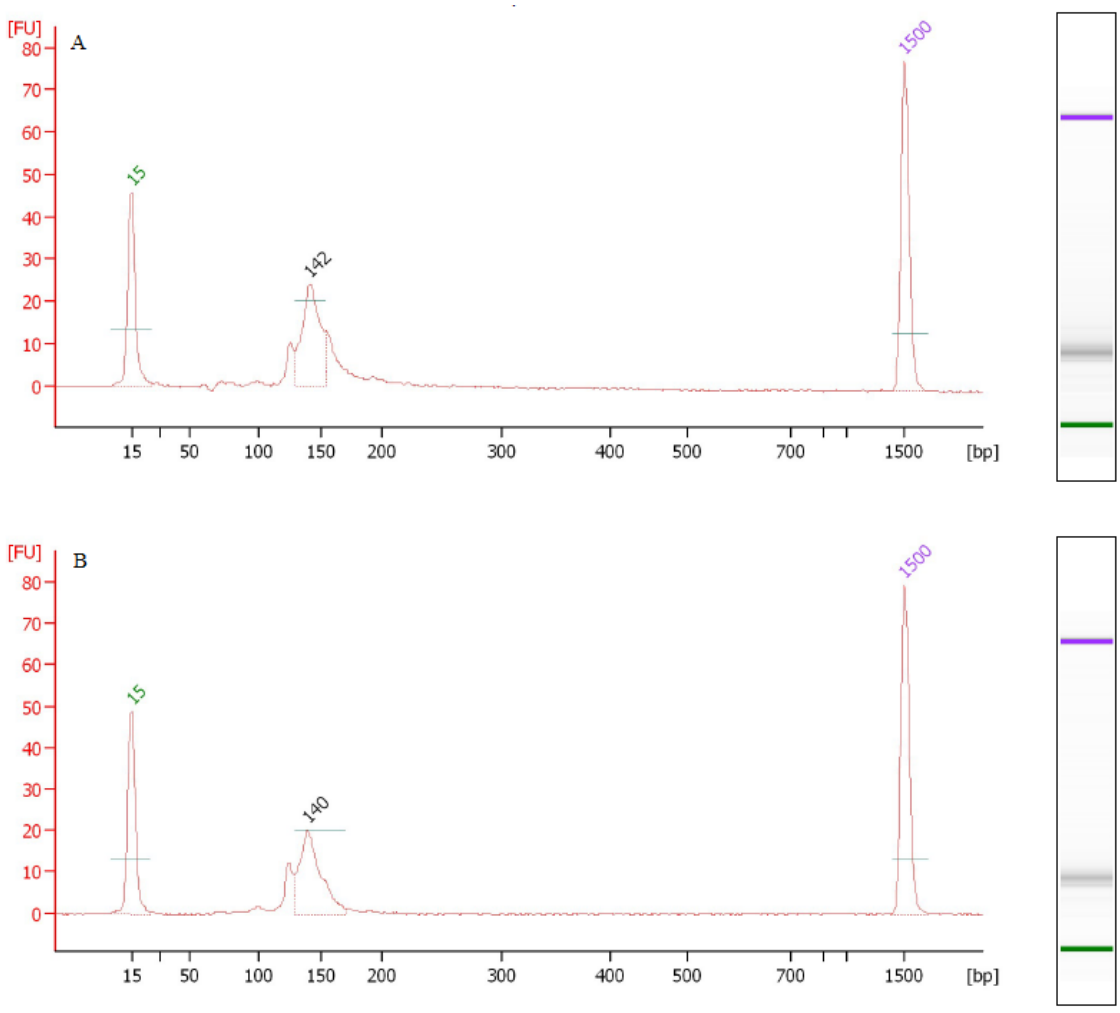

Figure 4.2 Analysis of Mp719 21882 replicate 1 sample by Bioanalyzer DNA 1000 prior to (A) and after (B) AMPure XP bead treatment

The capillary electrophoresis outputs (right picture) show the intensity of DNA relative to size, which corresponds to the graphical representation (left picture) with intensity ([FU]) as a function of size (nt). The green and purple bands represent the lower and upper markers, which correspond to the peaks at 15 and 1500 nt, respectively. Peaks at 142 (A) and 140 (B) represent small RNA samples, which have the concentration of 3.04 ng/µl and 2.91 ng/µl and the molarity of 32.5 nmol/l and 31.5 nmol/l, respectively.

After removal of the adaptors, the sorted reads including the number and percentage that survived or were dropped for being too short are presented in Table 4.3.

There was a wide range of raw reads from each sample, but most of the samples lost

about 1% of the reads due to small size. The length distribution of the sequences and their percentage mapped to the *A. flavus* NRRL 3357 genome are shown in Figure 4.3. Samples marked in red were determined to be outliers, based on both the length distribution patterns and the mapping to the *A. flavus* genome, and those samples were eliminated from further analysis.

Table 4.3 Trimming statistics of small RNA sequence data

Sample	Raw Reads	Surviving	Surviving Percent	Dropped	Dropped Percent
Mp719-3357-1	4,320,210	4,283,116	99.14	37,094	0.85
Mp719-3357-2	8,299,712	8,228,451	99.14	71,261	0.85
Mp719-3357-3	7,077,568	7,015,944	99.12	61,624	0.87
Mp719-21882-1	5,017,257	4,962,542	98.90	54,715	1.09
Mp719-21882-2	6,514,190	6,445,533	98.94	68,657	1.05
Mp719-21882-3	6,364,869	6,298,793	98.96	66,076	1.03
Mp719-H_2O-1	10,062,400	9,983,318	99.21	79,082	0.78
Mp719-H_2O-2	7,754,618	7,694,802	99.22	59,816	0.77
Mp719-H_2O-3	7,233,906	7,167,452	99.08	66,454	0.91
Mp719-Control-1	7,606,729	7,554,896	99.31	51,833	0.68
Mp719-Control-2	7,498,463	7,446,379	99.30	52,084	0.69
Mp719-Control-3	4,812,484	4,777,600	99.27	34,884	0.72
Va35-3357-1	8,321,526	8,256,581	99.21	64,945	0.78
Va35-3357-2	7,729,030	7,649,892	98.97	79,138	1.02
Va35-3357-3	1,512,181	1,497,313	99.01	14,868	0.98
Va35-21882-1	4,739,723	4,694,486	99.04	45,237	0.95
Va35-21882-2	10,097,167	9,985,614	98.89	111,553	1.10
Va35-21882-3	3,395,222	3,365,950	99.13	29,272	0.86
Va35-H_2O-1	6,017,442	5,967,367	99.16	50,075	0.83
Va35-H_2O-2	5,600,116	5,552,970	99.15	47,146	0.84
Va35-H_2O-3	4,518,898	4,481,370	99.16	37,528	0.83
Va35-Control-1	6,193,704	6,157,661	99.41	36,043	0.58
Va35-Control-2	5,255,753	5,211,619	99.16	44,134	0.83
Va35-Control-3	5,411,852	5,371,428	99.25	40,424	0.74

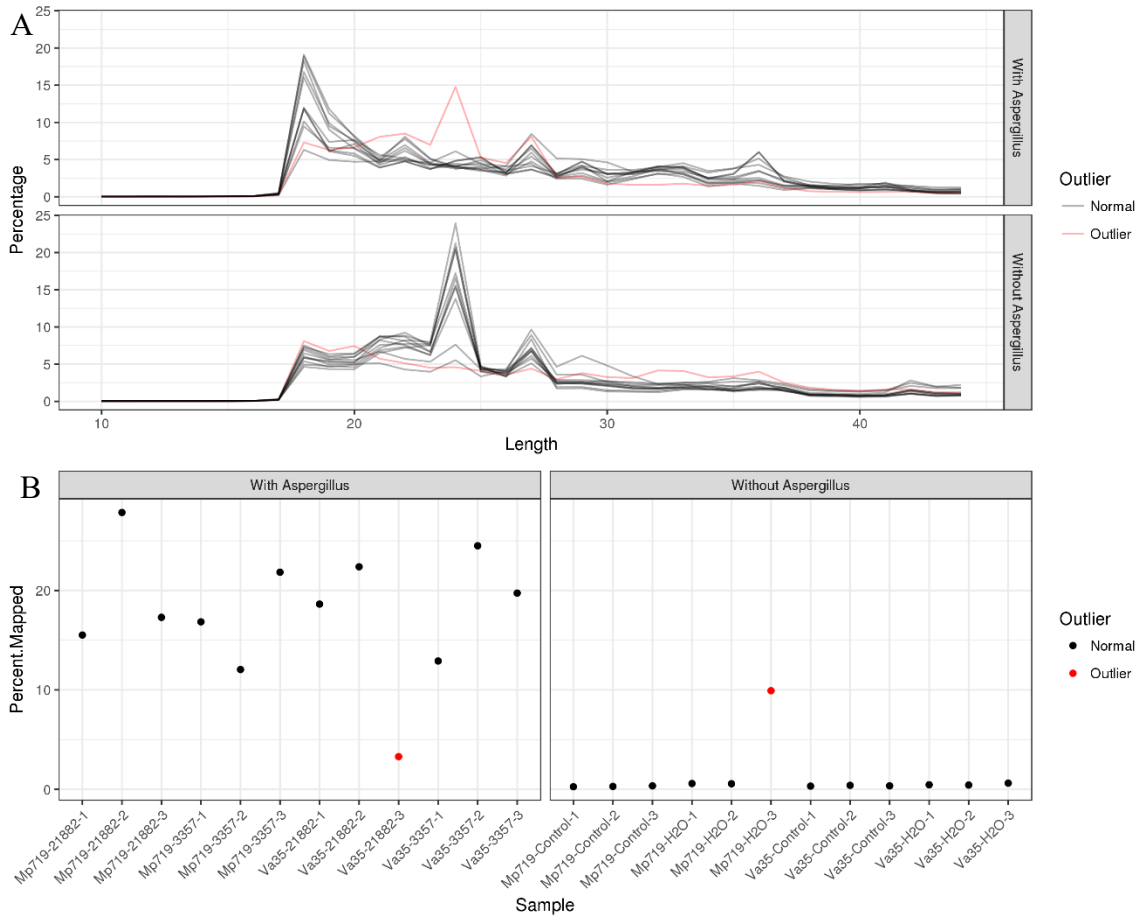

Figure 4.3 Normalized length distribution grouped by *A. flavus*-inoculation status and percentage of reads mapping to the *A. flavus* genome.

The distribution of sequence lengths (A) and percentage of sequences mapped to the *A. flavus* genome (B) in *A. flavus*-inoculated samples on top (A) and left (B) pictures and water-inoculated and control samples on bottom (A) and right (B) pictures, with outlier samples marked with red.

A. flavus milRNAs

From the sequence data, 69 unique *A. flavus* milRNAs were identified by computational analysis, including seven known milRNAs (Afl-milR-2, -3, -7, -9, -33, -43, -92) which were previously described by Bai et al (2015). The secondary structure of one pre-milRNA, All-m0029-3p, as an example was plotted in Figure 4.4. These milRNAs, along with the sequences, and their predicted targets are presented in Table

4.4. A principal component analysis (PCA) plot of the variance among these milRNAs along with water and control samples is shown in Figure 4.5. The plot shows the *A. flavus*-inoculated samples grouping separately from the water and control samples, with some overlap between the NRRL 3357 and NRRL 21882 inoculated samples, and there is no obvious separation based on the maize resistance or susceptibility. The large difference between the *A. flavus*-inoculated and the control samples is probably due to the lack of *A. flavus* milRNA sequences in the control samples.

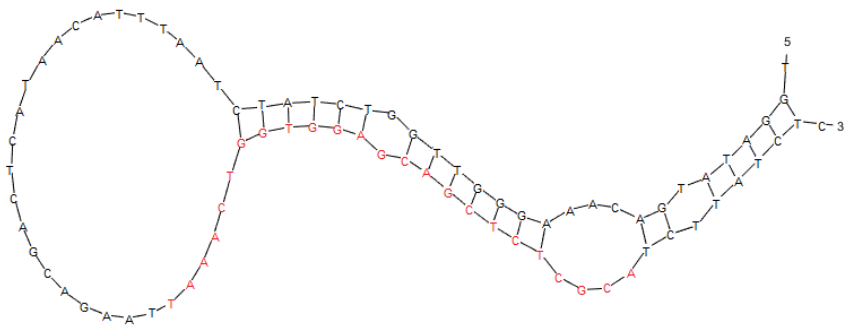

Figure 4.4 Secondary structure of pre-milRNA of All-m0029-3p.

The pre-milRNA has a stem-loop structure and the mature milRNA sequence is marked in red color. The sequence was folded using RNAPlot in MatLab (R2018a).

Table 4.4 *A. flavus* milRNA sequences and their predicted targets

milRNA	Sequence	Target mRNA Accession Number	Target Protein
Afl-milR-2	GGCAAGAUGACCGAGUGGUUA	XM_002375588.1	conserved hypothetical protein
		XM_002375968.1	conserved hypothetical protein
		XM_002379462.1	ZIP metal ion transporter, putative
		XM_002375588.1	conserved hypothetical protein
		XM_002375968.1	conserved hypothetical protein
		XM_002379462.1	ZIP metal ion transporter, putative
		XM_002375588.1	conserved hypothetical protein
		XM_002375968.1	conserved hypothetical protein
		XM_002379462.1	ZIP metal ion transporter, putative
		XM_002375588.1	conserved hypothetical protein
		XM_002375968.1	conserved hypothetical protein
		XM_002379462.1	ZIP metal ion transporter, putative
Afl-milR-3	GGCGAGAUGGCCGAGCGGUCU	XM_002375968.1	conserved hypothetical protein
		XM_002377351.1	conserved hypothetical protein
		XM_002375968.1	conserved hypothetical protein
		XM_002377351.1	conserved hypothetical protein
Afl-milR-7	GUGGGAGGUUGAGUGGGUGGUA	XM_002372832.1	conserved hypothetical protein
		XM_002373498.1	translation repressor/antiviral protein Ski3, putative
		XM_002376998.1	conserved hypothetical protein
		XM_002378919.1	polyubiquitin binding protein (Doa1/Ufd3), putative
		XM_002381083.1	C6 transcription factor (NirA), putative

Table 4.4 (continued)

Afl-milR-7	GUGGGAGGUUGAGUGGGUGGUA	XM_002381258.1	thioredoxin, putative
		XM_002381971.1	DNA damage repair protein Mus42, putative
		XM_002382125.1	mRNA decapping hydrolase, putative
		XM_002382126.1	ubiquitin C-terminal hydrolase L3
		XM_002372832.1	conserved hypothetical protein
		XM_002373498.1	translation repressor/antiviral protein Ski3, putative
		XM_002376998.1	conserved hypothetical protein
		XM_002378919.1	polyubiquitin binding protein (Doa1/Ufd3), putative
		XM_002381083.1	C6 transcription factor (NirA), putative
		XM_002381258.1	thioredoxin, putative
		XM_002381971.1	DNA damage repair protein Mus42, putative
		XM_002382125.1	mRNA decapping hydrolase, putative
		XM_002382126.1	ubiquitin C-terminal hydrolase L3
		XM_002372832.1	conserved hypothetical protein
		XM_002373498.1	translation repressor/antiviral protein Ski3, putative
		XM_002376998.1	conserved hypothetical protein
		XM_002378919.1	polyubiquitin binding protein (Doa1/Ufd3), putative
		XM_002381083.1	C6 transcription factor (NirA), putative
		XM_002381258.1	thioredoxin, putative
		XM_002381971.1	DNA damage repair protein Mus42, putative
		XM_002382125.1	mRNA decapping hydrolase, putative
		XM_002382126.1	ubiquitin C-terminal hydrolase L3
		XM_002372832.1	conserved hypothetical protein
		XM_002373498.1	translation repressor/antiviral protein Ski3, putative
		XM_002376998.1	conserved hypothetical protein
		XM_002378919.1	polyubiquitin binding protein (Doa1/Ufd3), putative
		XM_002381083.1	C6 transcription factor (NirA), putative

Table 4.4 (continued)

Afl-milR-7	GUGGGAGGUUGAGUGGGUGGUA	XM_002381258.1	thioredoxin, putative
		XM_002381971.1	DNA damage repair protein Mus42, putative
		XM_002382125.1	mRNA decapping hydrolase, putative
		XM_002382126.1	ubiquitin C-terminal hydrolase L3
Afl-milR-9	GGCGAGAUGGCCGAGCGGUCC	XM_002375968.1	conserved hypothetical protein
Afl-milR-33	GGCGAGAUGGCCGAGCGGUC	XM_002375968.1	conserved hypothetical protein
		XM_002376366.1	conserved hypothetical protein
		XM_002375968.1	conserved hypothetical protein
		XM_002376366.1	conserved hypothetical protein
		XM_002375968.1	conserved hypothetical protein
		XM_002376366.1	conserved hypothetical protein
Afl-milR-43	CCUAGGACAAGGGCGCACAGAGU		
Afl-milR-92	CGGGGUGGAAUAGGGGGAGGAG	XM_002385089.1	conserved hypothetical protein
		XM_002385527.1	flocculation suppression protein
all-m0002-3p	TTTTGGGGATTTGATCTCACTA	XM_002374476.1	DNA-directed RNA polymerase I, II, and III subunit Rpb6
		XM_002375259.1	mating alpha-pheromone PpgA
		XM_002376700.1	quinone oxidoreductase, putative
		XM_002376701.1	ankyrin repeat protein
		XM_002378314.1	conserved hypothetical protein
		XM_002380032.1	conserved hypothetical protein
all-m0007-5p	ATGGATTTATAGGTCTGTGCAG		
all-m0013-3p	GCAGTCGGCTGTTAACAAGGCC	XM_002372703.1	myosin I MyoA/Myo5
all-m0027-3p	ACTGGGCGAGTCCTCCTGAGGCTT		
all-m0029-3p	TAAACTGGTGGAGCAGCTCTCGCA		

Table 4.4 (continued)

all-m0029-5p	AAAGGGTTGGTCTATCTAAT	XM_002373293.1	conserved hypothetical protein
		XM_002375235.1	conserved hypothetical protein
		XM_002375267.1	pheromone response protein, putative
		XM_002381487.1	hypothetical protein
all-m0036-3p	TTGGGCCAAAGAGAACGGGG	XM_002374222.1	glycerol kinase, putative
		XM_002381069.1	oxidative stress protein Svf1, putative
all-m0036-5p	TATCTTTTCTCGTTGGCCTCTA	XM_002374222.1	glycerol kinase, putative
		XM_002374244.1	conserved hypothetical protein
		XM_002376062.1	GTPase activating protein (Gyp3), putative
		XM_002376771.1	nonribosomal siderophore peptide synthase SidC
		XM_002377252.1	sugar transporter, putative
		XM_002379855.1	facilitated glucose transporter, putative
all-m0048-5p	GCTTCGGGGTTCCTTGGCGATC	XM_002373774.1	C6 transcription factor, putative
		XM_002373775.1	MFS transporter, putative
		XM_002382734.1	DnaJ domain protein
		XM_002384347.1	alpha-1,3-glucan synthase Ags3
all-m0049-5p	CCATCGGATCAGGGGATCTCC	XM_002372802.1	alcohol dehydrogenase, putative
		XM_002373788.1	GNAT family N-acetyltransferase, putative
all-m0059-3p	ATTCTAGGACAGAACTGGAA	XM_002375816.1	nucleoporin (Nup184), putative
		XM_002385312.1	beta-xylosidase, putative
		XM_002385313.1	MFS allantoate transporter, putative
all-m0063-3p	TATCATCAGATTGTCCCTGGCCT	XM_002373961.1	conserved hypothetical protein
all-m0067-3p	ATTTCGAGGATTTCCGGGAC	XM_002374956.1	conserved hypothetical protein
		XM_002376035.1	phosphatidate cytidylyltransferase, putative
		XM_002377271.1	conserved hypothetical protein

Table 4.4 (continued)

all-m0067-3p	ATTTCGAGGATTTCCGGGAC	XM_002377847.1	kynureninase
		XM_002379509.1	diphthamide biosynthesis protein, putative
		XM_002380978.1	peptidyl-prolyl cis-trans isomerase
all-m0071-5p	CTATACTTCGCCGTCGGGGTA		
all-m0073-3p	TCATTGATCTGCCTTGGTAAGATA	XM_002376494.1	conserved hypothetical protein
		XM_002380162.1	conserved hypothetical protein
all-m0079-3p	TACTTCGGTGAGCCTGCATCCT		
all-m0091-5p	TAATACTGTAGGGTACACTAATG		
all-m0099-5p	TCCCTGCCCCATTTGCATTCTGG	XM_002378053.1	trafficking protein particle complex subunit 2/Sedlin, putative
		XM_002380220.1	jumonji family transcription factor, putative
		XM_002380221.1	conserved hypothetical protein
all-m0107-3p	CCGGGCTTGTGGAGATTAACATGG	XM_002372527.1	DEAD/DEAH box helicase, putative
all-m0110-5p	TTTGCGGATTTCTGAGAGGCT	XM_002372462.1	conserved hypothetical protein
all-m0118-5p	ACTTTTCACCAAGAGAGCAG	XM_002375264.1	SET domain protein
		XM_002380986.1	Ras GTPase activating protein, putative
all-m0119-5p	CTTTTATTCGTCCGAAGGTAT		
all-m0121-3p	TGTGGTGGACAGATCTGTTGACT		
all-m0123-3p	TTTGCTTGTGTTGAACAGGGGCT	XM_002375207.1	conserved hypothetical protein
		XM_002375824.1	tyrosinase, putative
all-m0130-5p	TATCAGCCGTCGGCGGCCCGCAG	XM_002382781.1	exopolyphosphatase, putative
all-m0133-5p	TTTCTGGAAGCCTCTTGTTTCT	XM_002375983.1	pyruvate decarboxylase, putative
		XM_002378818.1	alcohol dehydrogenase, putative
		XM_002378905.1	conserved hypothetical protein
		XM_002379370.1	NOT2 family protein

Table 4.4 (continued)

all-m0133-5p	TTTCTGGAAGCCTCTTGTTTCT	XM_002379427.1	HD family hydrolase, putative
		XM_002383834.1	nucleolin protein Nsr1, putative
		XM_002385220.1	conserved hypothetical protein
all-m0136-5p	TCAACGTTCTCTTGGACTCACC	XM_002379298.1	conserved hypothetical protein
all-m0140-3p	TAAGGATCAAGTGCTTCCGGGGT		
all-m0140-5p	ATCTCCAGTACTTGTGTGT	XM_002373395.1	asparaginyl-tRNA synthetase Slm5, putative
		XM_002373932.1	hypothetical protein
		XM_002374344.1	UMTA methyltransferase family protein
		XM_002375518.1	C6 transcription factor, putative
		XM_002376467.1	ATP binding protein, putative
		XM_002377473.1	hypothetical protein
		XM_002377474.1	bcs1 AAA-type ATPase, putative
		XM_002377606.1	phthalate transporter, putative
		XM_002379607.1	conserved hypothetical protein
		XM_002379916.1	FAD dependent oxidoreductase, putative
		XM_002380413.1	M protein repeat protein
		XM_002383587.1	conserved hypothetical protein
all-m0141-3p	GGTTAGTGTGACTGTAGGGTGA	XM_002380013.1	conserved hypothetical protein
all-m0144-3p	GGTGGTAGTAGCAGATACTTT	XM_002372924.1	HD superfamily hydrolase, putative
		XM_002373033.1	hypothetical protein
		XM_002378781.1	hydrophobin family protein
		XM_002382197.1	nuclear division Rft1 protein, putative
		XM_002382870.1	secretion related GTPase SrgB/Ypt1
all-m0145-5p	CCTGTGGTGAATCTCTGCCC	XM_002375619.1	glutathione S-transferase, putative
		XM_002379944.1	phenol 2-monooxygenase, putative

Table 4.4 (continued)

all-m0145-5p	CCTGTGGTGAATCTCTGCCC	XM_002380333.1	quinate utilisation oxidoreductase QutH
all-m0156-5p	GGCAGATGTAGCCGAGTGGT	XM_002380328.1	hypothetical protein
		XM_002380980.1	HMG-CoA reductase
		XM_002381450.1	hypothetical protein
		XM_002384258.1	hypothetical protein
all-m0162-3p	ACTGCAAGGGGCACACGATC	XM_002382454.1	glycosyl hydrolase, putative
all-m0164-5p	GTTCTACATGTTTGCGACTCA	XM_002374050.1	SYF2 splicing factor family protein
all-m0168-3p	ACTACAGCGGTTACGGACAGC		
all-m0170-3p	AGGCGAGATGGCCGAGCGGTCT	XM_002375968.1	conserved hypothetical protein
		XM_002380018.1	conserved hypothetical protein
		XM_002384030.1	MFS sugar transporter, putative
all-m0171-5p	GTCAGACCAGTAGCTACAGGA		
all-m0173-5p	TACGAGACAACCTTCACTGGGT	XM_002382066.1	rootletin, putative
all-m0178-3p	TATCATCCGTGCCAACATTT	XM_002373464.1	Coatomer subunit alpha, putative
		XM_002376284.1	conserved hypothetical protein
		XM_002378050.1	conserved hypothetical protein
		XM_002382244.1	efflux pump antibiotic resistance protein, putative
		XM_002382599.1	conserved hypothetical protein
		XM_002385485.1	SAC3/GANP domain protein
		XM_002385486.1	vacuolar protein sorting protein (Vps36), putative
all-m0184-3p	ATAGGACGATAGTTGCTCTGTA	XM_002375687.1	isoamyl alcohol oxidase, putative
		XM_002384096.1	conserved hypothetical protein
		XM_002384881.1	NADH oxidase
all-m0185-5p	TTCTGCTAGGCCTTTGCACCTG	XM_002372554.1	ribonucleoprotein, putative

Table 4.4 (continued)

all-m0185-5p	TTCTGCTAGGCCTTTGCACCTG	XM_002374065.1	Nucleoside transporter family
		XM_002383563.1	conserved hypothetical protein
		XM_002383564.1	conserved hypothetical protein
all-m0187-3p	ACTTACCCTTTTTTTTTCATTC	XM_002372979.1	AAA family ATPase Rvb2/Reptin, putative
		XM_002373920.1	conserved hypothetical protein
		XM_002374152.1	40S ribosomal protein S6
		XM_002374361.1	IQ and HECT domain protein
		XM_002374572.1	conserved hypothetical protein
		XM_002375483.1	importin beta-5 subunit, putative
		XM_002375570.1	MFS transporter, putative
		XM_002376067.1	transcriptional corepressor of histone genes (Hir3), putative
		XM_002376352.1	conserved hypothetical protein
		XM_002376353.1	short-chain type dehydrogenase, putative
		XM_002376370.1	conserved hypothetical protein
		XM_002376832.1	cupin domain protein
		XM_002376902.1	conserved hypothetical protein
		XM_002376972.1	hypothetical protein
		XM_002377072.1	endosomal cargo receptor (Erp5), putative
		XM_002377225.1	conserved hypothetical protein
		XM_002377922.1	SNARE protein (Ufe1), putative
		XM_002378256.1	alpha-1,2-mannosyltransferase (Mnn2), putative
		XM_002378910.1	hypothetical protein
		XM_002379125.1	arsenite resistance protein Ars2, putative
		XM_002379612.1	hypothetical protein
		XM_002379768.1	conserved hypothetical protein
		XM_002379861.1	hypothetical protein

Table 4.4 (continued)

all-m0187-3p	ACTTACCCTTTTTTTTTCATTC	XM_002379862.1	monooxygenase, putative
		XM_002380996.1	conserved hypothetical protein
		XM_002382441.1	tRNA nucleotidyltransferase
		XM_002382510.1	thioesterase family protein
		XM_002383053.1	short-chain dehydrogenase, putative
		XM_002383097.1	conserved hypothetical protein
		XM_002383188.1	conserved hypothetical protein
		XM_002383279.1	conserved hypothetical protein
		XM_002383760.1	3-methylcrotonyl-CoA carboxylase, beta subunit (MccB), putative
		XM_002383832.1	t-complex protein 1, delta subunit, putative
		XM_002383938.1	sorting nexin Snx3, putative
		XM_002385335.1	vps9-ankyrin repeat-containing protein, putative
all-m0188-5p	CTGCGAGACGCGGTAGCGCT		
all-m0191-5p	ACACGAGTTCCAGTAGTTGGT	XM_002375001.1	RanGTP-binding protein
		XM_002379434.1	mitochondrial DnaJ chaperone (Mdj1), putative
		XM_002381631.1	GNAT family acetyltransferase, putative
		XM_002381632.1	conserved hypothetical protein
		XM_002383253.1	conserved hypothetical protein
all-m0193-3p	CAGGACTTTTAGTTGCATGT	XM_002385111.1	conserved hypothetical protein
all-m0195-5p	GCAAGGCGTGTTCGGCTCTA	XM_002373336.1	AMP binding domain protein, putative
		XM_002374791.1	amidase family protein
		XM_002375716.1	AP-2 adaptor complex subunit sigma, putative
		XM_002376499.1	conserved hypothetical protein
		XM_002377286.1	fatty acid synthase alpha subunit, putative
		XM_002378862.1	conserved hypothetical protein

Table 4.4 (continued)

all-m0195-5p	GCAAGGCGTGTTCGGCTCTA	XM_002379362.1	DNA replication complex GINS protein (Psf2), putative
		XM_002380223.1	Acyl CoA binding protein, putative
		XM_002381156.1	ubiquitin ligase subunit CulD, putative
all-m0201-5p	TAGAAGGTCCTCAAGGCTCAGA	XM_002372973.1	conserved hypothetical protein
all-m0202-3p	TCGGGCTGTTGTCTTGTTGA	XM_002372133.1	5-oxoprolinase, putative
		XM_002372222.1	copper amine oxidase, putative
		XM_002372930.1	DEAD box helicase Mph1, putative
		XM_002373404.1	DNA polymerase epsilon, catalytic subunit A/POL2, putative
		XM_002373694.1	cell cycle control protein cwf18, putative
		XM_002374639.1	cell wall protein, putative
		XM_002375000.1	conserved hypothetical protein
		XM_002375391.1	conserved hypothetical protein
		XM_002376110.1	conserved hypothetical protein
		XM_002376398.1	HEAT repeat protein
		XM_002377084.1	cAMP-mediated signaling protein Sok1, putative
		XM_002377178.1	pentafunctional AROM polypeptide, putative
		XM_002377179.1	fungal specific transcription factor, putative
		XM_002377215.1	conserved hypothetical protein
		XM_002377781.1	Golgi membrane protein (Rer1), putative
		XM_002377817.1	SAGA complex subunit (Ada2), putative
		XM_002377818.1	enoyl-CoA hydratase
		XM_002378076.1	ubiquitin C-terminal hydrolase, putative
		XM_002379414.1	MFS monosaccharide transporter, putative
		XM_002380011.1	1,3-beta-glucanosyltransferase gel4 precursor, putative
		XM_002380864.1	tRNA-splicing endonuclease, putative

Table 4.4 (continued)

all-m0202-3p	TCGGGCTGTTGTCTTGTTGA	XM_002380956.1	integral membrane protein
		XM_002382947.1	succinyl-CoA synthetase alpha subunit, putative
		XM_002382989.1	ribosome biogenesis GTPase Lsg1, putative
		XM_002383040.1	conserved hypothetical protein
		XM_002383888.1	ankyrin repeat domain protein, putative
		XM_002384347.1	alpha-1,3-glucan synthase Ags3
		XM_002385134.1	AMP dependent ligase, putative
		XM_002385553.1	riboflavin-specific deaminase
all-m0212-3p	GCCGATCGGCTCGGCGCGTG	XM_002377811.1	conserved hypothetical protein
all-m0214-3p	TAACCGGGTCGTAGTATCTTT	XM_002373605.1	peroxisome biosynthesis protein (PAS8/Peroxin-6), putative
		XM_002377936.1	conserved hypothetical protein
		XM_002378527.1	conserved hypothetical protein
		XM_002379732.1	conserved hypothetical protein
		XM_002381293.1	pectinesterase precursor, putative
		XM_002383387.1	hscarg dehydrogenase, putative
all-m0217-3p	GGTTGTATCGTAGGCTCTCCAAG		
all-m0221-3p	GGAGTGGGCGAACGGCTCGGA	XM_002374348.1	GARP complex subunit (Sac2), putative
		XM_002378956.1	protein kinase, putative
		XM_002384963.1	MFS sugar transporter, putative
all-m0224-3p	AGGAATCTTTGAAAACAGAG	XM_002385128.1	serine protein kinase, putative
all-m0225-3p	CCAGAAGATGAGGAGTCATA	XM_002374376.1	ribosome assembly and transport protein Srp40, putative
		XM_002376771.1	nonribosomal siderophore peptide synthase SidC
		XM_002381366.1	conserved hypothetical protein
		XM_002385340.1	conserved hypothetical protein

Table 4.4 (continued)

all-m0229-3p	AAGAGATCAGAACTGTGGTTGTC	XM_002375490.1	conserved hypothetical protein
all-m0233-3p	TTGCCGTCGTCCGACCCGGACA	XM_002375516.1	DUF92 domain protein
		XM_002383024.1	glutamine synthetase, putative
all-m0233-5p	GTTGACGGGCGCTCTTGATACCGCTG	XM_002379203.1	PAXNEB protein superfamily
		XM_002380366.1	serine/threonine protein kinase Kin1, putative
all-m0234-5p	GGCTTAATTCTTTCCATGGTCGGC	XM_002375959.1	extracellular phytase, putative
all-m0235-5p	TCATGGGCGATTTAGACAACTG		
all-m0236-3p	TGTGTTGGGTCGTCGTCCC	XM_002373542.1	SNF2 family helicase/ATPase, putative
		XM_002375182.1	WD repeat protein
		XM_002377112.1	polyketide synthase, putative
		XM_002385396.1	G-patch domain protein, putative
all-m0236-5p	CATGCCTGTCCGAGCGTCATT	XM_002377458.1	membrane copper amine oxidase, putative

milRNAs labelled “Afl-milR” are previously known, while “all-m” milRNAs are previously undescribed.

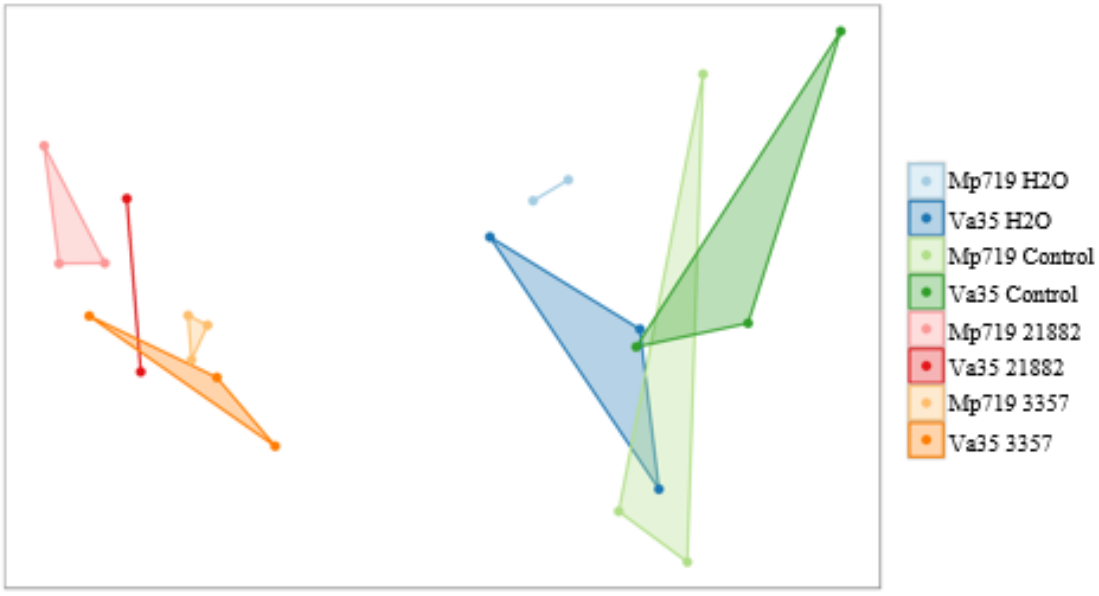

Figure 4.5 A PCA plot of *A. flavus* small RNAs

The RNA-seq data analysis software, edgeR, was used to determine differential expression of identified milRNAs. The statistically significant (based on false discovery rate) differentially expressed milRNAs are reported in Figure 4.6. The most significant differential expression occurs when comparing the two *A. flavus* strains and ignoring the maize lines (3357–21882), which results in seven significantly differentially expressed milRNAs.

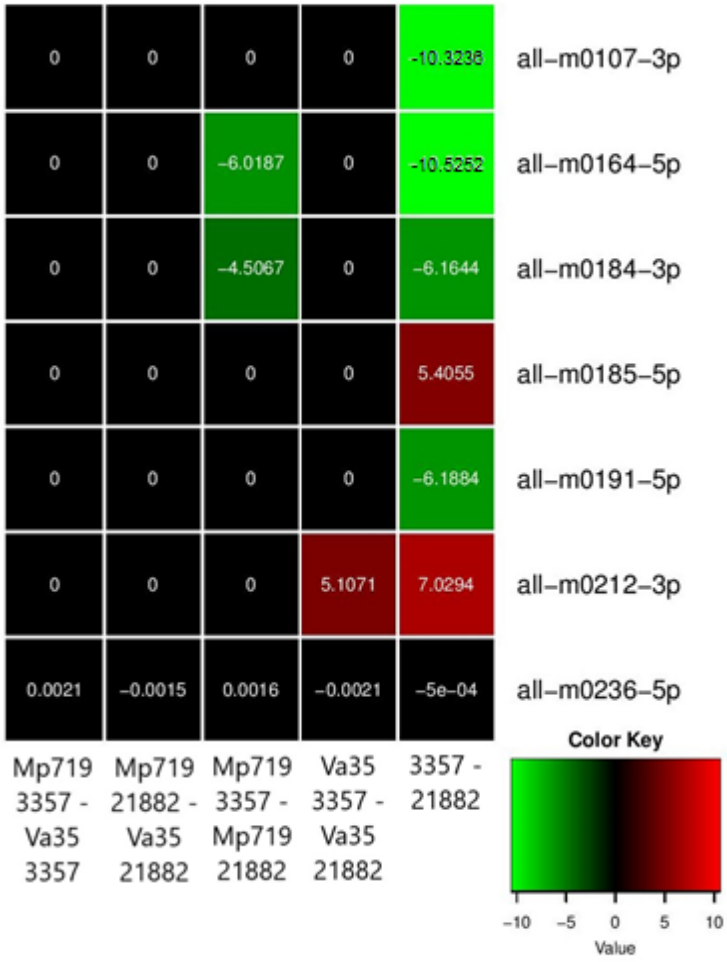

Figure 4.6 Heat map of differentially expressed *A. flavus* milRNAs

The differential expression is based on the $\log_2$(Fold Change) of milRNAs between treatments. The white text is the $\log_2$(FC) number for each comparison. Decreased expression is represented by a green color, while increased expression is indicated by a red color, with the brightness indicating relative intensity. Significance of the differential expression is determined by FDR ($p <= 0.05$).

There were very few significantly differentially expressed milRNAs between the experimental groups. Of the 135 known milRNAs previously described by Bai *et al.* (2015), seven (Afl-milR-2, -3, -7, -9, -33, -43, -92) were aligned to our samples and they were subjected to further expression analysis. None of these samples, however, had any

significant differential expression. The differential expression seems to rely on infecting *A. flavus* strain, rather than the resistance of the maize inbred line. The PCA plot shows that the infected samples grouped together but minimally separated, which might explain these low levels of differential expression.

In all comparisons, the predicted milRNA all-m0236-5p was differentially expressed, about 2-fold increase in expression in Mp719 3357 to Va35 3357 and Mp719 3357 to Mp719 21882 and 2-fold decrease in expression in Mp719 21882 to Va35 21882 and Va35 3357 to Va35 21882 (Figure 4.6). This milRNA was predicted to target a putative membrane-bound copper amine oxidase (Table 4.4). When comparing Mp719 3357 to Mp719 21882, all-m0164-5p and all-m0184-3p had a 22-64 fold decrease in expression (Figure 4.6), which might lead to an increased expression of the predicted targets including a SYF2 splicing factor family protein, two oxidases and a hypothetical protein (Table 4.4). When comparing Va35 3357 to Va35 21882, all-m0212-3p had a 32-fold increased expression, which might lead to a decrease in the hypothetical protein it was predicted to target. When comparing all samples inoculated with NRRL 3357 to those inoculated with NRRL 21882, there were some similarities in the expression of Mp719 3357 to Mp719 21882, in that all-m0184-3p and all-m0164-5p had decreased expression (Figure 4.6). Similarly, all-m0212-3p had increased expression as it did in the comparison of Va35 3357 toVa35 21882 (Figure 4.6). In addition, all-m0191-5p and all-m0107-3p had decreased expression (Figure 4.6), suggesting increased expression of their targets which include a RanGTP-binding protein, a DnaJ chaperone, and an acetyltransferase along with some hypothetical proteins and a helicase (Table 4.4). In the same comparison, all-m0185-5p had increased expression (Figure 4.6), which might lead

to a downregulation in its targets including a ribonucleoprotein, a nucleoside transporter, and hypothetical proteins (Table 4.4). The predicted targets of all identified milRNAs are listed in Table 4.4. However, none of these targets are related to aflatoxin biosynthesis, implying that *A. flavus* may not utilize milRNAs as a way to control the production of aflatoxins. Additionally, there does seems to be no difference between the strains of *A. flavus* in terms of milRNAs, nor does *A. flavus* appear to have a milRNA response when inoculated on a resistant or susceptible maize host.

Z. mays miRNAs

From the RNA sequence data, 523 unique *Z. mays* miRNAs, named as Predict-miR, were identified by computational analysis. Including 168 known miRNAs, as zma-mir, previously reported in the miRNA data base miRBase, this brings the total number of maize miRNAs to 691. These 691 maize miRNAs and their sequences are presented in Table 4.5, and their predicted targets are listed in a supplementary table (Table S1). A PCA plot of the variance between these miRNAs is shown in Figure 4.7. The plot shows that the *A. flavus*-inoculated samples group separately from the water and control samples with some overlap between the NRRL 3357 inoculated and the NRRL 21882 inoculated samples. There is more variance among the *A. flavus* infected samples than the water and control samples, with the most variance in the susceptible maize line Va35.

Table 4.5 *Z. mays* miRNA sequences

miRNA	Sequence
Predict-miR-002	AAATTAGGCAGCGAACCAAACAGG
Predict-miR-003	GCGAGCTGTTCTGGTATTGGTT
Predict-miR-004	GGTACCGACGTTCTTACATGAGTT
Predict-miR-006	GCACTGTCCGGTGCCCGATTTCTT
Predict-miR-007	GCACTGTCCGGTGCCCGATTTCTT
Predict-miR-008	GCACTGTCCGGTGCCCGATTTCTT
Predict-miR-009	TCATTTTGCTACGTTCTT
Predict-miR-011	GTGTTTGGTTTCTAGTGACTAATT
Predict-miR-012	ACACTATGTGTAGAAACCTAAGAA
Predict-miR-013	ACACTATGTGTAGAAACCTAAGAA
Predict-miR-015	ACAGGCACTGTAGACTGTCCGA
Predict-miR-016	ACAGTTAGCCACGAACCAAACATG
Predict-miR-017	TCTACGCAGTCGTTATGT
Predict-miR-018	ACATTAGTCCATAGAAACCAAAC
Predict-miR-019	ACCTAGAACACTCGGCAAAGGCGC
Predict-miR-020	ACGTGTCATGATATCATATGTAGAC
Predict-miR-021	ACTCCCTCCGTCCTAAAATATAGT
Predict-miR-022	ACTATTAGCTAGGTTGTTTGGATG
Predict-miR-023	ACTGGCGGACTGCTTAAGAAAACC
Predict-miR-024	TCCGTCTTACAGTTCAGTTTATCT
Predict-miR-026	AGCGACTGTGGTCACTTCGACCTT
Predict-miR-027	GCACTGTCCGGTGCCCGATTTCCT
Predict-miR-028	AGGAAGTTAGTCGGCTGACGGCGT
Predict-miR-029	AGGGCTGCAAACACTCTGGTTTGC
Predict-miR-031	CTTCATTTTATTCTATTTTAGTAT
Predict-miR-032	CTTGTTCGGTTATTCCAATTCTAT
Predict-miR-033	ATATATGGTAGGTATAACGGGAGC
Predict-miR-034	TATCACAGCCTCTAGATATGATAT
Predict-miR-035	ATATGTACAGACTGTGATAAAAAT
Predict-miR-036	ATGAAAACAAGTAGAAGA
Predict-miR-037	ATGAACGTATGTGAGCTCACTCTC
Predict-miR-039	TTAGTCCCTCTATTTTAGTCTCAT
Predict-miR-040	ATGATATCATATGTAGAGGCCGTG

Table 4.5 (continued)

Predict-miR-041	ATGATATCATATGTAGAGGCCGTG
Predict-miR-042	GCTGTTCACTGTCCGGTGTGCCAT
Predict-miR-044	ATGGCTAGAACCGTTACTAAAGGT
Predict-miR-045	AGAGTTGGTACCTCTCAGCCAT
Predict-miR-046	ATGTAGACGGAATGTAGGAAA
Predict-miR-047	ATTATATAAGTTGGATTATGA
Predict-miR-048	ATTATATAAGTTGGATTATGA
Predict-miR-049	TGGCTTGTTCGGTTAGCTCTCAAT
Predict-miR-050	GGTTCTCAAACTAGCCCTAAAT
Predict-miR-051	ATTTGCTCCTAAAACTGTAGAAGA
Predict-miR-052	ATTTTATAAAAGCTGTCGGAAGTT
Predict-miR-053	AGCCCACGTACACCAATCCTTG
Predict-miR-054	CAATCCGACATAAACGAACAAGGC
Predict-miR-055	TCATTCCTTGTGTGCCACTGAGTG
Predict-miR-056	GCCGGACAGTCTACAGTGCCTG
Predict-miR-057	CCCTAACTGACTCTGCGCACGCGT
Predict-miR-058	GGACCGTTCGGCCCACAGGCGCGG
Predict-miR-062	GGTGCCCACACGCCGGACTGTTCG
Predict-miR-063	GGTGCCCACACGCCGGACTGTTCG
Predict-miR-064	ACGTTCCTTTTAGTGCCAGTGCCG
Predict-miR-065	AGCTCGAGTGAAGCAGACCG
Predict-miR-067	TTGTGAGTCCAAAAACCGGAG
Predict-miR-068	GGCAGCGGCGGCGCGAGAGGAG
Predict-miR-069	CTCCTGGTCGTGGATCTCCCAC
Predict-miR-070	CTGGATTGGCCTAACCGAACAAGC
Predict-miR-071	CATGAGCATAAGATACGTCCTAAG
Predict-miR-072	CTTATATCCTAGGACGGAGGGAGT
Predict-miR-073	CCGTTGTCCACTGCTGGCGAAG
Predict-miR-074	CTTGTTTCCACATGCGGTTTTCTT
Predict-miR-075	CTTTTCGGGCTTGGGTCGGGCCGG
Predict-miR-077	AATTAGTCTCTAAAAACCAAACACTC
Predict-miR-078	GATCTCCTTGTCACCAAATCAATC
Predict-miR-079	GCCCTCAATGTCTGTGTCATC
Predict-miR-080	ACCCTCCACATCCAACGGTGCTGC

Table 4.5 (continued)

Predict-miR-081	TCTCCGTTTCTTTTTAGTTGTCGC
Predict-miR-082	GCTGATTTGGTGACTAGGGATCAC
Predict-miR-083	GGATATAATGATCTTCGGACGAAGGTA
Predict-miR-084	GGATTGAGGTAGAACCGAACAAGC
Predict-miR-085	GGATTGAGGTAGAACCGAACAAGC
Predict-miR-086	GGATTGAGGTAGAACCGAACAAGC
Predict-miR-087	GGCACTCGGCAAAGAGCTCG
Predict-miR-090	CCCTAGAAACCAAACATCCCC
Predict-miR-091	GGGGATTTGAGTTTCTAAACTAGT
Predict-miR-092	GTGGATTGAGGGGACTAGAATCCC
Predict-miR-093	ACATGATCTCTTAGGTTTCTACAC
Predict-miR-094	TAAAATCACAATTGCAAGGTG
Predict-miR-095	CACCTCAATCCATGTGTATTA
Predict-miR-097	TAGGGAGAAGAGAACTCATGCA
Predict-miR-098	TTGGTCAACCAATCCATCCCTA
Predict-miR-099	CTGGTCACCAAATCAGCCCTA
Predict-miR-100	TATATATCTAAAGTTGTAATCTTT
Predict-miR-101	GCTGGTCCTGGAACCCGAGATGGA
Predict-miR-102	TCGAACTGGTCCCTCGGAGGGT
Predict-miR-104	TCTCTGGTCAGGCGCGGACGGTCA
Predict-miR-105	TGCTCCTAAGACTGTAGAACGC
Predict-miR-106	TGCTCCTAAGACTGTAGAAGCC
Predict-miR-108	TGTATGAGCTGTGTTAAGGACA
Predict-miR-109	TGTATGAGCTGTGTTAAGGACA
Predict-miR-110	TGTCATGATATCATATGTAGAGGA
Predict-miR-112	TGTCTATTTGTATGTGAACCT
Predict-miR-113	GCATAGTTAGCCACAAACCAAACA
Predict-miR-114	TTAGGGCTAGTTTGGGAACCACAAT
Predict-miR-115	TTAGGTGTGGGAGTCCAGACGT
Predict-miR-116	GGGTGGAGGTGCGGGGAA
Predict-miR-117	ATAGTCTCATACTTCTCCGGAA
Predict-miR-118	TTCTTTAATTCGGGCCTGAGCT
Predict-miR-119	TTGAAGTTTCTTGTGACGTTGC
Predict-miR-120	TTGAAGTTTCTTGTGACGTTGC

Table 4.5 (continued)

Predict-miR-121	TTGATTGTCAACTTTGCGAGTA
Predict-miR-122	TTGTCATATAGAACCGCCAGT
Predict-miR-123	TTGTCATATAGAACCGCCAGT
Predict-miR-124	TTGTTGTAGATAAATGACA
Predict-miR-125	TTTATTTTGGCATCTCTTCCGC
Predict-miR-129	AGTTGCAAAGTAGATCGAAAAA
Predict-miR-130	AGTTGCAAAGTAGATCGAAAAA
Predict-miR-131	GCAAAGTATTTGCCGAGTGTTTTT
Predict-miR-132	TTACTACTCCCTCCGTTTCTTTTT
Predict-miR-133	AAAACTGCGTAGAACGTCCGTTCT
Predict-miR-134	AAATCTTCTTCTATTCAATTTTGA
Predict-miR-135	AACGAGCCAGCTCGAACTCGGACA
Predict-miR-136	GGTACCGACGTTCTTACATGAGTT
Predict-miR-137	AAGCATCGGCCTACACTCTCAGGT
Predict-miR-138	AATAGAATAAAATCTAGGGACTAA
Predict-miR-139	ACAGGCACTGTAGACTGTCCGA
Predict-miR-140	ACCGGACAGGTCCTGTAGACTGC
Predict-miR-141	GCTGTATAAAGTACACCGTCAGT
Predict-miR-142	AATTGGGGTTCCCAAACTAGCCCT
Predict-miR-143	AGGTCTGTGTTCTTTGCCGAGTGT
Predict-miR-144	ATATATGGTAGGTATAACGGGAGC
Predict-miR-145	ATATTATATAAGTTGGATTA
Predict-miR-146	ATCGGGCCGGCCCGACACGACTA
Predict-miR-148	ATCTGGACAGATTATAATCTC
Predict-miR-149	ATGATATCATATGTAGAGGCCGTG
Predict-miR-150	GGTGTTTGATTTCTAGGGACTAAT
Predict-miR-151	GCATCATGAGTCTATTCCACAAAT
Predict-miR-152	ATTTTATAAAAGCTGTCGGAAGTT
Predict-miR-153	ATTTTGTGGCTCTCAAACTAG
Predict-miR-155	CATCTCGACCGGATATTATGCC
Predict-miR-156	CCCTGGATAAAGAAGTACA
Predict-miR-157	CGCGGCGCTGACCATCTGAGTG
Predict-miR-159	CCGTCGGATATTACCTTATGTCCG
Predict-miR-160	GGTTTTCAGCAAGGTCCCCG

Table 4.5 (continued)

Predict-miR-161	GGTTTTCAGCAAGGTCCCCG
Predict-miR-162	CGGTGTGCACCGGACTGTCCGC
Predict-miR-163	CGGTGTGCACCGGACTGTCCGC
Predict-miR-164	CTAACTTCCTACGGCCGTCTCTAG
Predict-miR-165	CTCAAGACGCCTAATTCTCAGCC
Predict-miR-168	GCGGACAGTGTCTGGTGG
Predict-miR-169	TGCCATAGCCTATGGCGCCGAGC
Predict-miR-170	GTGTAGTGTCTCTGTCTGAGTT
Predict-miR-171	TGGTTCTTTCTTTCCACAACAC
Predict-miR-173	TAAAAAGAAACGGAGGGAGTACGT
Predict-miR-178	CTCAAGTTTTTATCACAGCCTCTA
Predict-miR-180	TAGGGAGAAGAGAACTCATGCA
Predict-miR-181	TTGGTCAACCAATCCATCCCTA
Predict-miR-182	TATGTCCGGATGTGTGGTCAA
Predict-miR-183	GAGTTCCCCCAAACACTTCA
Predict-miR-184	TGGGCGGTCTCCTTGGCTAGC
Predict-miR-185	TGGGTGTGCTTAATGAACC
Predict-miR-186	GGGCCTGTCACCGAACATTACA
Predict-miR-187	TGTATGAGCTGTGTTAAGGACA
Predict-miR-190	TTAGGGCTTATTCCCGTCGGTTGC
Predict-miR-191	TTGTCATATAGAACCGCCAGT
Predict-miR-192	TTGTCATATAGAACCGCCAGT
Predict-miR-193	TTTGAACTTGAAATTTTGTAT
Predict-miR-194	AATCTTGTTTCCACAGGCGGTTTT
Predict-miR-195	AACCATAGTTGACTAGGAGATGAC
Predict-miR-196	GGTACCGACGTTCTTACATGAGTT
Predict-miR-197	AAGGAATGAGTATAAATTTTGATG
Predict-miR-198	AAGGCACTCGGCAAAGATACTAGC
Predict-miR-199	AAGGTGTCTGGGTAGAAGTCAGGC
Predict-miR-200	ACACTACGTGTAGAAACCTAAGAG
Predict-miR-201	ACACTACGTGTAGAAACCTAAGAG
Predict-miR-202	ACACTACTGGAAACACTTTCTTGC
Predict-miR-203	ACACTCGGCAAAGAACCTATACCA
Predict-miR-204	ACAGGCACTGTAGACTGTCCGA

Table 4.5 (continued)

Predict-miR-205	ACAGGCACTGTAGACTGTCCGA
Predict-miR-206	ACCGACGTTCTTACTCTAATAGGC
Predict-miR-207	ACCGGACAGGCACTGTAGACTA
Predict-miR-208	ACTATGTCCGGATGTGTGGTCG
Predict-miR-209	ACTGGACTGTCCGATGTGCCC
Predict-miR-210	CGAGCCCGAGCCGAGCCTAATTCT
Predict-miR-211	AGGGAAAGATGAAAAGGAT
Predict-miR-212	AATTGGGGTTCCCAAACTAGCCCT
Predict-miR-213	AATTGGGGTTCCCAAACTAGCCCT
Predict-miR-214	CCTGTGGGTCCTATCGGGTCGGAT
Predict-miR-215	GTGTTTGAATGCACTAGATCTAAT
Predict-miR-216	ATTATATAAGTTGGATTATGA
Predict-miR-217	ATTATATAAGTTGGATTATGA
Predict-miR-218	GGTGGTTCAATGCCCAACACAAAT
Predict-miR-219	ATTTTTAGTTTGAATAGGGAAT
Predict-miR-220	CAAGGGGATCCATGGGGGAGG
Predict-miR-221	GGCGCGGACAGTCCGGACCCTG
Predict-miR-222	ACTCAGATTTTGACTATG
Predict-miR-223	CATTGACTCGTCGTCGGTGAGATT
Predict-miR-225	GCAGTCTACAGTGCCTGTCCGG
Predict-miR-226	CCGGAGGAGATTGGAGGGGCT
Predict-miR-228	CGGACAGTGTCTGGTGGG
Predict-miR-229	AGCTCGAGTGAAGCAGACCG
Predict-miR-230	AGCTCGAGTGAAGCAGACCG
Predict-miR-231	AGCTCGAGTGAAGCAGACCG
Predict-miR-232	TGCAGTGTCCAGTTTATTACG
Predict-miR-233	CGTGGCTGGCGCACCGGACAGTGC
Predict-miR-234	CTCCTGGTCGTGGATCTCCCAC
Predict-miR-236	CTTTTCTAGGTACATAGCTTT
Predict-miR-238	GATGTGAGGGACTGTAAAATAGTG
Predict-miR-239	GTATTTCCATCTCGTGACTCTGCA
Predict-miR-241	GTTTTATCGCAAGAGTGAGCTCAC
Predict-miR-244	GCTGGCGGTTGTGTTAAGATA
Predict-miR-245	TCGAACTGGTCCCTCGGAGGGT

Table 4.5 (continued)

Predict-miR-246	AACTAAACATTAGTCCCTAGA
Predict-miR-247	TCTTGTGACGTTGTGTTTGATA
Predict-miR-248	GTGCTCACTCTCTTCTGTCA
Predict-miR-249	GTGCTCACTCTCTTCTGTCA
Predict-miR-250	TGAGCCGGTGTACTCTGTCCAGA
Predict-miR-251	TGGTCTACTGAAGCTTGGTTCC
Predict-miR-253	TGGTTTCCAAACTAGCCCTAA
Predict-miR-254	TTAGGTGTGGGAGTCCAGACGT
Predict-miR-255	TTAGGTGTGGGAGTCCAGACGT
Predict-miR-256	ATAGTCTCATACTTCTCCGGAA
Predict-miR-257	TTGAAGTTTCTTGTGACGTTGC
Predict-miR-258	GTCTGGTGCGCCATGCGACAGCAA
Predict-miR-260	TCCCTAAGTCCTTCATAGAAAA
Predict-miR-261	GCGTACATGGTTCACATTCGGTTT
Predict-miR-262	GCACTGTCCGGTGCCCGATTTCTT
Predict-miR-263	AAGCATCGGCCTACACTCTCAGGT
Predict-miR-264	GACATAGATTATTTCCGACGGCTT
Predict-miR-265	AAGGAATGAGTATAAAATCTGATG
Predict-miR-266	AAGGGCTAGTTTGAGAACT
Predict-miR-267	ACACTATGTGTAGAAACCTAAGAA
Predict-miR-268	ACACTCGGCAAAGAACCTATACCA
Predict-miR-269	ACCGAGTTGGAGTAGGCAGGTA
Predict-miR-270	GGCATCTTTTTAGCGACCGACCGT
Predict-miR-271	ACTGGCGGCTGTATTAAGCAAACC
Predict-miR-272	CTTCATTTTATTCCTTTTTAGTCT
Predict-miR-273	CTTCATTTTATTCCTTTTTAGTCT
Predict-miR-274	AGACTAAAGTGGAATAAAATGAAG
Predict-miR-277	ATATAATCTAACAATTTTTGAACT
Predict-miR-278	ATCTCTATACACTCTGTTATTATG
Predict-miR-285	CTTGTTCGGTTATTTTCAATTCAT
Predict-miR-286	ATTGGGGTAGAACCGAACAAGCCT
Predict-miR-287	ATTGTTCGTTGTAGTTGAACCA
Predict-miR-288	CCATATGGATTGGGGTAGAACCA
Predict-miR-289	CCCAAGCTGTGCTCGATGATGA

Table 4.5 (continued)

Predict-miR-290	CCCGTAGACTAGGAAGAACGGCGC
Predict-miR-292	GGACCGTTCGGCCCACAGGCGCGG
Predict-miR-293	CGATGTAGGCTTGATGATCGAGA
Predict-miR-294	AGCTCGAGTGAAGCAGACCG
Predict-miR-295	AGCTCGAGTGAAGCAGACCG
Predict-miR-296	CTCGGCTCGGGCTCGTTCGGAGCG
Predict-miR-298	CTGGAGTAGAACATGGAAACT
Predict-miR-299	ACAAAGAGCTCTTTGCCGAGTGTC
Predict-miR-300	TGTGATTATACCCTTCTCTC
Predict-miR-301	GCACTAGGTCGCGGACCGTCCGGC
Predict-miR-303	ACCCTCCACATCCAACGGTGCTGC
Predict-miR-305	GTGTAGTGTCTCTGTCTGAGTT
Predict-miR-306	GTGTAGTGTCTCTGTCTGAGTT
Predict-miR-307	GTGTGGCACTATGTGTAGAAACCT
Predict-miR-308	TAAACTAAGAACTTCGGAGACA
Predict-miR-309	GTTTCTAGTGACTAATATTTA
Predict-miR-310	TAAGGCTAAAGATTTTGATGTC
Predict-miR-311	TAAGGGCTAGTTTGGGAACCTCA
Predict-miR-313	CTCAAATTTTTATCAGAGTCTCTA
Predict-miR-314	TAGCTGGGTACTGAGGAACTCC
Predict-miR-315	TAGGGAGCGGAGAACTCGTGCA
Predict-miR-316	TATCCTGTGCGGTTATTATGT
Predict-miR-317	TATCCTGTGCGGTTATTATGT
Predict-miR-318	TATGAACGACTTGAAAACATCC
Predict-miR-319	TCTCTGGTCAGGCGCGGACGGTA
Predict-miR-320	TCTGCACCGGACTGTGAACAGTGC
Predict-miR-321	TGGAATTAGGTGTAGCTAT
Predict-miR-322	TGTCTTAACACAACCGCCA
Predict-miR-323	TGGTGGGGTACTGTGCTCTCGA
Predict-miR-324	TGTAGTTTAGTAGCATTCC
Predict-miR-325	TGTCATGATATCATATGTAGAGGA
Predict-miR-326	TGTCATGATATCATATGTAGAGGA
Predict-miR-327	TGTCATGATATCATATGTAGAGGA
Predict-miR-328	TTCCGTTGAGACGCCGAGGACC

Table 4.5 (continued)

Predict-miR-329	TTCCTCAAATCTGAGTTCTCCC
Predict-miR-330	TTCGAATCAAGAACAAGACAACA
Predict-miR-331	TTCTTTGTCGAGTGCCAGATC
Predict-miR-332	TTGCTCCTAAAACTGTAGAAGA
Predict-miR-333	TTTAAAATGTGCATGTGAGC
Predict-miR-334	GAGTCATTCCGTTCTAGTTCCTTT
Predict-miR-335	AAGAGAAGCGCACAGATGAAGT
Predict-miR-336	AAGAGAAGCGCACAGATGAAGT
Predict-miR-337	AAGGAATGAATATAAAATCTGATG
Predict-miR-338	GGTGAAATATAAGCCCTT
Predict-miR-339	AAGTGAAGATTGGAGTGACTCT
Predict-miR-340	AATCCTTCAGTGGTATCAGAGC
Predict-miR-341	ACCGAGTTGGAGTAGGCAGGTA
Predict-miR-342	ACCGAGTTGGAGTAGGCAGGTA
Predict-miR-343	ACCGAGTTGGAGTAGGCAGGTA
Predict-miR-344	ACCGGCTCACCATCGTCTGGCT
Predict-miR-345	ACTTCTTTAACTTTGACCAAG
Predict-miR-346	AGCTGAGAATTAGGAGCCTTGAGA
Predict-miR-347	AGGACTAGTTTGGAAACTCAAATC
Predict-miR-348	AAATGGAGTTTCCAAACTAGCCCT
Predict-miR-349	AGGTCTGTGCTCTTTGTCGAGTGT
Predict-miR-351	ATAGCTCAGTGGTAGAGC
Predict-miR-354	GATGTCTACATGCACCTTTCAT
Predict-miR-355	GCTGTTCACTGTCCGGTGTGCCAT
Predict-miR-356	ATTAGTCCCTAGAAACCAAACACA
Predict-miR-357	ATTAGTCCCTAGAAACCAAACACT
Predict-miR-358	ATTAGTCCCTAGAAACCAAACACT
Predict-miR-359	ATTAGTCCCTAGTAACCAAACACC
Predict-miR-360	ATTGTGAGAGTTAAGTAGACTAGT
Predict-miR-361	GGCCGTTGGCCCGGCCGACCGTTG
Predict-miR-363	GCCATGTTCGGTTACTAGTGG
Predict-miR-364	CCCACTGCAACATCTACAC
Predict-miR-365	GCAGTCTACAGTGCCTGTCCGG
Predict-miR-366	CCGGACAGTCTACAGTGCCTGC

Table 4.5 (continued)

Predict-miR-368	GGGGTCTTAGCCCGAGTCCGAG
Predict-miR-369	CTCTGGTGGAGGCTCGAG
Predict-miR-371	CTTTTCTAGGTACATAGCTTT
Predict-miR-372	CGCAGCCTCTACATATGATATC
Predict-miR-373	GCTATAATTCACCGGACCGTCTGG
Predict-miR-374	ACAAAGAGCTCTTTGCCGAGTGCC
Predict-miR-375	GGTAGCTTCAGCCCCGTAGAC
Predict-miR-376	GGTAGCTTCAGCCCCGTAGAC
Predict-miR-377	TAAACTAAGAACTTCGGAGACA
Predict-miR-378	TAAGGACTCACTTTAGTAAGCC
Predict-miR-379	TAAGGACTCACTTTAGTAAGCC
Predict-miR-381	TAGGGAGCGGAGAACTCGTGCA
Predict-miR-382	TAGTGCGTGACAACTTTCATG
Predict-miR-383	TAGTGCGTGACAACTTTCATG
Predict-miR-384	CCGCTTGCTCAACAGACTCAGATA
Predict-miR-385	TCGAACTGGTCCCTCGGAGGGT
Predict-miR-387	TGATAAAAATTTGAGACTGTT
Predict-miR-388	TGCAACGGAACTGTATAATAACAC
Predict-miR-389	TGCTCCTAAGACTGTAGAACGC
Predict-miR-390	TGCTCCTAAGACTGTAGAACGC
Predict-miR-391	GGCATGTTCGGTTATACCAATCCA
Predict-miR-392	CACGTAATCCTGTTGTCACCA
Predict-miR-393	TGTATGAGCTGTGTTAAGGACA
Predict-miR-394	TGTCATGATATCATATGTAGAGGA
Predict-miR-395	TGTCATGATATCATATGTAGAGGA
Predict-miR-396	TTAGTGTCTTATAGAGTAGTAGA
Predict-miR-397	TTGGATTTTGATTGGATGCAC
Predict-miR-398	AGTTGCAAAGTAGATCGAAAAA
Predict-miR-399	GTCTTTTCAAAGTCCTTTT
Predict-miR-400	AAGAAAACCGTCACTAGAAATCGT
Predict-miR-401	AAGAAACTGGTTTATAGAAATTGA
Predict-miR-402	GCACTGTCCGGTGCCCGATTTCTT
Predict-miR-403	AAGAGAAGCGCACAGATGAAGT
Predict-miR-404	AAGAGAAGCGCACAGATGAAGT

Table 4.5 (continued)

Predict-miR-405	AAGGCTAAAGATTTTGATGTTTGT
Predict-miR-406	GGTGAAATATAAGCCCTT
Predict-miR-407	AATACATATGGATTGGATGAGATT
Predict-miR-408	AATATTCCGGGAATGTAGCAGGTA
Predict-miR-409	GTGTTTGGTTTCTAGTGACTAATT
Predict-miR-410	AATTGGAATGAATTTTGGTTC
Predict-miR-411	ACACTATGTGTAGAAACCTAAGAA
Predict-miR-414	CTAGTCGGTCTACATTGAAACTCT
Predict-miR-415	AGATTACATCGGATATGACC
Predict-miR-416	GCACTGTCCGGTGCCCGATTTCCT
Predict-miR-417	AGGCACTGTAGACTGTCCGGTA
Predict-miR-420	AGATTATATAATCCAACAT
Predict-miR-421	ATTAGTCCCTAGAAACCAAACACT
Predict-miR-422	ATTAGTCCCTAGAAACCAAACACT
Predict-miR-423	CATCTCGACCGGATATTATGCC
Predict-miR-425	CGGACATAAGCTATCTCCGACGGT
Predict-miR-426	CGGACTGTCCGGTGTGTACCAGAC
Predict-miR-427	CGTGATCTCTGTCCACCAAATCAG
Predict-miR-428	CTTACGGTTGGTTGCTAAAAC
Predict-miR-429	CTTACGGTTGGTTGCTAAAAC
Predict-miR-430	GTACGTGGGCCTAATAACTTGG
Predict-miR-431	GTGACCCGGGCTAAACTTTAGCAA
Predict-miR-432	TGGTTCTTTCTTTCCACAACAC
Predict-miR-433	TAAACTAAGAACTTCGGAGACA
Predict-miR-434	GCCCAAAGTTCTTGTGTCTA
Predict-miR-436	TCCGGTTTTATGGCTCCCA
Predict-miR-437	TCGAACTGGTCCCTCGGAGGGT
Predict-miR-438	GGCATACAGGGAGCCAGGCA
Predict-miR-439	TGCTCCTAAGACTGTAGAACGC
Predict-miR-440	TGCTCCTAAGACTGTAGAAGCC
Predict-miR-441	TGCTCCTAAGACTGTAGAAGCC
Predict-miR-442	GCGAGGTCCAGACCCCACACAGCA
Predict-miR-443	TGTATGAGCTGTGTTAAGGACA
Predict-miR-447	TTTAGAATGTTTGAAGAAAGTTGT

Table 4.5 (continued)

Predict-miR-450	TTTTGGATTAGAGAAATATGACGT
Predict-miR-452	AAGAACGTGGGTACCGTCGAACTC
Predict-miR-453	GGGTATCTGAGTGCCCAGCGTCTT
Predict-miR-454	AAGCATCGGCCTACACTCTCAGGT
Predict-miR-455	AAGGAATGAGTATAAAATCTGATG
Predict-miR-456	AATCCTCTCCGATTTTTGGACTCC
Predict-miR-457	ACACACTATATGTAGAAACCTAGC
Predict-miR-458	ACCGAGTTGGAGTAGGCAGGTA
Predict-miR-459	ACTCGGCAAAGAAACTCTTTACCG
Predict-miR-460	TTATTTTATTCCATTTTAGTCT
Predict-miR-461	AGCTCAGCTGGTCTCTGA
Predict-miR-462	AGCTTATGTCCGACGGCTTTGGCC
Predict-miR-463	ATCTGCTCCGACTTTTCTGACAGC
Predict-miR-464	ATTATATAAGTTGGATTATGA
Predict-miR-465	ATTTGGAGGTTGTGCCCT
Predict-miR-467	CAATTCAACCGTTGGGGTAGGCTG
Predict-miR-468	CATCTCGACCGGATATTATGCC
Predict-miR-470	CGGAATTTAGCTCTTTGCCGAGTG
Predict-miR-471	TTCCGGTGTACACCGGACAGTCCG
Predict-miR-472	CGGCCTTTCCGACTTTGAAGCA
Predict-miR-473	AGCTCGAGTGAAGCAGACCG
Predict-miR-474	AGCTCGAGTGAAGCAGACCG
Predict-miR-475	AGCTCGAGTGAAGCAGACCG
Predict-miR-476	GGTTCGTGAGAGGTCTAG
Predict-miR-477	CTGAGCCCGGAGGACTTGGAAT
Predict-miR-478	CTTGTTGAATTTACTCCCGCC
Predict-miR-479	ACCCTCCACATCCAACGGTGCTGC
Predict-miR-480	GCCACGTCGACATCCGGTTTGAGC
Predict-miR-482	TAACATATGATGAATTTGAAC
Predict-miR-483	TCACCGAGTTGGAGTAGGCAGA
Predict-miR-484	GCTGGTCCTGGAACCCGAGATGGA
Predict-miR-485	GCTGGTCCTGGAACCCGAGATGGA
Predict-miR-486	TCCCCACGGACGGCGCCC
Predict-miR-487	GCGAGGTCCAGACCCCACACAGCA

Table 4.5 (continued)

Predict-miR-488	GGTAGTTCAGGGGCACCTACA
Predict-miR-489	GCATAGTTAGCCACAAACCAAACA
Predict-miR-490	GCTAAACATTAGTCCCTAGAA
Predict-miR-491	TTGTCATATAGAACCGCCAGT
Predict-miR-493	GGATCCTACACTCTTTACTAAA
Predict-miR-494	TTTGTACTAGATGTAGAGATGC
Predict-miR-495	AAAGACGTTAGATCTAAAATGAGT
Predict-miR-496	GCCTTCTTCTTTTTGCCGTCCTTT
Predict-miR-497	AACGAGCCAGCTCGAACTCGGACA
Predict-miR-498	GCACTGTCCGGTGCCCGATTTCTT
Predict-miR-500	AATCCCTTGCTATTCAATTTTGAAT
Predict-miR-501	AATTCACCGGACTGTCTGGC
Predict-miR-502	ACACTATGTGTAGAAACCTAAGAA
Predict-miR-503	ACACTCGGCAAAGAGCTTCTTCGT
Predict-miR-504	ACTCGGCAAAGGCTCTGTCACCGT
Predict-miR-506	CTTCATTTTATTCCTTTTTAGTCT
Predict-miR-507	AGCACTCGGCAAAGGGACT
Predict-miR-508	CAGTCTTTGCCGAGTGCTGGGCT
Predict-miR-509	AAATGGAGTTACCAAACTAGCCCT
Predict-miR-510	AGGGGTCGGCGCCATAGATCTTGG
Predict-miR-512	CCATGCTCTACTCCTATCCGAGAT
Predict-miR-517	ATGCTTGTGATTTGTGACATGTGT
Predict-miR-518	AGGCTTGTTCGGTTAGCTCTCAAT
Predict-miR-519	TGGTGTTTGACGTCCATCACAAAT
Predict-miR-520	GGCCGTTGGCCCGGCCGACCGTTG
Predict-miR-521	CACCCGGATATGGTGATCCTCA
Predict-miR-523	CATTTTCACTGGCGGTTATCT
Predict-miR-524	CCGGACAGTCTACAGTGCCTGC
Predict-miR-528	CGGACAGTGTCTGGTGGG
Predict-miR-529	CGGTGTGCACCGGACTGTCCGC
Predict-miR-530	CTCTACCACTGTATAAAATTTCAAGT
Predict-miR-531	TGGTCAGAGGAGCGGCGAAG
Predict-miR-532	CTTTGTAAAGGCTACGTAGC
Predict-miR-533	TACCTTCATTAGCCAAACAAAG

Table 4.5 (continued)

Predict-miR-534	GCTCGTCCGGTTCCTGCAGGAT
Predict-miR-537	TAGGATTGGGAATAGAAACATT
Predict-miR-538	TCTGGTCAGGCGCGGACGGTCTGT
Predict-miR-539	TGCCAGTGGAGGCTCTGCTCTC
Predict-miR-540	TGTCATGATATCATATGTAGAGGA
Predict-miR-541	TGTGATATTATGGACTTAAGCA
Predict-miR-543	TTCACCGATCACAAGAGTCTA
Predict-miR-545	TTGGAAACTGTGTGAAACCA
Predict-miR-546	GCAACTTTCTCCAAACATTCTAAA
Predict-miR-548	TTTTTGGACGTGTCGTACTTTT
Predict-miR-549	AAAACGACTACTATTTTAGAACGG
Predict-miR-550	TAGCCACAAACCAAACATGCCCTT
Predict-miR-551	CCTATAGATGTTCCTGAATCACTT
Predict-miR-552	GTGTTTGGTTTATAGAGACTAATT
Predict-miR-553	ACTGGACTGTCCGGTGAACCA
Predict-miR-555	TATAAGGTTCAATGGACT
Predict-miR-556	GAGCATACATTATACTAGTCACT
Predict-miR-557	ACAACTAGATCACAAGTTCACGAT
Predict-miR-559	ATCTTTGCCGAGTGCTGTGGTCAA
Predict-miR-560	ATTAGTCCCTAGAAACCAAACACT
Predict-miR-561	ATTAGTCCCTAGTAACCAAACACC
Predict-miR-562	CATGTGGATTGAGTGAGATTGAAT
Predict-miR-564	ATTTGCTCCTAAAACTGTAGAAGA
Predict-miR-565	ACAGTGCACAGTAGCTGTCCGGTG
Predict-miR-566	CACTTCGATCTTGCCGACTGAGGC
Predict-miR-567	CCCCAAATTGAGCGAGCGGACGGT
Predict-miR-568	ACGGTTGCCAGGCCGACGGTGGCG
Predict-miR-569	CTCCGTCGTTTCCAGGATCCGT
Predict-miR-571	GAGGCATTGGGGTTGAAA
Predict-miR-572	GCGGACCGTCCGGTGAATTATAGC
Predict-miR-573	CCACTAAACTATACCCGC
Predict-miR-574	GCTTCGGATCTGAGTGGTC
Predict-miR-575	GGACACATCGGGCGTCGACCTCGC
Predict-miR-577	GTGTAGTGTCTCTGTCTGAGTT

Table 4.5 (continued)

Predict-miR-578	TAAACTAAGAACTTCGGAGACA
Predict-miR-579	TAAAGGATTATAGGTTGGATT
Predict-miR-580	TCTTTTTATTTGTCGCTGGATAGC
Predict-miR-581	TGAGCCGGTGTACTCTGTCCAGA
Predict-miR-582	GCGAGGTCCAGACCCCACACAGCA
Predict-miR-583	GCTAACATCAAATCTTGTCCA
Predict-miR-584	TGGCGCTCTCTGTTGACGTGGC
Predict-miR-585	TTAGAAAGACTCTTGGAGATG
Predict-miR-586	ATAGTCTCATACTTCTCCGGAA
Predict-miR-587	GCTAAACATTAGTCCCTAGAA
Predict-miR-593	AATCTTGTTTCCACAGGCGGTTTT
Predict-miR-594	AAGCATCGGCCTACACTCTCAGGT
Predict-miR-595	ACACTCGGCAAAGAACCTAAACCG
Predict-miR-596	ACCGAGTTGGAGTAGGCAGGTA
Predict-miR-597	ACCGAGTTGGAGTAGGCAGGTA
Predict-miR-598	GATCCATGACTTTCGCCCT
Predict-miR-599	GATCCATGACTTTCGCCCT
Predict-miR-600	ATGGAATGGTACGACGATGAATCC
Predict-miR-601	ATGGCTAACTGTGTCACACTTTGC
Predict-miR-602	ATGGCTAACTGTGTCACACTTTGC
Predict-miR-603	AGAGTTGGTACCTCTCAGCCAT
Predict-miR-604	AGTCATCTTAGGTTTCTACACAT
Predict-miR-605	ATTTGCTCCTAAAACTGTAGAAGA
Predict-miR-606	CAATTTAGGGCTTGTTCGGTTAGC
Predict-miR-607	CACATCCGGACAGAGTACACCA
Predict-miR-608	TCTTTGCCGAGTGCCAGATCGTG
Predict-miR-610	GAAGAGAGTCTCGGTGTAGTGC
Predict-miR-611	ACCCTCCACATCCAACGGTGCTGC
Predict-miR-612	GCGCCTATAGGCCGGACGGTCCGC
Predict-miR-613	GCGGACCGTCCGGTGAATTATAGC
Predict-miR-614	GGATTGAGGTAGAACCGAACAAGC
Predict-miR-615	GTGTGGCACTATGTGTAGAAACCT
Predict-miR-616	TGGTTCTTTCTTTCCACAACAC
Predict-miR-617	ACTTTATAGTACGGCTAAAAC

Table 4.5 (continued)

Predict-miR-618	TAACATATGATGAATTTGAAC
Predict-miR-619	GGTTGACAAACTAGCCCTTA
Predict-miR-621	TGAATGGATTAACGAGATA
Predict-miR-622	TGAGCCGGTGTACTCTGTCCAGA
Predict-miR-623	TGGTTGAAGTCTCTAGCGACGC
Predict-miR-624	TGTATGAGCTGTGTTAAGGACA
Predict-miR-625	TGTCATGATATCATATGTAGAGGA
Predict-miR-626	TTGGCGAAAGCTCTTGATGACA
Predict-miR-628	GGTACCGACGTTCTTACATGAGTT
Predict-miR-629	GGTACCGACGTTCTTACATGAGTT
Predict-miR-630	TTGCTCCTAAAACTGTAGAAGC
Predict-miR-631	TTGCTCCTAAAACTGTAGAAGC
Predict-miR-632	TGATAAAAATTTGAGACTGTT
Predict-miR-634	GTGAGCCTCTGGTCGATGATCAAT
zma-miR156a-3p	GCTCACTTCTCTCTCTGTCAGT
zma-miR156a-5p	TGACAGAAGAGAGTGAGCAC
zma-miR156b-3p	GCTCACCCTCTATCTGTCAGT
zma-miR156b-5p	TGACAGAAGAGAGTGAGCAC
zma-miR156d-3p	GCTCACTTCTCTTTCTGTCAGC
zma-miR156d-5p	TGACAGAAGAGAGTGAGCAC
zma-miR156e-3p	GCTCACTGCTCTCTCTGTCATC
zma-miR156e-5p	TGACAGAAGAGAGTGAGCAC
zma-miR156f-3p	GCTCACTTCTCTTTCTGTCAGC
zma-miR156f-5p	TGACAGAAGAGAGTGAGCAC
zma-miR156g-3p	GCTCACTTCTCTTTCTGTCAGC
zma-miR156g-5p	TGACAGAAGAGAGTGAGCAC
zma-miR156h-3p	GCTCACTGCTCTTTCTGTCATC
zma-miR156h-5p	TGACAGAAGAGAGTGAGCAC
zma-miR156i-3p	GCTCACTGCTCTATCTGTCATC
zma-miR156i-5p	TGACAGAAGAGAGTGAGCAC
zma-miR156j-3p	TGCTCTCTGCTCTCACTGTCATC
zma-miR156j-5p	TGACAGAAGAGAGAGAGCACA
zma-miR156k-3p	GCTCGCTTCTCTTTCTGTCAGC
zma-miR156k-5p	TGACAGAAGAGAGCGAGCAC

Table 4.5 (continued)

zma-miR156l-3p	GCTCACTGCTCTATCTGTCACC
zma-miR156l-5p	TGACAGAAGAGAGTGAGCAC
zma-miR159a-3p	TTTGGATTGAAGGGAGCTCTG
zma-miR159a-5p	GAGCTCCTATCATTCCAATGA
zma-miR159b-3p	TTTGGATTGAAGGGAGCTCTG
zma-miR159c-3p	CTTGGATTGAAGGGAGCTCCT
zma-miR159c-5p	GAGCTCCCTTCGATCCAATCC
zma-miR159d-3p	CTTGGATTGAAGGGAGCTCCT
zma-miR159d-5p	GAGCTCCCTTCGATCCAATCC
zma-miR159f-3p	TTTGGATTGAAGGGAGCTCTG
zma-miR159f-5p	GAGCTCCTCTCATTCCAATGA
zma-miR159j-3p	TTTGGATTGAAGGGAGCTCTG
zma-miR159k-3p	TTTGGATTGAAGGGAGCTCTG
zma-miR160c-5p	TGCCTGGCTCCCTGTATGCCA
zma-miR160d-5p	TGCCTGGCTCCCTGTATGCCA
zma-miR160f-5p	TGCCTGGCTCCCTGTATGCCG
zma-miR160g-3p	GCGTGCAAGGAGCCAAGCATG
zma-miR160g-5p	TGCCTGGCTCCCTGTATGCCA
zma-miR162-3p	TCGATAAACCTCTGCATCCA
zma-miR164a-5p	TGGAGAAGCAGGGCACGTGCA
zma-miR164b-5p	TGGAGAAGCAGGGCACGTGCA
zma-miR164c-3p	CATGTGCCCTTCTTCTCCATC
zma-miR164c-5p	TGGAGAAGCAGGGCACGTGCA
zma-miR164d-5p	TGGAGAAGCAGGGCACGTGCA
zma-miR164e-5p	TGGAGAAGCAGGACACGTGAG
zma-miR164f-3p	CACGTGCGCTCCTTCTCCAAC
zma-miR164f-5p	TGGAGAAGCAGGGCACGTGCT
zma-miR164g-3p	CACGTGCTCCCCTTCTCCACC
zma-miR164g-5p	TGGAGAAGCAGGGCACGTGCA
zma-miR164h-3p	CATGTGCCCTTCTTCTCCATC
zma-miR164h-5p	TGGAGAAGCAGGGCACGTGTG
zma-miR166a-3p	TCGGACCAGGCTTCATTCCCC
zma-miR166a-5p	GGAATGTTGTCTGGCTCGGGG
zma-miR166b-3p	TCGGACCAGGCTTCATTCCC

Table 4.5 (continued)

zma-miR166b-5p	GGAATGTTGTCTGGTTCAAGG
zma-miR166c-3p	TCGGACCAGGCTTCATTCCC
zma-miR166c-5p	GGAATGTTGTCTGGCTCGAGG
zma-miR166d-3p	TCGGACCAGGCTTCATTCCC
zma-miR166d-5p	GGAATGTTGTCTGGTTCAAGG
zma-miR166g-3p	TCGGACCAGGCTTCATTCCC
zma-miR166g-5p	GGAATGTTGTCTGGTTGGAGA
zma-miR166h-3p	TCGGACCAGGCTTCATTCCC
zma-miR166h-5p	GGAATGACGTCCGGTCCGAAC
zma-miR166i-3p	TCGGACCAGGCTTCATTCCC
zma-miR166j-3p	TCGGACCAGGCTTCAATCCCT
zma-miR166k-3p	TCGGACCAGGCTTCAATCCCT
zma-miR166l-3p	TCGGACCAGGCTTCATTCCTC
zma-miR166m-3p	TCGGACCAGGCTTCATTCCTC
zma-miR167a-5p	TGAAGCTGCCAGCATGATCTA
zma-miR167b-3p	GATCATGCTGTGACAGTTTCACT
zma-miR167b-5p	TGAAGCTGCCAGCATGATCTA
zma-miR167c-3p	GATCATGCTGTGGCAGCCTCACT
zma-miR167c-5p	TGAAGCTGCCAGCATGATCTA
zma-miR167d-5p	TGAAGCTGCCAGCATGATCTA
zma-miR167e-3p	GATCATGCTGTGCAGTTTCATC
zma-miR167e-5p	TGAAGCTGCCAGCATGATCTG
zma-miR167f-5p	TGAAGCTGCCAGCATGATCTG
zma-miR167g-3p	GGTCATGCTGTAGTTTCATC
zma-miR167g-5p	TGAAGCTGCCAGCATGATCTG
zma-miR167h-3p	GATCATGTTGCAGCTTCAC
zma-miR167h-5p	TGAAGCTGCCAGCATGATCTG
zma-miR167i-3p	GATCATGTTGCAGCTTCAC
zma-miR167i-5p	TGAAGCTGCCAGCATGATCTG
zma-miR167j-3p	GATCATGTGGCAGTTTCATT
zma-miR167j-5p	TGAAGCTGCCAGCATGATCTG
zma-miR168a-3p	CCCGCCTTGCACCAAGTGAA
zma-miR168a-5p	TCGCTTGGTGCAGATCGGGAC
zma-miR168b-3p	CCCGCCTTGCATCAAGTGAA

Table 4.5 (continued)

zma-miR168b-5p	TCGCTTGGTGCAGATCGGGAC
zma-miR169c-3p	GGCAAGTCTGTCCTTGGCTACA
zma-miR169k-5p	TAGCCAAGGATGACTTGCCTG
zma-miR169o-3p	GGCAGGTCTTCTTGGCTAGC
zma-miR169o-5p	TAGCCAAGAATGACTTGCCTA
zma-miR169p-5p	TAGCCAAGGATGACTTGCCGG
zma-miR171b-3p	TTGAGCCGTGCCAATATCAC
zma-miR171c-3p	TGACTGAGCCGTGCCAATATC
zma-miR171d-3p	TGATTGAGCCGTGCCAATATC
zma-miR171d-5p	TGTTGGCTCGGCTCACTCAGA
zma-miR171e-3p	TGATTGAGCCGTGCCAATATC
zma-miR171e-5p	TGTTGGCTCGGCTCACTCAGA
zma-miR171f-3p	TTGAGCCGTGCCAATATCACA
zma-miR171f-5p	CGATGTTGGCATGGCTCAATC
zma-miR171i-3p	TGATTGAGCCGTGCCAATATC
zma-miR171i-5p	TGTTGGCACGGTTCAATCAAA
zma-miR171j-3p	TGATTGAGCCGTGCCAATATC
zma-miR171l-3p	GGATTGAGCCGCGTCAATATC
zma-miR171n-3p	TGATTGAGCCGCGCCAATATC
zma-miR319a-3p	TTGGACTGAAGGGTGCTCCC
zma-miR319b-3p	TTGGACTGAAGGGTGCTCCC
zma-miR319b-5p	AGAGCGTCCTTCAGTCCACTC
zma-miR319c-3p	TTGGACTGAAGGGTGCTCCC
zma-miR319d-3p	TTGGACTGAAGGGTGCTCCC
zma-miR319d-5p	AGAGCGTCCTTCAGTCCACTC
zma-miR390a-3p	CGCTATCTATCCTGAGCTCCA
zma-miR390a-5p	AAGCTCAGGAGGGATAGCGCC
zma-miR390b-3p	CGCTATCTATCCTGAGCTCCA
zma-miR390b-5p	AAGCTCAGGAGGGATAGCGCC
zma-miR393a-3p	ATCAGTGCAATCCCTTTGGAAT
zma-miR393a-5p	TCCAAAGGGATCGCATTGATCT
zma-miR393b-5p	TCCAAAGGGATCGCATTGATCC
zma-miR393c-3p	GTCAGTGCAATCCCTTTGGAAT
zma-miR393c-5p	TCCAAAGGGATCGCATTGATCT

Table 4.5 (continued)

zma-miR394a-5p	TTGGCATTCTGTCCACCTCC
zma-miR394b-5p	TTGGCATTCTGTCCACCTCC
zma-miR395a-3p	GTGAAGTGTTTGGGGGAACTC
zma-miR395a-5p	GTTCTCCTCAAACCACTTCAGTT
zma-miR395b-3p	GTGAAGTGTTTGGGGGAACTC
zma-miR395b-5p	GTTCCCTACAAGCACTTCACAA
zma-miR395f-3p	GTGAAGTGTTTGGGGGAACTC
zma-miR395i-3p	GTGAAGTGTTTGGGGGAACTC
zma-miR395i-5p	GTTCCCTACAAGCACTTCACGA
zma-miR395n-3p	GTGAAGTGTTTGGGGGAACTC
zma-miR395n-5p	GTTCTCTACAAGCACTTCACGA
zma-miR395p-3p	GTGAAGTGTTTGGGGGAACTC
zma-miR395p-5p	GTTCCCTTCAAGCACTTCACAT
zma-miR396a-3p	GTTCAATAAAGCTGTGGGAAA
zma-miR396a-5p	TTCCACAGCTTTCTTGAACTG
zma-miR396b-3p	GTTCAATAAAGCTGTGGGAAA
zma-miR396b-5p	TTCCACAGCTTTCTTGAACTG
zma-miR396c	TTCCACAGGCTTTCTTGAACTG
zma-miR396d	TTCCACAGGCTTTCTTGAACTG
zma-miR396e-5p	TTCCACAGCTTTCTTGAACTT
zma-miR396f-5p	TTCCACAGCTTTCTTGAACTT
zma-miR396g-3p	GTTCAAGAAAGCTGTGGAAGA
zma-miR396g-5p	TCCCACAGCTTTATTGAACTG
zma-miR396h	TCCCACAGCTTTATTGAACTG
zma-miR397a-5p	TCATTGAGCGCAGCGTTGATG
zma-miR397b-3p	CCAGCGCTGCACTCAATTACG
zma-miR397b-5p	TCATTGAGCGCAGCGTTGATG
zma-miR398a-3p	TGTGTTCTCAGGTCGCCCCCG
zma-miR398a-5p	GGGGCGAACTGAGAACACATG
zma-miR398b-3p	TGTGTTCTCAGGTCGCCCCCG
zma-miR398b-5p	GGGGCGGACTGGGAACACATG
zma-miR399e-3p	TGCCAAAGGAGAGTTGCCCTG
zma-miR399h-3p	TGCCAAAGGAGAATTGCCCTG
zma-miR399i-3p	TGCCAAAGGAGAGTTGCCCTG

Table 4.5 (continued)

zma-miR399j-5p	AGGCAGCTCTCCTCTGGCAGG
zma-miR408b-3p	CTGCACTGCCTCTTCCCTGGC
zma-miR408b-5p	CAGGGACGAGGCAGAGCATGG
zma-miR528a-3p	CCTGTGCCTGCCTCTTCCATT
zma-miR528a-5p	TGGAAGGGGCATGCAGAGGAG
zma-miR528b-3p	CCTGTGCCTGCCTCTTCCATT
zma-miR528b-5p	TGGAAGGGGCATGCAGAGGAG
zma-miR529-3p	GCTGTACCCTCTCTCTTCTTC
zma-miR529-5p	AGAAGAGAGAGAGTACAGCCT
zma-miR827-3p	TTAGATGACCATCAGCAAACA
zma-miR827-5p	TTTGTTGGTGGTCATTTAACC
zma-miR1432-5p	CTCAGGAGAGATGACACCGAC

miRNAs labelled as “zma-miR” are previously known, while “Predict-miR” miRNAs are previously undescribed.

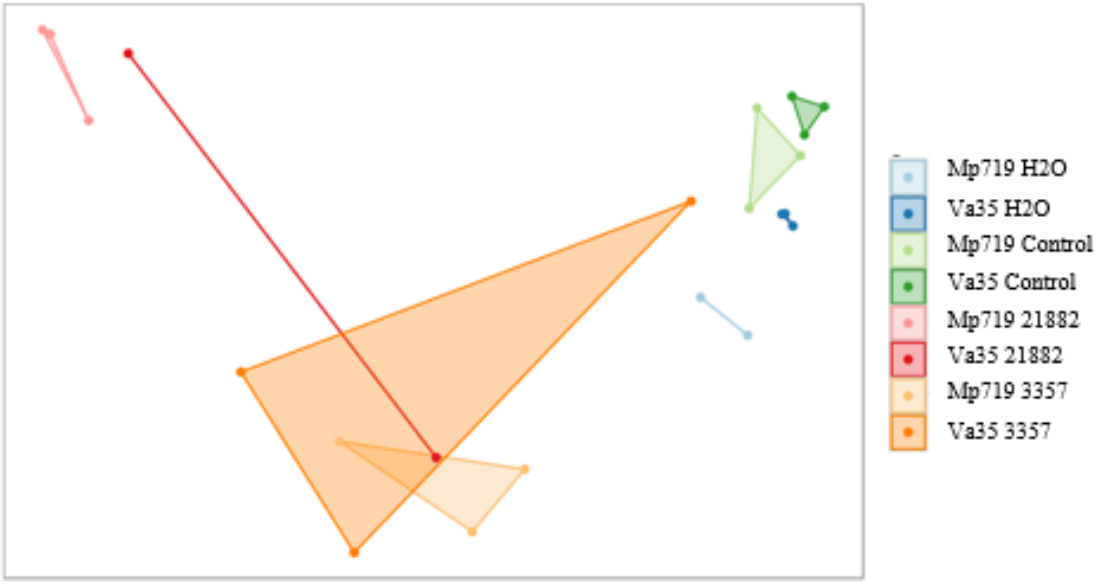

Figure 4.7 A PCA plot of *Z. mays* small RNAs

The RNA-seq data analysis software, edgeR, was used to determine differential expression of these miRNAs. The statistically significant (based on false discovery rate) differentially expressed miRNAs are shown in Figures 4.8-4.11. These results are congruent with what is visualized in the PCA plot. Much of the differential expression occurs when comparing inoculated with control samples.

The comparison of differential expression of miRNAs in the control and water inoculation samples is shown in Figure 4.8. When comparing the expression of Mp719 Control–Va35 Control with Mp719 H_2O–Va35 H_2O samples, there was a similar differential expression pattern, meaning that with or without inoculation, the miRNA expression was different between the two maize lines.

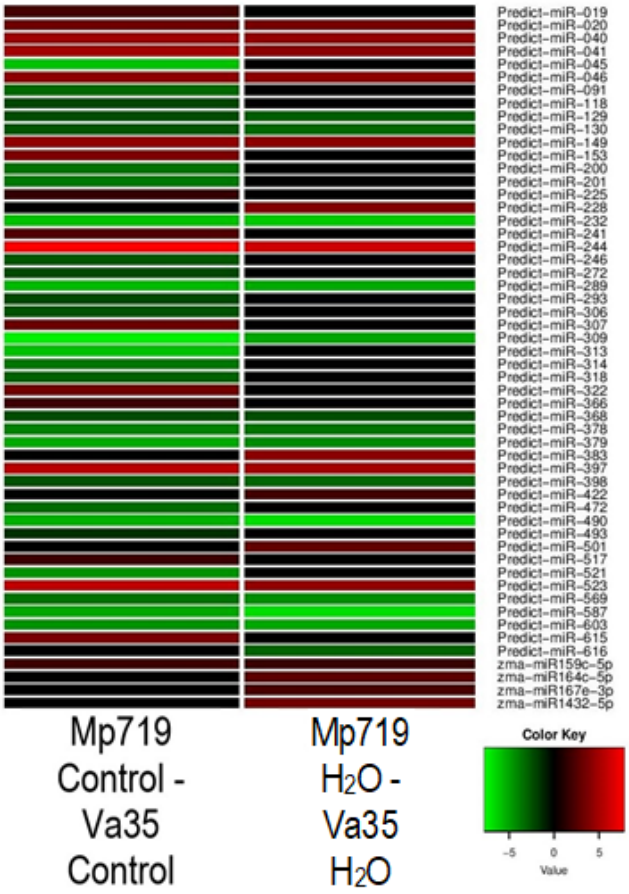

Figure 4.8 Heat map of differentially expressed *Z. mays* miRNAs comparing control and water inoculations

The differential expression of maize miRNAs is indicated when the $\log_2$(Fold Change) values are larger or equal to 1. Decreased expression is represented by a green color, while increased expression is represented by a red color, with the brightness indicating relative intensity. Significance of the differential expression is determined by FDR ($p <= 0.05$).

The comparison of differential expression of miRNAs in the *A. flavus* inoculation samples is shown in Figure 4.9. When comparing the two maize lines that were inoculated individually with *A. flavus* NRRL 3357 or 21882 (Mp719 3357–Va35 3357 and Mp719 21882–Va35 21882), there were few miRNAs that were differentially expressed in either case. This is surprising when compared to results reported in Figure 4.8, which seem to indicate a difference in miRNA expression between the maize lines.

The greater variation between the *A. flavus*-inoculated samples when compared to the control and water-inoculated samples, seen in Figure 4.7, may explain this large difference in significantly differentially expressed miRNAs.

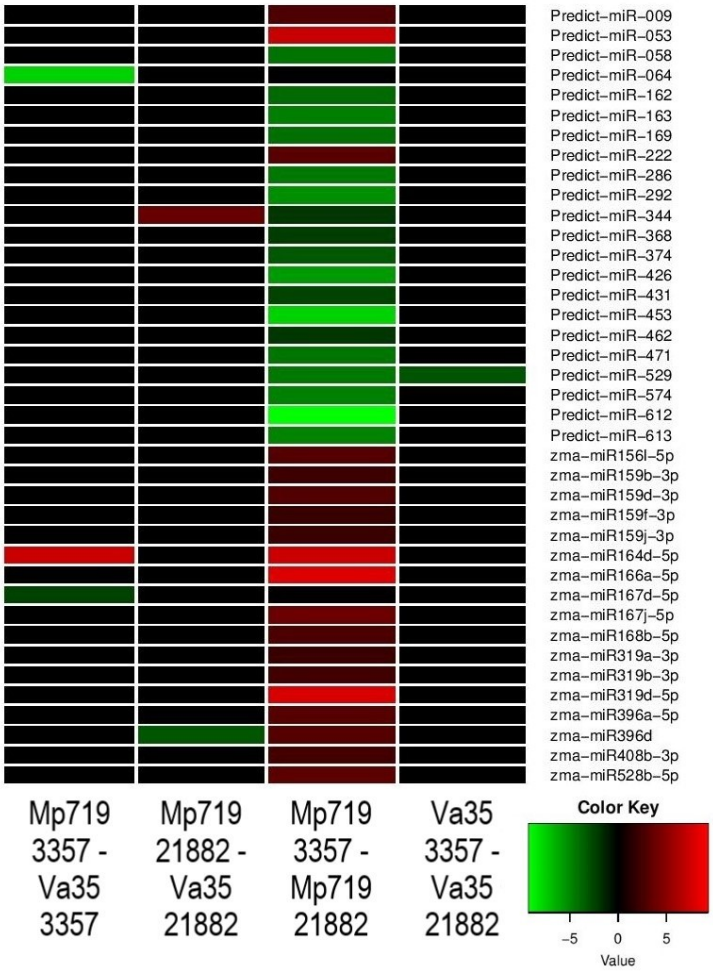

Figure 4.9 Heat map of differentially expressed *Z. mays* miRNAs comparing *A. flavus* inoculations

The differential expression of maize miRNAs is indicated when the $\log_2$(Fold Change) values are larger or equal to 1. Decreased expression is represented by a green color, while increased expression is represented by a red color, with the brightness indicating relative intensity. Significance of the differential expression is determined by FDR ($p <= 0.05$).

As shown in Figure 4.9, the comparison of both Mp719 3357–Mp719 21882 and Va35 3357–Va35 21882 aligned well with how these samples were grouped in Figure 4.7, in that the Va35 samples were similar, while the Mp719 samples were more separate in Figure 4.7. There was obviously more differentially expressed miRNAs in Mp719 than those in Va35, which might indicate a response based on resistance to the aflatoxigenic strain when compared to the nonaflatoxigenic strain. Except for a single miRNA (Predict-miR-529) which was down-regulated in both Mp719 3357-Mp719 21882 and Va35 3357-Va35 21882 samples, there are 19 up-regulated (Predict-miR-009, 053, 222, zma-miR156l-5p, 159b-3p,159d-3p, 159f-3p, 159j-3p, 164d-5p, 166a-5p, 167j-5p, 168b-5p, 319a-3p, 319b-3p, 319d-5p, 396a-5p, 396d, 408b-3p, and 528b-5p) and 18 down-regulated (Predict-miR-058, 162, 163, 169, 286, 292, 344, 368, 374, 426, 431, 453, 462, 471, 529, 574, 612, 613) miRNAs in Mp719 3357-Mp719 21882, and they might be part of resistance mechanisms related to the maize response to aflatoxin production.

The comparison of differential expression of maize miRNAs between the inoculation and control samples in Mp719 and Va35 is shown in Figures 4.10 and 4.11. Three miRNAs including Predict-miR-361, zma-miR159f-3p, and zma-miR160c-5p had similar differential expression (one upregulated and two downregulated) in the Mp719 H_2O–Mp719 Control and Va35 H_2O–Va35 Control samples, and they might represent a physical damage response by inoculation of water to the maize lines (Figures 4.10 and 4.11). Most of the targets for these miRNAs were uncharacterized proteins. The 21 miRNAs (Predict-miR-064, 075, 159, 168, 228, 374, 385, 452, 528, 616, zma-miR164c-5p, 164h-5p, 166a-5p, 167e-5p, 168a-3p, 168b-3p, 408b-3p, 528a-3p, 528a-5p, 528b-5p, and 1432-5p) that were differentially expressed in Mp719 but not in Va35 might play a

role in the resistance of Mp719 to fungal infection, in explaining how maize kernels respond to the initial infection (Figures 4.10 and 4.11). In these comparisons, it was also noteworthy that the maize miRNAs were more differentially expressed in the resistant line (Mp719 H_2O–Mp719 Control) than the susceptible line (Va35 H_2O–Va35 Control) (Figures 4.10 and 4.11).

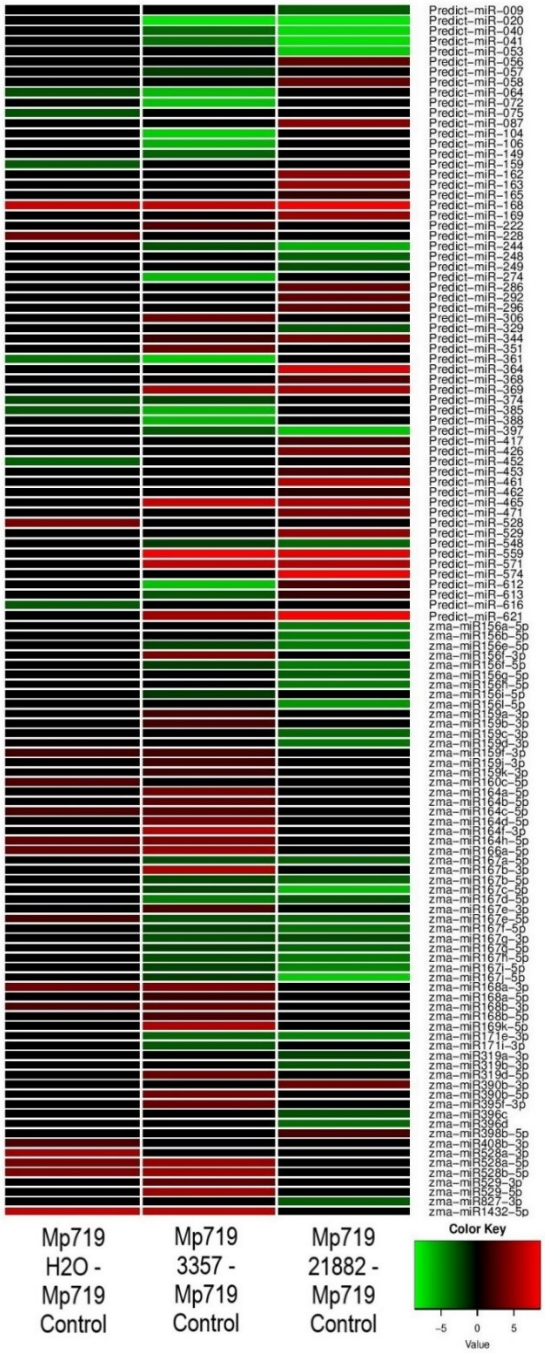

Figure 4.10 Heat map of differentially expressed *Z. mays* miRNAs comparing inoculations in the resistant maize line

The differential expression of maize miRNAs is indicated when the $\log_2$(Fold Change) values are larger or equal to 1. Decreased expression is represented by a green color, while increased expression is represented by a red color, with the brightness indicating relative intensity. Significance of the differential expression is determined by FDR ($p <= 0.05$).

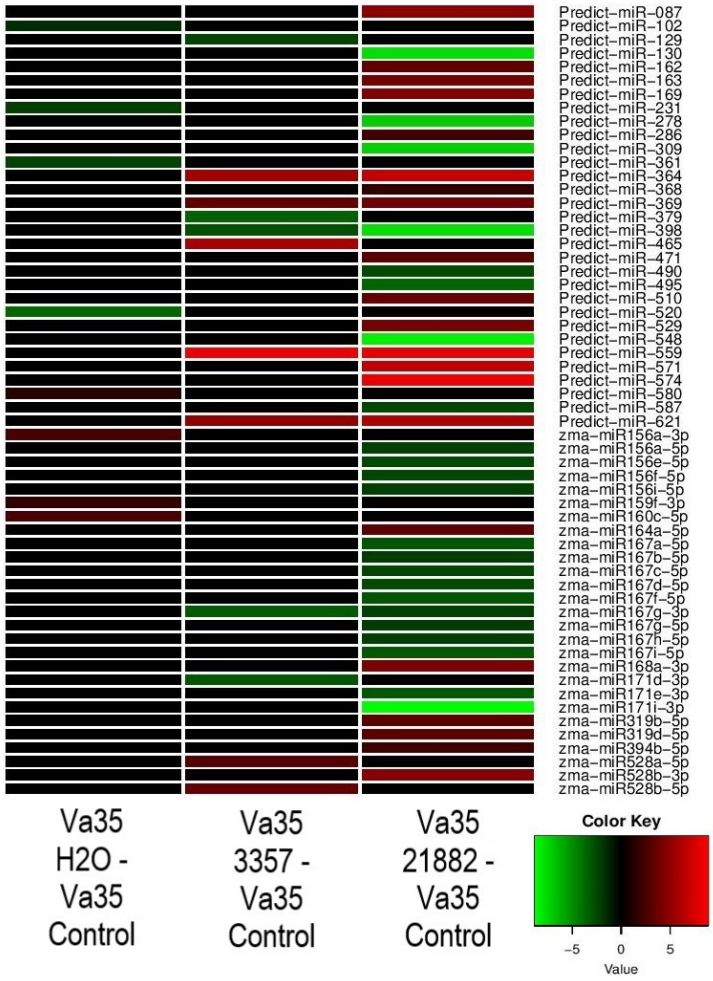

Figure 4.11 Heat map of differentially expressed *Z. mays* miRNAs comparing inoculations in the susceptible maize line

The differential expression of maize miRNAs is indicated when the $\log_2$(Fold Change) values are larger or equal to 1. Decreased expression is represented by a green color, while increased expression is represented by a red color, with the brightness indicating relative intensity. Significance of the differential expression is determined by FDR ($p <= 0.05$).

When comparing the *A. flavus* inoculated and control (non-inoculated) samples (Mp719 3357–Mp719 Control, Mp719 21882–Mp719 Control, Va35 3357–Va35 Control, Va35 21882–Va35 Control), four miRNAs – Predict-miR-369, Predict-miR-559, Predict-miR-621, and zma-miR167g-3p – were found to share similar differential

expression patterns across all four comparisons (Figures 4.10 and 4.11). Again, a major portion of these targets were uncharacterized (Table S1). These miRNAs could be part of the response to *A. flavus* infection as well.

Except for those miRNAs that were similarly differentially expressed in either Mp719 H_2O–Mp719 control or Mp719 21882-Mp719 control samples, eleven miRNAs (Predict-miR-057, 072, 104, 106, 149, 274, 388, 612, 613, zma-miR156i-5p, and 171i-3p) had decreased expression and twenty-two miRNAs (Predict-miR-222, 306, 351, zma-miR156f-3p, 159a-3p, 159b-3p, 159j-3p, 159k-3p, 164a-5p, 164b-5p, 164d-5p, 164f-3p, 167b-5p,167e-3p, 168a-5p, 168b-5p, 169k-5p, 319d-5p, 390b-5p, 395f-3p, 529-3p, 529-5p) had increased expression in Mp719 3357–Mp719 control (Figure 4.10). Except for those that were similarly differentially expressed in either Va35 H_2O–Va35 control or Va35 21882–Va35 control, three (Predict-miR-129, 379, zma-miR171d-3p) had decreased expression and two (Predict-miR-465 and zma-miR528a-5p) with increased expression in Va35 3357–Va35 control (Figure 4.11). None of these miRNAs had similar expression when compared with the Mp719 3357-Mp719 control samples. The differentially expressed miRNAs in the comparison of Mp719 3357 to Mp719 control may play a role in resistant maize response to aflatoxin production, that is distant from the response to either inoculation or *A. flavus* growth.

RT-qPCR

The qPCR analysis of the 135 *A. flavus* milRNAs identified by Bai *et al.* (2015) was performed to better understand the expression of these milRNAs in the two maize lines inoculated with the *A. flavus* 3357 or 21882 strain. Several milRNAs, shown in Figure 4.12, including Afl-milR-12, 16, 19, 22, 25, 27, 29, 31 and 39 had more than 50-

fold downregulation when compared the Mp719-3357 to Va35-3357 samples. These milRNAs were not differentially expressed under the experimental conditions described by Bai *et al.* (2015); however, one milRNA (Afl-milR-33) was found to be upregulated and it might be involved in the biosynthesis of ustiloxin B. Two of these milRNAs (Afl-milR-7 and Afl-milR-92) were identified from the small RNA-seq experiments reported here, but neither was differentially expressed under our experimental conditions.

These milRNAs with high levels of differential expression, particularly Afl-milR-12, may represent a response by *A. flavus* to the growth on a resistant compared to a susceptible host. These milRNAs, along with milRNAs and miRNAs described previously, represent an interaction between *A. flavus* and its maize host at the miRNA/milRNA level.

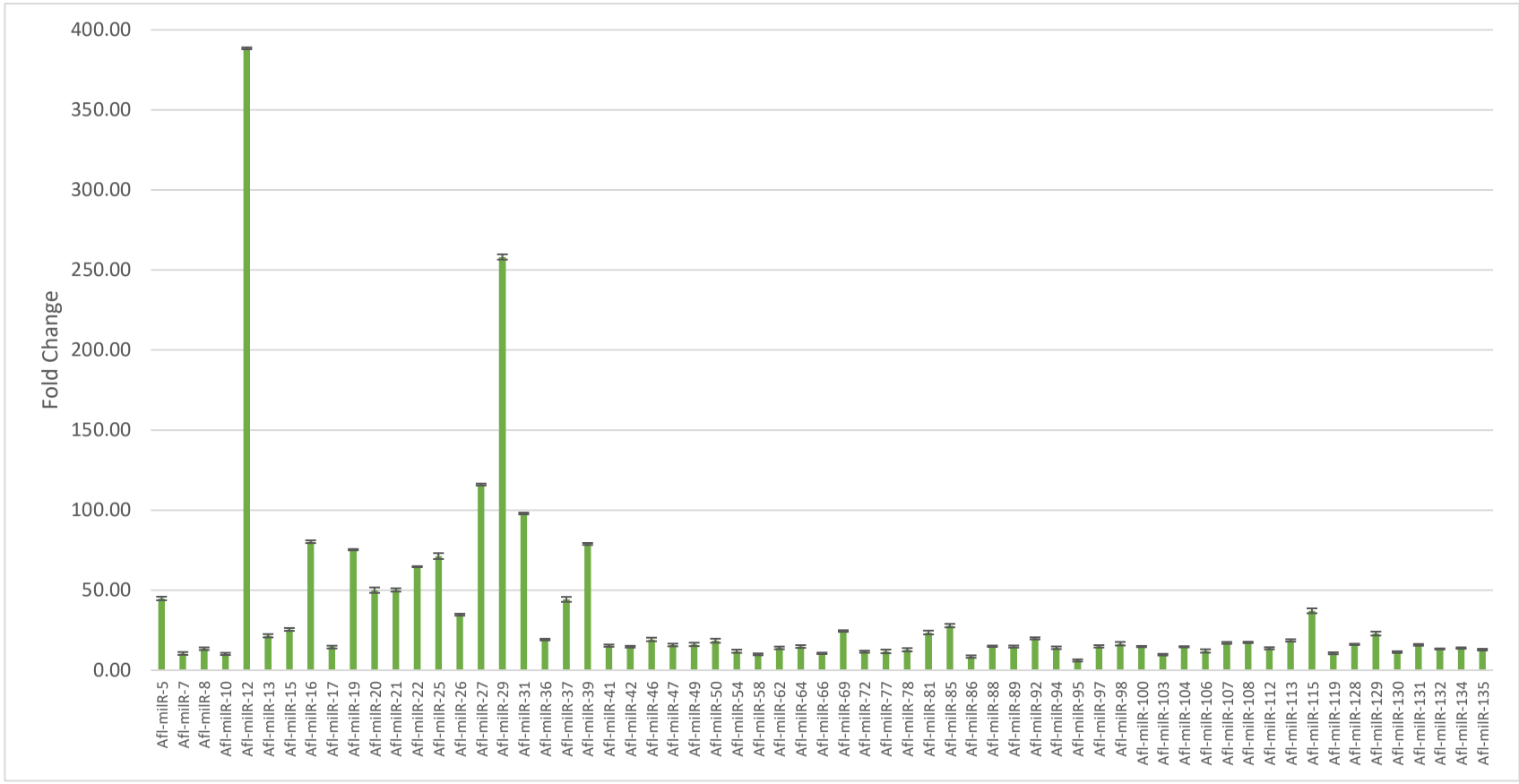

Figure 4.12 Expression analysis of *A. flavus* milRNAs between Mp719 – 3357 and Va35 – 3357 samples determined by RT-qPCR

Bars represent the decrease in expression in comparing Mp719 – 3357 to Va35 – 3357. Fold change was determined by the delta-delta C_t method. Error bars represent standard deviation. Statistical significance was determined by a T-test.

CHAPTER V

DISCUSSION

This research has provided insight into the host-pathogen relationship between *A. flavus* and maize at the molecular level. The small RNA sequencing analysis identified 62 *A. flavus* milRNAs and 523 *Z. mays* miRNAs that were previously undescribed. Differential expression analysis of *A. flavus* milRNAs and *Z. mays* miRNAs via comparison under different experimental conditions would be useful for studying the mechanisms of maize response to fungal inoculation, *A. flavus* growth, and aflatoxin production. So far, no *A. flavus* milRNAs were found to be related to aflatoxin biosynthesis; however, some of the differentially expressed maize miRNAs were shown to target the mRNA of chitinases, proteases, and other proteins relevant to antifungal activity, although they are not the enzymes that are known as antifungals (De Lucca et al. 2005).

Further research into the maize miRNAs in response to inoculation, *A. flavus* growth, and aflatoxin biosynthesis may lead to a better understanding of maize resistance to *A. flavus* and aflatoxin production. Additionally, these miRNAs may also respond to other pathogens affecting corn, and the identified miRNAs could be used by other agriculturally important plants to protect against the infection by pathogens. This research could facilitate further research into the interaction of plant miRNAs with fungal pathogens.

Another path for this research is toward the development of either *A. flavus* milRNAs or maize miRNAs as biomarkers of *A. flavus* infection and aflatoxin production. Although aflatoxin biomarkers have traditionally been metabolites (Kensler et al. 2011; Lau et al. 2006; Wild 2002), small non-coding RNAs like miRNAs have been presented as an additional avenue for biomarkers that, with next-generation sequencing technology, could be cheap and easy to quantify (Lopez et al. 2015). The research from this study has provided a promising number of *A. flavus* milRNAs and maize miRNAs that could be utilized as biomarkers of either *A. flavus* growth or aflatoxin production. With further investigation, these hypothetical biomarkers could enhance the current methods of testing for aflatoxin contamination in maize and other affected agricultural products, which could have impacts on the global economy and health worldwide.

This research adds to the growing number of known fungal milRNAs. Recently, milRNAs have been identified in an increasing number of fungal species including *Neurospora crassa, Fusarium oxysporum, Penicillium* spp., and others (Lau et al. 2013; Wang et al. 2017; Dahlmann and Kück 2015; Lin et al. 2015; Zhou et al. 2012; Kang et al. 2013; Liu et al. 2016; Yang et al. 2013; Huang and Evans 2016; Jiang et al. 2017; Chen et al. 2014; Zhou et al. 2012; Mueth et al. 2015; Lau et al. 2017). These results provide important insight into various fungal pathogens, and overall there is a generally standardized method of milRNA prediction. However, many methods utilize the miRNA database (miRBase) to identify homologous sequences, with the majority of newly found milRNAs having no homologous sequences (Jiang et al. 2017; Lin et al. 2015; Zhou et al. 2012; Zhou et al. 2012; Kang et al. 2013; Liu et al. 2016; Lau et al. 2013; Chen et al. 2014). This is likely due to the lack of fungal milRNAs in miRBase. Inclusion of all

miRNAs and milRNAs in the database could help to better understand the evolution of fungal milRNAs and milRNA families.

CHAPTER VI

CONCLUSION

This research has identified 62 new *A. flavus* milRNAs and 523 undescribed *Z. mays* miRNAs. Based on differential expression of RNA-seq data, the milRNA and miRNA response to the experimental conditions have been described. Several miRNAs responding to *A. flavus* infection, growth, and aflatoxin production, as well as possibly having a role in maize resistance to *A. flavus* were identified. With further investigation, these small RNAs could be utilized as biomarkers of *A. flavus* growth or aflatoxin production, which could have positive health and economic benefits around the world.

REFERENCES

Abbas, HK, RM Zablotowicz, BW Horn, NA Phillips, BJ Johnson, X Jin, and CA Abel. 2011. "Comparison of Major Biocontrol Strains of Non-Aflatoxigenic *Aspergillus flavus* for the Reduction of Aflatoxins and Cyclopiazonic Acid in Maize." *Food Additives and Contaminants - Part A Chemistry, Analysis, Control, Exposure and Risk Assessment* 28 (2). Taylor & Francis Group: 198–208. doi:10.1080/19440049.2010.544680.

Amaike, Saori, and Nancy P Keller. 2011. "*Aspergillus Flavus*." *Annual Review of Phytopathology* 49 (1): 107–33. doi:10.1146/annurev-phyto-072910-095221.

Asters, Matthew C, W Paul Williams, Andy D Perkins, J Erik Mylroie, Gary L Windham, and Xueyan Shan. 2014. "Relating Significance and Relations of Differentially Expressed Genes in Response to *Aspergillus flavus* Infection in Maize." *Scientific Reports* 4: 4815. doi:10.1038/srep04815.

Axtell, Michael J, Jakub O Westholm, and Eric C Lai. 2011. "Vive La Différence : Biogenesis and Evolution of microRNAs in Plants and Animals." *Genome Biology* 12: 221.

Bai, Youhuang, Faxiu Lan, Weiqiang Yang, Feng Zhang, Kunlong Yang, Zhenguo Li, Peili Gao, and Shihua Wang. 2015. "sRNA Profiling in *Aspergillus flavus* Reveals Differentially Expressed miRNA-like RNAs Response to Water Activity and Temperature." *Fungal Genetics and Biology* 81: 113–19. doi:10.1016/j.fgb.2015.03.004.

Baldrich, Patricia, Sonia Campo, Ming-Tsung Wu, Tze-Tze Liu, Yue-Ie Caroline Hsing, and Blanca San Segundo. 2015. "microRNA-Mediated Regulation of Gene Expression in the Response of Rice Plants to Fungal Elicitors." *RNA Biology* 12 (8): 847–63. doi:10.1080/15476286.2015.1050577.

Bennett, W Joan. 2010. "An Overview of the Genus *Aspergillus*." Edited by Masayuki Machida and Katsuya Gomi. *Aspergillus: Molecular Biology and Genomics*. Caister Academic Press, 1–17. doi:doi:10.1201/9781420008517.sec1.

Bhatnagar-Mathur, Pooja, Sowmini Sunkara, Madhurima Bhatnagar-Panwar, Farid Waliyar, and Kiran Kumar Sharma. 2015. "Biotechnological Advances for Combating *Aspergillus flavus* and Aflatoxin Contamination in Crops." *Plant Science*. Elsevier. doi:10.1016/j.plantsci.2015.02.009.

Borges, Filipe, and Robert A Martienssen. 2016. "The Expanding World of Small RNAs in Plants." *Nature Reviews Molecular and Cell Biology* 16 (12): 727–41. doi:10.1038/nrm4085.

Chen, Rui, Nan Jiang, Qiyan Jiang, Xianjun Sun, Yong Wang, Hui Zhang, and Zheng Hu. 2014. "Exploring microRNA-like Small RNAs in the Filamentous Fungus *Fusarium oxysporum*." *PLoS ONE* 9 (8): e104956. doi:10.1371/journal.pone.0104956.

Dahlmann, Tim A, and Ulrich Kück. 2015. "Dicer-Dependent Biogenesis of Small RNAs and Evidence for microRNA-like RNAs in the Penicillin Producing Fungus *Penicillium chrysogenum*." *PLoS ONE* 10 (5): e0125989. doi:10.1371/journal.pone.0125989.

De Lucca, AJ, TE Cleveland, and DE Wedge. 2005. "Plant-Derived Antifungal Proteins and Peptides." *Canadian Journal of Microbiology* 51 (12): 1001–14. doi:10.1139/w05-063.

Eldem, Vahap, Sezer Okay, and Turgay Ünver. 2013. "Plant microRNAs: New Players in Functional Genomics." *Turkish Journal of Agriculture and Forestry* 37 (1): 1–21. doi:10.3906/tar-1206-50.

Farfan, Ivan D Barrero, Gerald N De La Fuente, Seth C Murray, Thomas Isakeit, Pei-Cheng Huang, Marilyn Warburton, Paul Williams, Gary L Windham, and Mike Kolomiets. 2015. "Genome Wide Association Study for Drought, Aflatoxin Resistance, and Important Agronomic Traits of Maize Hybrids in the Sub-Tropics." *PLoS ONE* 10 (2): e0117737. doi:10.1371/journal.pone.0117737.

Fountain, Jake C, Brian T Scully, Xinzhi Ni, Robert C Kemerait, Robert D Lee, Zhi Yuan Chen, and Baozhu Guo. 2014. "Environmental Influences on Maize-*Aspergillus flavus* Interactions and Aflatoxin Production." *Frontiers in Microbiology*. doi:10.3389/fmicb.2014.00040.

Hedayati, MT, AC Pasqualotto, PA Warn, P Bowyer, and DW Denning. 2007. "*Aspergillus flavus*: Human Pathogen, Allergen and Mycotoxin Producer." *Microbiology* 153: 1677–92. doi:10.1099/mic.0.2007/007641-0.

Horn, Bruce W, Geromy G Moore, and Ignazio Carbone. 2009. "Sexual Reproduction in *Aspergillus flavus*." *Mycologia* 101 (3). Taylor & Francis: 423–29. doi:10.3852/09-011.

Huang, Qiang, and Jay D Evans. 2016. “Identification of microRNA-like Small RNAs from Fungal Parasite *Nosema ceranae*.” *Journal of Invertebrate Pathology* 133. Elsevier Inc.: 107–9. doi:10.1016/j.jip.2015.12.005.

Huntley, Rachael P, Dmitry Sitnikov, Marija Orlic-Milacic, Rama Balakrishnan, Peter D’Eustachio, Marc E Gillespie, Doug Howe, Anastasia Z Kalea, Lars Maegdefessel, David Osumi-Sutherland, Victoria Petri, Jennifer R Smith, Kimberly Van Auken, Valerie Wood, Anna Zampetaki, Manuel Mayr, Ruth C Lovering. 2016. “Guidelines for the Functional Annotation of microRNAs Using the Gene Ontology.” *RNA* 22 (5). Cold Spring Harbor Laboratory Press: 667–76. doi:10.1261/rna.055301.115.

Jiang, Xuefei, Fei Qiao, Yali Long, Hanqing Cong, and Huapeng Sun. 2017. “microRNA-like RNAs in Plant Pathogenic Fungus *Fusarium oxysporum* f. Sp. Niveum Are Involved in Toxin Gene Expression Fine Tuning.” *3 Biotech* 7 (5). doi:10.1007/s13205-017-0951-y.

Kang, Kang, Jiasheng Zhong, Liang Jiang, Gang Liu, Christine Yuan Gou, Qiong Wu, You Wang, Jun Luo, and Deming Gou. 2013. “Identification of microRNA-Like RNAs in the Filamentous Fungus *Trichoderma reesei* by Solexa Sequencing.” *PLoS ONE* 8 (10): e76288. doi:10.1371/journal.pone.0076288.

Kelley, Rowena Y, W Paul Williams, J Erik Mylroie, Deborah L Boykin, Leigh K Hawkins, Gary L Windham, Thomas D Brooks, Susan M Bridges, Brian E Scheffler, and Jeff R Wilkinson. 2009. “Genomic Profile of Maize Response to *Aspergillus flavus* Infection.” *Toxin Reviews* 28 (2–3): 129–41. doi:10.1080/15569540903089239.

Kensler, Thomas W, Bill D Roebuck, Gerald N Wogan, and John D Groopman. 2011. “Aflatoxin : A 50-Year Odyssey of Mechanistic and Translational Toxicology.” *Toxological Sciences* 120 (S1): 28–48. doi:10.1093/toxsci/kfq283.

Klich, Maren A. 2007. “*Aspergillus flavus* : The Major Producer of Aflatoxin.” *Molecular Plant Pathology* 8 (6): 713–22. doi:10.1111/J.1364-3703.2007.00436.X.

Kozomara, Ana, and Sam Griffiths-Jones. 2014. “miRBase: Annotating High Confidence microRNAs Using Deep Sequencing Data.” *Nucleic Acids Research* 42 (D1). Oxford University Press: D68–73. doi:10.1093/nar/gkt1181.

Kulcheski, Franceli R, Luiz Fv de Oliveira, Lorrayne G Molina, Maurício P Almerão, Fabiana a Rodrigues, Juliana Marcolino, Joice F Barbosa, Renata Stolf-Moreira, Alexandre L Nepomuceno, Francismar C Marcelino-Guimarães, Ricardo V Abdelnoor, Leandro C Nascimento, Marcelo F Carazzolle, Gonçalo Ag Pereira, Rogério Margis. 2011. "Identification of Novel Soybean microRNAs Involved in Abiotic and Biotic Stresses." *BMC Genomics* 12. BioMed Central Ltd: 307. doi:10.1186/1471-2164-12-307.

Lau, Arthur PS, Alex KY Lee, Chak K Chan, and Ming Fang. 2006. "Ergosterol as a Biomarker for the Quantification of the Fungal Biomass in Atmospheric Aerosols." *Atmospheric Environment* 40: 249–59. doi:10.1016/j.atmosenv.2005.09.048.

Lau, Susanna KP, Chi Ching Tsang, and Patrick CY Woo. 2017. "*Talaromyces marneffei* Genomic, Transcriptomic, Proteomic and Metabolomic Studies Reveal Mechanisms for Environmental Adaptations and Virulence." *Toxins* 9: 192. doi:10.3390/toxins9060192.

Lau, Susanna KP, Wang Ngai Chow, Annette YP Wong, Julian MY Yeung, Jessie Bao, Na Zhang, Si Lok, Patrick CY Woo, and Kwok Yung Yuen. 2013. "Identification of microRNA-Like RNAs in Mycelial and Yeast Phases of the Thermal Dimorphic Fungus *Penicillium marneffei*." *PLoS Neglected Tropical Diseases* 7 (8): e2398. doi:10.1371/journal.pntd.0002398.

Law, Meiyee, Kevin L Childs, Michael S Campbell, Joshua C Stein, Andrew J Olson, Carson Holt, Nicholas Panchy, Jikai Lei, Dian Jiao, Carson M Andorf, Carolyn J Lawrence, Doreen Ware, Shin-Han Shiu, Yanni Sun, Ning Jiang, Mark Yandell. 2015. "Automated Update, Revision, and Quality Control of the Maize Genome Annotations Using MAKER-P Improves the B73 RefGen_v3 Gene Models and Identifies New Genes." *Plant Physiology* 167 (1): 25–39. doi:10.1104/pp.114.245027.

Lee, Heng-chi, Liande Li, Weifeng Gu, Zhihong Xue, Susan K Crosthwaite, Alexander Pertsemlidis, Zachary A Lewis, Michael Freitag, Eric U Selker, Craig C Mello, Yi Liu. 2010. "Diverse Pathways Generate microRNA-like RNAs and Dicer-Independent Small Interfering RNAs in Fungi." *Molecular Cell* 38 (6): 803–14. doi:10.1016/j.molcel.2010.04.005.

Lin, Yan Liang, Li Ting Ma, Yi Ru Lee, Shih Shun Lin, Sheng Yang Wang, Tun Tschu Chang, Jei Fu Shaw, Wen Hsiung Li, and Fang Hua Chu. 2015. "microRNA-like Small RNAs Prediction in the Development of *Antrodia cinnamomea*." *PLoS ONE* 10 (4): e0123245. doi:10.1371/journal.pone.0123245.

Liu, Tong, John Hu, Yuhu Zuo, Yazhong Jin, and Jumei Hou. 2016. "Identification of microRNA-like RNAs from *Curvularia lunata* Associated with Maize Leaf Spot by Bioinformation Analysis and Deep Sequencing." *Molecular Genetics and Genomics : MGG* 291. Springer Berlin Heidelberg: 587–96. doi:10.1007/s00438-015-1128-1.

Livak, Kenneth J, and Thomas D Schmittgen. 2001. "Analysis of Relative Gene Expression Data Using Real-Time Quantitative PCR and the $2^{-\Delta\Delta CT}$ Method." *Methods* 25 (4): 402–8. doi:10.1006/meth.2001.1262.

Lopez, Juan Pablo, Alpha Diallo, Cristiana Cruceanu, Laura M Fiori, Sylvie Laboissiere, Isabelle Guillet, Joelle Fontaine, Jiannis Ragoussis, Vladimir Benes, Gustavo Turecki, Ernst, Carl. 2015. "Biomarker Discovery: Quantification of microRNAs and Other Small Non-Coding RNAs Using Next Generation Sequencing." *BMC Medical Genomics* 8 (July). BioMed Central: 35. doi:10.1186/s12920-015-0109-x.

Luo, Meng, Robert L Brown, Zhi-Yuan Chen, and Thomas E Cleveland. 2009. "Host Genes Involved in the Interaction between *Aspergillus flavus* and Maize." *Toxin Reviews* 28 (2–3): 118–28. doi:10.1080/15569540903089197.

MATLAB and Statistics Toolbox Release R2018a, The MathWorks, Inc., Natick, Massachusetts, United States.

Mellon, Jay E, Michael K Dowd, and Peter J Cotty. 2005. "Substrate Utilization by *Aspergillus flavus* in Inoculated Whole Corn Kernels and Isolated Tissues." *Journal of Agricultural and Food Chemistry* 53 (6): 2351–57. doi:10.1021/jf040276g.

Mueth, Nicholas A, Sowmya R Ramachandran, and Scot H Hulbert. 2015. "Small RNAs from the Wheat Stripe Rust Fungus (*Puccinia striiformis* f.Sp. Tritici)." *BMC Genomics* 16. BMC Genomics: 718. doi:10.1186/s12864-015-1895-4.

Mylroie, J Erik, Seval Ozkan, Renuka Shivaji, Gary L Windham, Michael N Alpe, and W Paul Williams. 2016. "Identification and Quantification of a Toxigenic and Non-Toxigenic *Aspergillus flavus* Strain in Contaminated Maize Using Quantitative Real-Time PCR." *Toxins* 8 (1): 15. doi:10.3390/toxins8010015.

Nierman, William C, Jiujiang Yu, Natalie D Fedorova-Abrams, Liliana Losada, Thomas E Cleveland, Deepak Bhatnagar, Joan W Bennett, Ralph Dean, and Gary A Payne. 2015. "Genome Sequence of *Aspergillus flavus* NRRL 3357, a Strain That Causes Aflatoxin Contamination of Food and Feed." *Genome Announcements* 3 (2). American Society for Microbiology: e00168-15. doi:10.1128/genomeA.00168-15.

Peethambaran, Bela, Leigh Hawkins, Gary L Windham, W Paul Williams, and Dawn S Luthe. 2010. "Anti-Fungal Activity of Maize Silk Proteins and Role of Chitinases in *Aspergillus flavus* Resistance." *Toxin Reviews* 29 (1): 27–39. doi:10.3109/15569540903402874.

Rogers, Kestrel, and Xuemei Chen. 2013. "Biogenesis, Turnover, and Mode of Action of Plant microRNAs." *The Plant Cell* 25: 2383–99. doi:10.1105/tpc.113.113159.

Rosas-cárdenas, Flor De Fátima, Noé Durán-figueroa, and Andrés Cruz-hernández. 2011. "A Simple and Efficient Method for Isolating Small RNAs from Different Plant Species." *Plant Methods* 7. BioMed Central Ltd: 4. doi:10.1186/1746-4811-7-4.

Schnable, Patrick S, Doreen Ware, Robert S. Fulton, Joshua C Stein, Fusheng Wei, Shiran Pasternak, Chengzhi Liang, et al. 2009. "The B73 Maize Genome: Complexity, Diversity, and Dynamics." *Science* 326 (5956). American Association for the Advancement of Science: 1112–15. doi:10.1126/science.1178534.

Shan, Xueyan, and W Paul Williams. 2014. "Toward Elucidation of Genetic and Functional Genetic Mechanisms in Corn Host Resistance to *Aspergillus flavus* Infection and Aflatoxin Contamination." *Frontiers in Microbiology* 5: 364. doi:10.3389/fmicb.2014.00364.

Smart, MG, DT Wicklow, and RW Caldwell. 1990. "Pathogenesis in *Aspergillus* Ear Rot of Maize - Light-Microscopy of Fungal Spread from Wounds." *Phytopathology*. https://naldc.nal.usda.gov/download/24323/PDF.

Thakare, Dhiraj, Jianwei Zhang, Rod A Wing, Peter J Cotty, and Monica A Schmidt. 2017. "Aflatoxin-Free Transgenic Maize Using Host-Induced Gene Silencing." *Science Advances* 3: e1602382.

Umemura, Myco, Nozomi Nagano, Hideaki Koike, Jin Kawano, Tomoko Ishii, Yuki Miyamura, Moto Kikuchi, Koichi Tamano, Jiuiang Yu, Kazuo Shin-ya, Masayuki Machida. 2014. "Characterization of the Biosynthetic Gene Cluster for the Ribosomally Synthesized Cyclic Peptide Ustiloxin B in *Aspergillus flavus*." *Fungal Genetics and Biology* 68: 23–30.

Wang, Bing, Yanfei Sun, Na Song, Mengxin Zhao, Rui Liu, Hao Feng, Xiaojie Wang, and Zhensheng Kang. 2017. "*Puccinia striiformis* f. Sp. Tritici MicroRNA-like RNA 1 (Pst-MilR1), an Important Pathogenicity Factor of Pst, Impairs Wheat Resistance to Pst by Suppressing the Wheat Pathogenesis-Related 2 Gene." *New Phytologist* 215: 338–50. doi:10.1111/nph.14577.

Warburton, Marilyn L, and W Paul Williams. 2014. "Aflatoxin Resistance in Maize: What Have We Learned Lately?" *Advances in Botany* 2014: 352831. doi:10.1155/2014/352831.

Wild, C.P. 2002. “The Toxicology of Aflatoxins as a Basis for Public Health Decisions.” *Mutagenesis* 17 (6). Oxford University Press: 471–81. doi:10.1093/mutage/17.6.471.

Williams, W Paul, and Gary L Windham. 2012. “Registration of Mp718 and Mp719 Germplasm Lines of Maize.” *Journal of Plant Registrations* 6 (2): 200–202. doi:10.3198/jpr2011.09.0489crg.

Xiao, Yingjie, Haijun Liu, Liuji Wu, Marilyn Warburton, and Jianbing Yan. 2017. “Genome-Wide Association Studies in Maize: Praise and Stargaze.” *Molecular Plant*. Cell Press. doi:10.1016/j.molp.2016.12.008.

Yang, Qiuying, Liande Li, Zhihong Xue, Qiaohong Ye, Lin Zhang, Shaojie Li, and Yi Liu. 2013. “Transcription of the Major *Neurospora crassa* microRNA-Like Small RNAs Relies on RNA Polymerase III.” *PLoS Genetics* 9 (1): e1003227. doi:10.1371/journal.pgen.1003227.

Yu, Jiujiang. 2012. “Current Understanding on Aflatoxin Biosynthesis and Future Perspective in Reducing Aflatoxin Contamination.” *Toxins* 4: 1024–57. doi:10.3390/toxins4111024.

Yu, Jiujiang, Perng-kuang Chang, Kenneth C Ehrlich, Jeffrey W Cary, Deepak Bhatnagar, Thomas E Cleveland, Gary A Payne, John E Linz, Charles P Woloshuk, and Joan W Bennett. 2004. “Clustered Pathway Genes in Aflatoxin Biosynthesis.” *Applied and Environmental Microbiology* 70 (3): 1253–62. doi:10.1128/AEM.70.3.1253.

Zhang, Baohong, Xiaoping Pan, and Todd A Anderson. 2006. “Identification of 188 Conserved Maize microRNAs and Their Targets.” *FEBS Letters* 580 (15). Wiley-Blackwell: 3753–62. doi:10.1016/j.febslet.2006.05.063.

Zhang, Lifang, Jer Ming Chia, Sunita Kumari, Joshua C Stein, Zhijie Liu, Apurva Narechania, Christopher A Maher, Katherine Guill, Michael D McMullen, and Doreen Ware. 2009. “A Genome-Wide Characterization of microRNA Genes in Maize.” *PLoS Genetics* 5 (11): e1000716. doi:10.1371/journal.pgen.1000716.

Zhang, Yijun, Miaomiao Fan, Xue Zhang, Feng Huang, Kang Wu, Junsong Zhang, Jun Liu, Zhuoqiong Huang, Haihua Luo, Liang Tao, Hui Zhang. 2014. “Cellular microRNAs Up-Regulate Transcription via Interaction with Promoter TATA-Box Motifs.” *RNA* 20 (12). Cold Spring Harbor Laboratory Press: 1878–89. doi:10.1261/rna.045633.114.

Zhou, Jiahong, Yanping Fu, Jiatao Xie, Bo Li, Daohong Jiang, Guoqing Li, and Jiasen Cheng. 2012. “Identification of microRNA-like RNAs in a Plant Pathogenic Fungus *Sclerotinia sclerotiorum* by High-Throughput Sequencing.” *Molecular Genetics and Genomics* 287: 275–82. doi:10.1007/s00438-012-0678-8.

Zhou, Quan, Zhangxun Wang, Jun Zhang, Huimin Meng, and Bo Huang. 2012. “Genome-Wide Identification and Profiling of microRNA-like RNAs from *Metarhizium anisopliae* During Development.” *Fungal Biology* 116. Elsevier Ltd: 1156–62. doi:10.1016/j.funbio.2012.09.001.

APPENDIX A

SUPPLEMENTAL TABLES

Table A.1 Primers for RT-qPCR analysis of 135 milRNAs (Afl-milR-1~135)

Name	Primer Sequence	Tm (°C)
Afl-milR-1	5'-GCTGGTATCTGCGAACGACTTGC-3'	60.4
Afl-milR-2	5'-GGCAAGATGACCGAGTGGTTA-3'	57.0
Afl-milR-3	5'-GGCGAGATGGCCGAGCGGTCT-3'	66.5
Afl-milR-4	5'-GTGGAGGATTGGGACGGGGT-3'	61.8
Afl-milR-5	5'-CTTTGGAGGGATTGGTGGGA-3'	57.0
Afl-milR-6	5'-GAGGGCGGAGAGGGGTGGAA-3'	63.9
Afl-milR-7	5'-GTGGGAGGTTGAGTGGGTGGTA-3'	60.8
Afl-milR-8	5'-TTTTGTGGAATCTGCCTCGCGCT-3'	61.7
Afl-milR-9	5'-GGCGAGATGGCCGAGCGGTCC-3'	67.5
Afl-milR-10	5'-CTGGATTCGTCCCGGGAACCC-3'	62.3
Afl-milR-11	5'-AGCGGTCTAAGGCGCACGGTTCA-3'	65.1
Afl-milR-12	5'-CTTCTATCTCGTCGGGGGTCA-3'	58.0
Afl-milR-13	5'-CTTTCTGGTTGATGGCGTCGGA-3'	59.7
Afl-milR-14	5'-AAAGGGGCATGGGTAGTATGA-3'	55.8
Afl-milR-15	5'-CTGGTCGGGTTTGATGATGGA-3'	57.1
Afl-milR-16	5'-ATTGCTTGCATGTTCGTTCTGGA-3'	57.6
Afl-milR-17	5'-CTTTCTCATATATACGTCGGAA-3'	49.4
Afl-milR-18	5'-CCATGATACTTTGTTGGTCGGA-3'	54.9
Afl-milR-19	5'-AGCGAGACGACCTGCCTGGCA-3'	65.8
Afl-milR-20	5'-CATCTCTCTTGTCGGTTCGAGA-3'	56.1
Afl-milR-21	5'-ATGGGGGTCTGTATGTGATGGA-3'	57.7
Afl-milR-22	5'-GGAAGTTGATCTTGATTGTTGGA-3'	53.2
Afl-milR-23	5'-GAGGGGAGAGGGGGCCGTTG-3'	65.0
Afl-milR-24	5'-TGGCTATCGATCGATCGTCGGA-3'	59.6
Afl-milR-25	5'-GTGTAGGGTGTGGTAGTGCTC-3'	57.2
Afl-milR-26	5'-CCTGTCTATCGAGGATTGTTGGA-3'	56.1
Afl-milR-27	5'-GGATGATAGGTCGGGATGAGA-3'	55.4
Afl-milR-28	5'-TAGCTATCTCGTGACAGACAAT-3'	52.9
Afl-milR-29	5'-ACTCCTTGGGCGCATCGTTGGA-3'	63.5
Afl-milR-30	5'-TTACTGTACATAAGCTAGACA-3'	47.8
Afl-milR-31	5'-CAAGGATTGTGATTGTTCTGGA-3'	53.1
Afl-milR-32	5'-CTTGTTCGTCGGGGGGATGGCA-3'	64.1
Afl-milR-33	5'-GGCGAGATGGCCGAGCGGTC-3'	65.7
Afl-milR-34	5'-AAGGCGGACGTTGGCGGCTGATA-3'	65.3
Afl-milR-35	5'-GGCGGACTGCTTCAAACGACGGA-3'	63.9

Table A.1 (continued)

Afl-milR-36	5'-ACTTTAGATGGTCGTGTTGGGGA-3'	58.1
Afl-milR-37	5'-CATTGTTTAAGCGTCGTTGGAA-3'	54.1
Afl-milR-38	5'-CCATGGGATTCTAATCGTCGGA-3'	56.4
Afl-milR-39	5'-GGTTTTGATGATCGTGTCGGA-3'	55.2
Afl-milR-40	5'-CCTATCGGCATTGTGAGACGGA-3'	58.8
Afl-milR-41	5'-GTCGTGGTAAGTGTGGCGTCGGA-3'	63.2
Afl-milR-42	5'-GTTCTCAGCACGATCGGCCGGA-3'	63.7
Afl-milR-43	5'-CCTAGGACAAGGGCGCACAGAGT-3'	62.9
Afl-milR-44	5'-GTATCAATGACAGATCGTAAGGA-3'	51.9
Afl-milR-45	5'-AGGCGACTGGTACATGTATGG-3'	56.6
Afl-milR-46	5'-ATGGCATTGAATCGGTCGGGA-3'	59.1
Afl-milR-47	5'-ATGTAGTACTGCATCGTTCTGGA-3'	55.6
Afl-milR-48	5'-TGGGTGGTGGGGTGGCGATGGCT-3'	69.8
Afl-milR-49	5'-AGGGGTAGTGGAGGATGAGGAA-3'	59.1
Afl-milR-50	5'-GGCGTATAAAGGAATGTGCTCTT-3'	55.3
Afl-milR-51	5'-AGATGTTGACGAGAGTGGGAT-3'	55.5
Afl-milR-52	5'-TGGGAACTCTTCAATCAGAATGA-3'	53.9
Afl-milR-53	5'-AAGAAAGGACGGAAGAGCAGG-3'	57.0
Afl-milR-54	5'-TTGCAGAAGTCGGATAGTGGATG-3'	56.7
Afl-milR-55	5'-GGCCGAGGCTGATACATGCGT-3'	62.2
Afl-milR-56	5'-TGGTTGGACTTGCTTTAGGCAT-3'	57.1
Afl-milR-57	5'-CGGCACGGAGATTGGGGGTCA-3'	64.3
Afl-milR-58	5'-AGCGGTCTAAGGCGCACGGTTC-3'	64.1
Afl-milR-59	5'-AGCATGTTAATTCAGGGGAA-3'	51.7
Afl-milR-60	5'-TAACTCGGTGGATTATGGCAG-3'	54.4
Afl-milR-61	5'-ACTGGGGGTAGAGTTCACGGTA-3'	59.3
Afl-milR-62	5'-AACCTAGGACAAGGGCGCAC-3'	60.0
Afl-milR-63	5'-GTGGGTTGGTTGTGGGTGGTT-3'	60.6
Afl-milR-64	5'-TAGGTCTGGTCCTTGTGCGGTTT-3'	60.5
Afl-milR-65	5'-TGAAGAAGTAGACACCAGGCGTT-3'	58.1
Afl-milR-66	5'-AGGATCTGAGACTGGCCGCGT-3'	62.9
Afl-milR-67	5'-GCGGGTGGGCGGGCCTGGTG-3'	71.6
Afl-milR-68	5'-TCAATTGCCCGGATGGTCTAGT-3'	58.3
Afl-milR-69	5'-GGATGGGCGTAAGATCTACT-3'	53.5
Afl-milR-70	5'-TCCGTAGAGCTTGCCGGAGGGA-3'	64.3
Afl-milR-71	5'-TGGCGACTTGTGAACGGAGCAGC-3'	64.1
Afl-milR-72	5'-TGATGGAAGGATGGTGTTGA-3'	53.7
Afl-milR-73	5'-TGGGTTTATGGGTAGGTTGGGG-3'	58.9

Table A.1 (continued)

Afl-milR-74	5'-TGGGGAGGGTTTCAGGGAGTGGA-3'	64.1
Afl-milR-75	5'-CGGGTAGCGGGTCGGGCGGGC-3'	72.2
Afl-milR-76	5'-AGATGAGAAGGAGAGCGAAGCA-3'	57.9
Afl-milR-77	5'-TTGGCTGTATGATGGAGGTTT-3'	54.2
Afl-milR-78	5'-CTGGGGAGGAGAGGGTGATGTTA-3'	59.8
Afl-milR-79	5'-AGATAGAGGATGAAAGTAGGC-3'	51.0
Afl-milR-80	5'-GAGGAGAGGGGGGGACGGAC-3'	63.9
Afl-milR-81	5'-CGGGTCAGGGTGGAGTGCGGGT-3'	68.1
Afl-milR-82	5'-CGGACTCGAGAGAATGGCGGA-3'	61.0
Afl-milR-83	5'-GAGGAAGGTGAGGGAAGGGA-3'	58.3
Afl-milR-84	5'-TTGGGTGTGGTGGGCGGTTTA-3'	61.8
Afl-milR-85	5'-GAAGAGAACTCGATCGTCGGAGG-3'	58.7
Afl-milR-86	5'-AGGGTAAAGGGCGGAGCGGGA-3'	65.5
Afl-milR-87	5'-TGGGCGATGTAGATACACGCGG-3'	61.3
Afl-milR-88	5'-GAGGCTGGGGAAGGGAGGGA-3'	63.6
Afl-milR-89	5'-ACGGAGAAGATGGATGAGCCG-3'	59.0
Afl-milR-90	5'-GCGGGAGAGGGGGTAGGCGTA-3'	65.4
Afl-milR-91	5'-CGATGGTAGCTGAAGGGTGTC-3'	57.5
Afl-milR-92	5'-CGGGGTGGAATAGGGGGAGGAG-3'	63.3
Afl-milR-93	5'-ACGGGAGTGGACAGGAGTGGGT-3'	64.4
Afl-milR-94	5'-TTCGCGCTGGGATGGATAATTG-3'	57.8
Afl-milR-95	5'-GGGGGCGGGTGGAGAGCGGAT-3'	68.8
Afl-milR-96	5'-CCGCAACGGCTGTGCGAGGTGTA-3'	66.1
Afl-milR-97	5'-TGGGGTGGATGTGGAAGCGGGCT-3'	67.4
Afl-milR-98	5'-GTGGGATGGGGCTGGGATGGTA-3'	63.4
Afl-milR-99	5'-AGGGGTAGGGCTAGGGTGGC-3'	63.7
Afl-milR-100	5'-GAGGGTTGGGCTGGACGGGA-3'	64.4
Afl-milR-101	5'-TGGACAGGTCTATGATGGCGATT-3'	58.0
Afl-milR-102	5'-GTGGCGGGCATAGTGGAGGGC-3'	65.4
Afl-milR-103	5'-GGATGTTGGCGAGGAAGGCGA-3'	62.2
Afl-milR-104	5'-GCATGGAACGGTAGCGGCAAGTG-3'	62.9
Afl-milR-105	5'-TGGGGTGGGATGGGTTGGCT-3'	64.2
Afl-milR-106	5'-TCCGGCTGTACTATAAATCGG-3'	53.9
Afl-milR-107	5'-TTGGGAGGGGGTGGAAGGAA-3'	60.9
Afl-milR-108	5'-AGGAAGTGGTGTAGACAGTCC-3'	55.9
Afl-milR-109	5'-GCGGGTTAGGAGGAGGTCGGG-3'	64.0
Afl-milR-110	5'-GCGGGTGGTGGGGCGAAGGTGAC-3'	68.9
Afl-milR-111	5'-GGGGGGGGGAAGGACGGGTT-3'	67.0

Table A.1 (continued)

Afl-milR-112	5'-TTCTGACATGAATGGCAACTCA-3'	54.6
Afl-milR-113	5'-AAGTAGTAGAATGTGGATAAAGA-3'	48.7
Afl-milR-114	5'-TGGTTGTAGCTGGCGATGGAAGT-3'	60.8
Afl-milR-115	5'-AGAAGTGGGTGTTGAGAGGACTC-3'	58.2
Afl-milR-116	5'-GGTTTTGGAATGTATCGGTGT-3'	53.1
Afl-milR-117	5'-TCGGGTGGAGAGTGTGGCGGATG-3'	65.1
Afl-milR-118	5'-TGACTGGAGTGGTTGGATGTTGG-3'	59.2
Afl-milR-119	5'-TGGGGAAGAGCTGAGGGAGGGGA-3'	65.8
Afl-milR-120	5'-AGGGTAGGGTAGGTAGAGGGC-3'	59.5
Afl-milR-121	5'-AGATGAGTGGCGGTAGACGCAA-3'	60.6
Afl-milR-122	5'-TGGTTGGGTAGGGGTGAGGTC-3'	60.9
Afl-milR-123	5'-TGGGGTTGTGTGGATGGGGGC-3'	64.9
Afl-milR-124	5'-CAGGATGTGGGGGGGCGGCTCG-3'	69.2
Afl-milR-125	5'-GGGGGGGTGGGGGCGGAGTAGA-3'	69.8
Afl-milR-126	5'-CCGGGGGGGTGGGCGGCGAC-3'	73.6
Afl-milR-127	5'-TTGAACACTGACCAAGCTTA-3'	52.2
Afl-milR-128	5'-GAGGGAGGATGATGTGGAGGTC-3'	58.8
Afl-milR-129	5'-AAGGGCTTGGTTAACGGAGTCAT-3'	58.6
Afl-milR-130	5'-GTGGGCTAACGAGGAGGGTTG-3'	60.0
Afl-milR-131	5'-TGGGTTTGTGGTTGTGGAGGTTG-3'	60.1
Afl-milR-132	5'-GTGGGAGGGAGGAGGAGGAT-3'	60.4
Afl-milR-133	5'-AGGGTGTGGTAGGGAAGGGG-3'	61.1
Afl-milR-134	5'-AGGGTTTCTGGAGTGGCGATG-3'	59.5
Afl-milR-135	5'-TGCAGTTCGTTGGCGGCAGT-3'	62.8

The targets of *Z. mays* miRNA targets are listed in Table S.1 and are accessible in

Harper_Supplemental File.xlsx.